EUROPEAN JOURNAL OF BIOMEDICAL AND PHARMACEUTICAL SCIENCES
http://www.ejbps.com

ISSN 2349-8870
Volume: 11
Issue: 12
Year: 2024

TRIFLUORO-ACETYLATION OF NATURALLY OCCURRING PHENOLS AND STUDY OF ANTI-PROLIFERATIVE ACTIVITY OF RESPECTIVE PRODUCTS

Ajoy K. Bauri*[1], Ines Castro Dionicio[2], Eric Salinas Arellano[2], Sabine Foro[3] and Esperanza J. Carcache de Blanco*[2]

[1]Bio-Organic Division, Bhabha Atomic Research Centre, Trombay, Mumbai 400085, India.
[2]College of Pharmacy, The Ohio State University, Ohio, Columbus, OH 43210, USA.
[3]Institute of Materials Science, Darmstadt University of Technology, Alarich-Weiss-Strasse 2, D-64287, Darmstadt, Germany.

***Corresponding Author: Ajoy K. Bauri**

Bio-Organic Division, Bhabha Atomic Research Centre, Trombay, Mumbai 400085, India.

Article Received on 10/10/2024 **Article Revised on 31/10/2024** **Article Accepted on 20/11/2024**

ABSTRACT

A methodology has been developed to introduce trifluoro acetyl moiety into acyl part of naturally occurring phenols, malabaricones (**A**-**D**) and acyl phenol (**AP**) isolated from methanol extract the rind of *Myristica malabarica*. This reaction is similar to Friedel Crafts acetylation reaction; a *regio*-selective trifluoro-acylation reaction has been achieved using of trifluoro acetic acid as reagent under specific reaction condition. These naturally occurring phenols undergo deacylation followed by trifluoro-acetylation to yield dihydroxy trifluoro-acetyl benzenes and respective fatty acids. The introduction of trifluoro acetyl moiety took place at *ortho* position to one of the hydroxy groups of their acyl moieties to yield compound (**1**) as major product [2, 4-dihydroxy trifluoro-acetyl benzene] along with *ipso* product (**2**) as very minor amount [2, 6-dihydroxy trifluoro-acetyl benzene]. When acyl phenol (**AP**) was used as substrate for trifluoro-acetylation reaction under similar reaction condition only product (**1**) was obtained as sole product without forming *ipso* product (**2**) [2, 4-dihydroxy trifluoro-acetyl benzene]. This trifluoro-acetylation reaction has also been conducted in presence of different transition metals and their salts, but no products were observed. In general, this methodology can be applied for synthesis of small molecules like dihydroxy trifluoro acetyl benzene; it can be used as [^{18}F] labeled radiopharmaceutical diagnosing agent for PET imaging using 2, 6-dihydroxy acetophenone or its related compounds as substrates. In contrast other dihydroxy acetophenone did not proceed trifluoro-acetylation reaction under this reaction conditions. The cell cytoxicity of these reaction products was screened against various human cancer cell lines in comparison with paclitaxel as control. It was found that compound **1** [2, 4-dihydroxy trifluoro acetyl benzene] exhibited anti-proliferative activity against different human cancer cell lines.

KEYWORDS: Natural phenols; *M. malabarica*; TFA reaction products; anti-proliferative activity; SRB assay.

INTRODUCTION

The introduction of the strong electron-withdrawing trifluoro-acetyl group into benzene ring can substantially alter the property of organic molecules such as lipophilicity, metabolic stability, bio-availability and bio-viability.[1-2] The findings of this reaction are introducing a strong electrophile trifluoro acetyl group to naturally occurring phenols isolated from *Myristica malabarica* by using trifluoroacetic acid as reagent with solvent heating at temperature 50 ^{0}C in presence of different transition metals,[2-4] different chloride salts of transition metals or catalyst.[5-7] In Friedel Crafts acylation/alkylation reaction, the alkylation or acylation has been introduced in aromatic nucleus using respective acyl chloride/alkyl chloride in presence of anhydrous $AlCl_3$ under reflux in an inert solvent, but trifluoro-acylation is not reported. The synthesis of small molecule like dihydroxy trifluoro-acetyl benzene can be carried out with help of aforesaid reaction without use of a catalyst and solvent which undergoes chelation with transition metal salt, solvated in aqueous medium. This type of reaction methodology may have a very good scope to synthesis of competent biomarkers specially fluorinated labeled compounds (^{18}F) useful in radiopharmaceuticals due to its less half-life for positron emission tomography (PET) and to detect pre-symptomatic biochemical transformation in body tissues where no abnormality is detected using existing facilities like computerized tomography (CT), magnetic resonance imaging (MRI) etc. The fluorinated-organic compounds can be used in pharmaceuticals,[8, 9] agrochemicals,[10] clinical,[11,12] and diagnostic biomarker-reagents etc.[13] In addition to these, trifluoro

alkylated organic molecules find application as materials such as liquid crystals[14] and fluorinated polymers[15] etc.

RESULTS AND DISCUSSION

When a solution of isolated malabaricones were heated at ambient temperature (50 ^{0}C) over period of three days (72 h) with continuous stirring to provide trifluoro-acetyl benzene and fatty acid depending upon the substrates used, the molecules possessed 2, 6-dihydroxy acetophenone and their derivatives undergo trifluoro-acetylation reaction to yield 2, 4-dihydroxy trifluoro acetyl benzene as major product (**1**); 2, 6-dihydroxy trifluoro acetyl benzene as very minor product (**2**) and respective fatty acid (**3**). The *regio*-selective trifluoro acetylation reaction took place smoothly when malabaricones were used as substrate in trifluoro acetic acid on heating at 50 ^{0}C (oil bath temperature) with continuous stirring over a period of 72 h. The same reactions have been carried out in the presence of different transition metals, their chloride salts under similar reaction condition. It has been observed that yields of the reactions are identical, except reaction duration. The reaction duration has been reduced from 72 h to 36-48 h. This indicated that trifluoro acetylation reaction has not been influenced by time reduction, in addition of different transition metals and their salts. In this reaction, trifluoroacetic acid acts as solvent as well as reagent. The scheme of the reaction is depicted below.

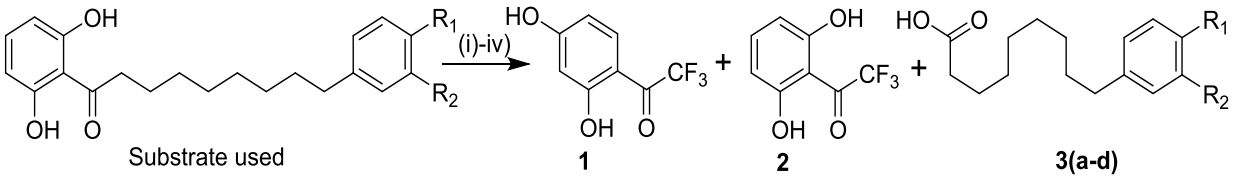

Substrate used 1 2 3(a-d)

$R_1 = R_2 = H$; Malabaricone A
$R_1 = H$ & $R_2 = H$; Malabaricone B
$R_1 = R_2 = OH$; Malabaricone C
$R_1, R_2 = -O-CH_2-O-$; Malabaricone D

(i). Reagent used TFA (ii). Heating 50 ^{o}C (iii). Stirred for 72 h

Scheme 1: Trifluoro acetylation reaction of Malabaricone (**A-D**)

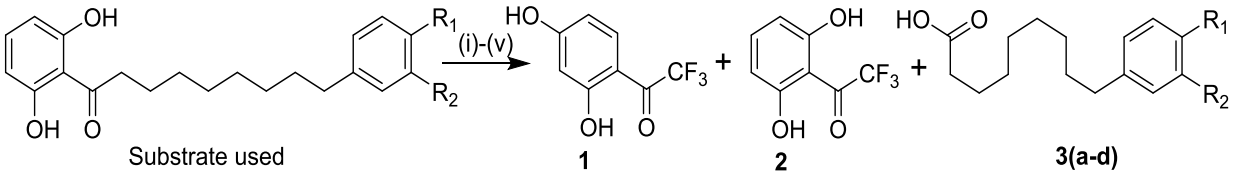

Substrate used 1 2 3(a-d)

$R_1 = R_2 = H$; Malabaricone A
$R_1 = H$ & $R_2 = H$; Malabaricone B
$R_1 = R_2 = OH$; Malabaricone C
$R_1, R_2 = -O-CH_2-O-$; Malabaricone D

(i). Reagent used TFA (ii). Heating 50 ^{o}C (iii). In presence of trasition metals (iv).Stirred for 72 h (v) standard work up

Scheme 2: Trifluoro acetylation reaction of Malabaricone (**A-D**)

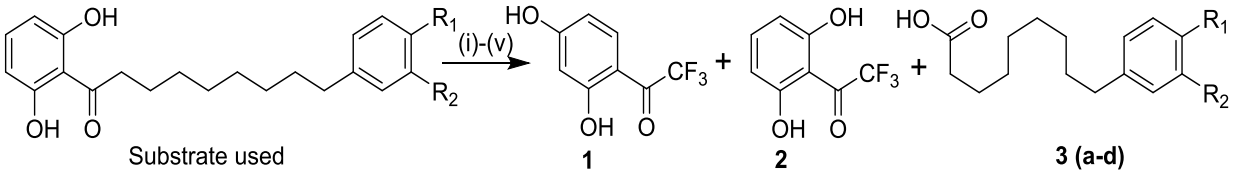

Substrate used 1 2 3 (a-d)

$R_1 = R_2 = H$; Malabaricone A
$R_1 = H$ & $R_2 = H$; Malabaricone B
$R_1 = R_2 = OH$; Malabaricone C
$R_1, R_2 = -O-CH_2-O-$; Malabaricone D

(i). Reagent used TFA (ii). Heating 50 ^{o}C (iii). In presence of salt of trasition metals (iv).Stirred for 72 h (v) standard work up

Scheme 3: Trifluoro acetylation reaction of Malabaricone (**A-D**)

When a solution of acyl phenol (2, 6-dihydroxy acetophenone or its derivatives) heated at ambient temperature (50 ^{0}C) over period of three days (72 h) with stirring to yield 2, 4-dihydroxy trifluoro-acetyl benzene and nonanoic acid, any 2, 6-dihydroxy benzene in association with aliphatic chain (smaller or bigger) at C-1 position used as substrates for trifluoro-acetylation reaction under the aforesaid reaction condition, 2, 6-dihydroxy trifluoro acetyl benzene and respective fatty acid has been formed as reaction products. The very selective trifluoro acetylation reaction occurred smoothly to the adjourning ortho position of one of the hydroxy groups of 2, 6-dihydroxy acyl phenol used as substrate. This trifluoro acetylation reaction was also conducted in presence of transition metals and their salts. It was noticed that there is no influence of effect of transition metals, their salts on the products. The only difference is reaction duration. In general, in this case, the reaction duration of trifluoro-acetylation reaction is around 72 h, but in presence of transition metals and their salts, the reaction duration has been less and lowered from 72h to 36-48h.

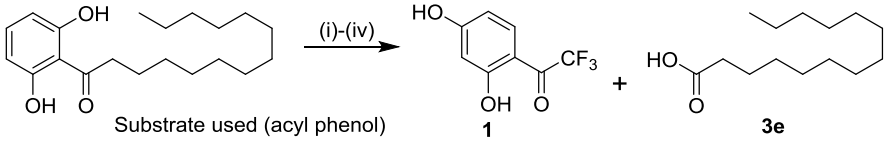

(i). Reagent and solvent used TFA (ii). Heating 50 ^{o}C (ii). Stirred for 72 h (iv) Standard worp up

Scheme 4: Trifluoro acylation reaction of acyl phenol (**AP**)

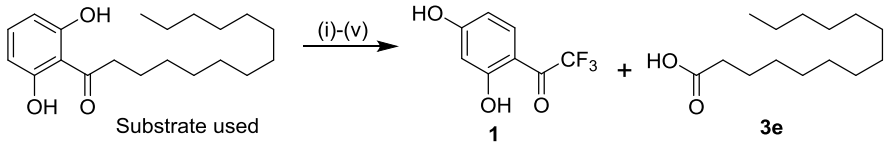

(i). Reagent used TFA (ii). Heating 50 ^{o}C (iii). In presence of transition metals (iv).Stirred for 72 h

Scheme 5: Trifluoro acylation reaction of acyl phenol (**AP**)

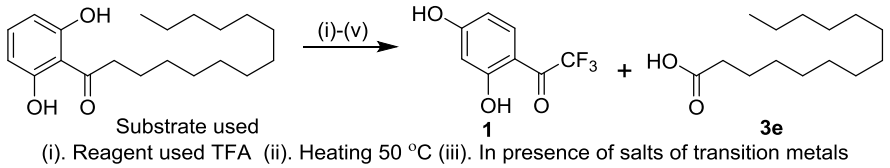

(i). Reagent used TFA (ii). Heating 50 ^{o}C (iii). In presence of salts of transition metals (iv). Stirred for 72 h

Scheme 6: Trifluoro acylation reaction of acyl phenol (**AP**)

The reaction products were worked up by the usual method. The crude reaction product was purified by column chromatography over silica gel with gradient elution using binary solvent system ethyl acetate in hexane followed by chloroform in methanol. The pure products were characterized by spectroscopic and spectrometric methods.

The probable mechanism for the formation of trifluoro acetylation of the naturally occurring phenols isolated from the dry fruit rind *Myristica malabarica* is depicted as in the scheme 7.

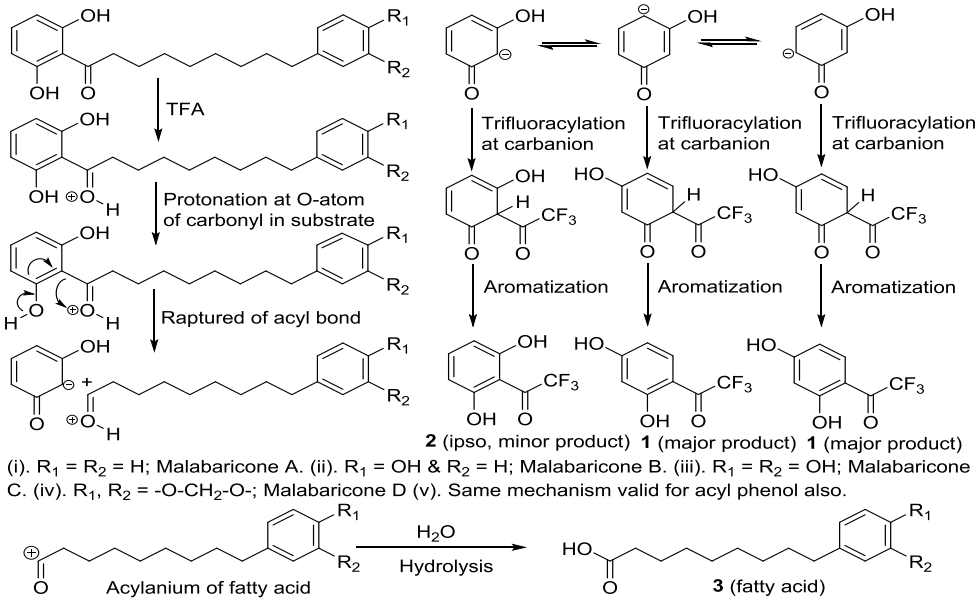

(i). $R_1 = R_2 = H$; Malabaricone A. (ii). $R_1 = OH$ & $R_2 = H$; Malabaricone B. (iii). $R_1 = R_2 = OH$; Malabaricone C. (iv). $R_1, R_2 = -O-CH_2-O-$; Malabaricone D (v). Same mechanism valid for acyl phenol also.

Scheme 7: Probable mechanism of trifluoro-acetylation raction of naturraly occurring isolated phenols

EXPERIMENTAL SECTION

General procedure for extraction and isolation of malabaricones used as substrates

The substrates used in this reaction were a series of malabaricones (**A-D**) and an acyl phenol (**AP**). These substrates were isolated from methanol extract of dry fruit rind of *Myristica malabarica*. Details extraction, isolation and purification of the substrates used in this reaction was described earlier.[16-25]

General procedure for synthesis of trifluoro acetyl phenols and respective fatty acids

A solution of malabaricones/acyl phenol in trifluoroacetic acid (TFA) were charged in a three neck round bottom flask fitted with a condenser along with

guard tube and a mechanical stirrer. The mixture was heated at temperature 50 °C in an oil bath over a period three days. The reaction vessel was removed from oil bath and allowed to cool at room temperature. The excess trifluoro acetic acid was removed by rotavapor. Chilled water was added to reaction mixture to complete extraction with diethyl ether or ethyl acetate. This extract was dried over Na_2SO_4 and solvent was removed using rotavapor to obtain crude reaction products. The crude reaction products were purified by column over silica gel with gradient solvent elution to obtain respective products [**1**, **2** and **3(a-e)**].

Structural characterization of purified products obtained from trifluoro acetyl reaction were mentioned below.

Structural determination of major trifluoro acetyl phenols

Characterization of product, **1** (major amt. ~ 80%): colorless needle shape crystal (5% EtOAc in hexane, slow evaporation at room temperature); mp: 128 °C; ^{1}H NMR data (200 MHz, $CDCl_3$): δ_H 7.76 (ddq, 1H, H-6), 6.66 (dd, 1H, *J* = 9.0 & 2.6 Hz, H-5), 6.51 (d, 1H, *J* = 2.4 Hz, H-3); ^{13}C NMR data (50 MHz, $CDCl_3$): ^{13}C NMR data ($CDCl_3$, 200 MHz): δ_C 205.10 (>C=O), 164.86 (C-2), 165.2 (C-6), 134.00 (C-4), 112.54 (-CF_3) 108.27 (C-3 & C-5), 102.56 (C-1); IR (neat): 3458.71 (-OH gr.), 3364.21.6 (-OH gr.), 1643.16 cm-1 (>C=O gr.); UV data (MeOH): λ_{max} 224 & 288 nm; EIMS data: *m/z* (%) 206 (14.0), 182 (3.0), 178 (2.0), 165 (3.0), 146 (9.0), 137 (100, base peak), 128 (15.5), 111 (11.2), 96 (5.5), 85 (8.2), 81 (50.1), 69 (79.5).

Structural determination of minor trifluoro acetyl phenols (2) yielded from TFA reaction

It is very minor product. Yield of **2** (~ 5%): It is a colorless needle shape crystal (5% EtOAc in hexane, slow evaporation at room temperature); mp 65 °C; ^{1}H NMR data ($CDCl_3$, 200 MHz): δ_H 6.95 (dd, 1H, J = 8.0 Hz, H-4), 6.32 (dd, 1H, J = 8.0 & 2.2 Hz, H-5), 6.28 (d, 1H, J = 8.0 & 2.2 Hz, H-3); ^{13}C NMR data ($CDCl_3$, 50 MHz): δ_C 162.39 (>C=O), 143.45 (C-2), 129.02 (C-6), 128.91 (C-1), 120.47 (-CF_3) 114.67 (C-3 & C-5), 102.56 (C-1); ^{19}F NMR: δ_F -121 ppm; IR (neat): 3458.75 (-OH gr.), 3368.21 (-OH gr.), 1633.16 (>C=O gr.) cm^{-1} ; UV data, λ_{max} (MeOH) : 206, 276 nm; EIMS data: *m/z* (%) 206 (40.0), 183 (7.5), 149 (9.0), 137 (100%, base peak), 125 (6.0), 111 (11.2), 95 (18.0), 95 (18.0), 87 (38.5), 81 (58.0), 69 (66).

Structural characterization of fatty acids (3a) obtained from TFA reaction

It is a viscous liquid; ^{1}H NMR data ($CDCl_3$, 200 MHz,): δ_H 7.30-7.20 (m, 5H, Ar-H), 2.64 (d, 2H, *J* = 7.4 Hz, H-2), 2.39 (d, 2H, *J* = 7.4 Hz, H-9, Ph-CH_2-), 1.67-1.49 (m, 4H, 2x-CH_2-, H-3 & H-8), 1.36 (s, 4x-CH_2-, 8H); ^{13}C NMR data ($CDCl_3$, 50 MHz): ^{13}C NMR data (CD_3COCD_3, 50 MHz): δ_C 180.06 (-COOH), 142.83 (Ar-C-H), 128.36 (Ar-CH), 128.20 (Ar-C-H), 125.54 (Ar-C-H), 35.92 (-CH_2-), 34.00 (-CH_2-), 31.44 (-CH_2-), 29.65 (-CH_2-), 29.34 (-CH_2-), 29.24 (-CH_2-), 29.20 (-CH_2-), 29.13 (-CH_2-), 28.99 (-CH_2-), 24.62 (-CH_2-); IR (neat): 1705.73 cm-1 (-COOH gr.); UV (MeOH) data, λ_{max}: 208 nm; EIMS data: *m/z* (%) 234 (5.1), 216 (3.4), 206 (2.0), 191 (5.5), 165 (3.1), 146 (22.5), 128 (74.3), 113 (8.2), 105 (21.0), 91 (100; base peak), 73 (47.0).

Characterization of fatty acid derivative, 3b [9-(4-hydroxyphenyl) nonanoic acid]: It is an off-white needle shaped crystal; mp 103 °C; ^{1}H NMR data ($CDCl_3$, 200 MHz,): δ_H 8.04 (1H, -OH), 6.99 (dd, 1H, *J* = 8.00 & 2.2 Hz, H-5′ & H-2′), 6.71 (dd, 1H, *J* = 1.4 & 8.0 Hz, H-6′), 2.48 (dd, 2H, *J* = 7.2 Hz, H-9), 2.30 (dd, 2H, *J* = 7.4 Hz, H-2), 1.69-1.49 (m, 4H, 2x-CH_2-, H-3 & H-8), 1.28 (s, 8H, 4x-CH_2-); ^{13}C NMR data ($CDCl_3$, 50 MHz): δ_C 174.71 (-COOH), 156.16 (Ar-C-OH), 134.14 (Ar-C-C), 129.97 (2xAr-C-H), 115.80 (2xAr-C-H), 35.58 (Ar-CH_2-), 34.15 (-CH_2-CO-), 32.61 (-CH_2-), 30.06 (-CH_2-), 25.60 (-CH_2-); IR (neat): 3407.6 (-OH), 1714.4 cm-1 (-COOH gr.); UV data, λ_{max} (MeOH): 224, 280 nm; EIMS data: *m/z* (%) 250 (40.0) [M]$^+$, 232 (15.0) [M$^+$-H_2O], 206 (12.0), 186 (11.0), 171 (10.0), 158 (12.0), 143 (13.0), 137 (35.0), 110 (52.0), 91 (86.0), 69 (100, base peak).

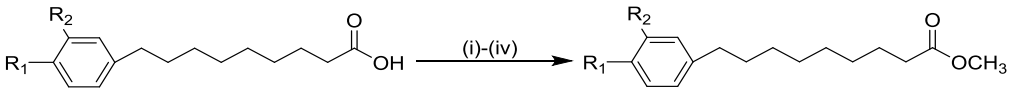

3 (**a-d**)/Substituted fatty acid from cleavage of phenols

$R_1 = R_2$ = H; 9(phenyl) nonanoic acid
R_1 = OH & R_2 = H; 9(3-phenyl) nonanoic acid
$R_1 = R_2$ = OH; 9(3, 4-diphenyl) nonanoic acid
R_1, R_2 = -O-CH_2-O-H; 9(3, 4- dihydroxy phenyl) nonanoic acid (deacylation occurred while TFA reaction)

4 (**a-d**)/Substituted fatty acid methyl ester

$R_1 = R_2$ = H; 9(phenyl) methyl nonanate
R_1 = OH & R_2 = H; 9(3-phenyl) methyl nonanate
$R_1 = R_2$ = OH; 9(3, 4-diphenyl) methyl nonanate
R_1, R_2 = -O-CH_2-O-H; 9(3, 4-dihydroxy phenyl) nonanate

(i). Solvent as well as reagent used: MeOH (ii). Added catalytic amount conc. H_2SO_4 (iii). Stirred (iv). Worked up by usual method and purification by standard procedure

Scheme 8: Esterification of substituted acid in the presence of a catalytic amount of H_2SO_4

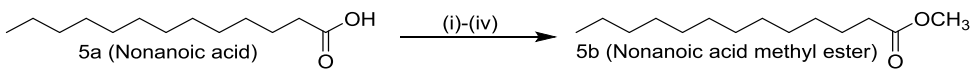

(i). Solvent as well as reagent used: MeOH (ii). Added catalytic amount conc. H_2SO_4 (iii). Stirred (iv). Worked up by usual method and purification by standard procedure

Scheme 9: Esterification of nonnoic acid in the presence of a catalytic amount of concetrated H_2SO_4

Methylation reaction of fatty acid 3b: About 10 mg of product **3b** was subjected to methylation by using MeOH in presence of a catalytic amount of H_2SO_4 with continuous mechanical stirring over a period of 12 hrs. The excess solvent was removed by means of rotavapor to afford respective methylated product in crude form. The scheme of reaction was depicted below in scheme 2.

The product was purified through open silica gel column by eluting with binary solvent systems hexane-ethyl acetate to afford pure product. The pure product was characterized by spectral methods.

Characterization of methylated product of molecule 4b: It is a light brown solid substance; mp 78-80 °C; ^{1}H NMR data (200 MHz, $CDCl_3$): δ 7.07 (d, 2H, *J* = 8.2 Hz, H-2′ & H-6′), 6.78 (d, 2H, *J* = 8.2 Hz, H-3′ & H-5′), 3.71 (s, 3H, -OCH_3), 2.56 (dd, 2H, *J* = 7.4 Hz, H-9), 2.34 (dd, 2H, *J* = 7.4 Hz, H-2), 1.64-1.61 (m, 4H, H-3 & H-9, 2x-CH_2-), 1.33 (s, 8H, 4x-CH_2-); ^{13}C NMR data: Unable to record due to insufficient amount of sample. IR: 3647.7 (-OH gr.), 1738.1 cm^{-1} (ester >C=O gr.); UV data, λ_{max} (MeOH): 224 and 270 nm; EIMS data: *m/z* (%): 264 (12.0) [M]$^+$, 232 (15.0) [M$^+$-OCH_3], 204 (7.0) [M$^+$-OCH_3-CO], 147 (2.0), 120 (20.0), 107 (100, base peak), 85 (3.0), 77 (12.0), 69 (10.0).

Characterization of fatty acid 3c [9(3, 4-dihydroxyphenyl) nonanoic acid]: It is colorless solid; mp 100 °C; ^{1}H NMR data ($CDCl_3$, 200 MHz): δ 6.77 (d, 1H, *J* = 8.0 Hz, H-5′), 6.69 (d, 1H, *J* = 1.4 Hz, H-2′), 6.60 (dd, 1H, *J* = 1.4 & 8.0 Hz, H-6′), 2.48 (dd, 2H, *J* = 7.2 Hz, H-9), 2.30 (dd, 2H, *J* = 7.4 Hz, H-2), 1.69-1.49 (m, 4H, 2x-CH_2-, H-3 & H-8), 1.28 (s, 8H, 4x-CH_2-); ^{13}C NMR data ($CDCl_3$, 50 MHz): δ_C 175.10 (-COOH), 159.36 (Ar-C-OH), 145.57 (Ar-C-OH), 143.59 (Ar-C-C), 130.59 (Ar-C-H), 120.29 (Ar-C-H), 116.14 (Ar-C-H), 115.79 (Ar-C-H), 35.76 (Ar-CH_2-), 34.14 (-CH_2-), 32.43 (-CH_2-), 32.43 (-CH_2-), 30.95 (-CH_2-), 30.16 (-CH_2-), 25.54 (-CH_2-); IR (neat): 3364.2 (-OH gr.), 1716.4 cm^{-1} (-COOH gr.); UV spectral data, λ_{max} (MeOH): 226 and 280 nm; EIMS data: m/z (%) 266 [M]$^+$ (not appeared), 203 (2.1) [M$^+$-(H_2O + CO_2)], 189 (5.5), 176 (7.2), 165 (11.5), 152 (67.5), 137 (100), 123 (4.5), 110 (4.3), 91 (2.5), 81 (8.3), 69 (8.5).

Methylation of fatty acid (3c) [9-(3, 4-dihydroxyphenyl) nonanoic acid]: A solution of 3c (10 mg, 0.034 mM) in MeOH along with a catalytic amount concentrated H_2SO_4 was stirred for overnight. The reaction was depicted in scheme 1. The excess solvent was removed by means of rotavapor to afford a residue. Water was poured into it. The product was extracted with diethyl ether, dried over anhydrous Na_2SO_4 and concentrated it to yield desired product in crude form. The product was passed over short silica gel column and eluted with binary solvent system hexane-ethyl acetate. The pure product was characterized by spectral means. Yield of the product was 90 % approximately.

Characterization of fatty acid (3d) [9-(3, 4-dihydroxyphenyl) nonanoic acid-demethylation occurred]: It is a colorless needle shape crystal (10% EtOAc in Hexane, slow evaporation at rt); mp 100 °C; ^{1}H NMR data ($CDCl_3$, 200 MHz): δ 6.77 (d, 1H, *J* = 8.0 Hz, H-5′), 6.69 (d, 1H, *J* = 1.4 Hz, H-2′), 6.60 (dd, 1H, *J* = 1.4 & 8.0 Hz, H-6′), 2.48 (dd, 2H, *J* = 7.2 Hz, H-9), 2.30 (dd, 2H, *J* = 7.4 Hz, H-2), 1.69-1.49 (m, 4H, 2x-CH_2-, H-3 & H-8), 1.28 (s, 8H, 4x-CH_2-); ^{13}C NMR data ($CDCl_3$, 50 MHz): δ 175.10 (-COOH), 159.36 (Ar-C-OH), 145.57 (Ar-C-OH), 143.59 (Ar-C-C), 130.59 (Ar-C-H), 120.29 (Ar-C-H), 116.14 (Ar-C-H), 115.79 (Ar-C-H), 35.76 (Ar-CH_2-), 34.14 (-CH_2-), 32.43 (-CH_2-), 32.43 (-CH_2-), 30.95 (-CH_2-), 30.16 (-CH_2-), 25.54 (-CH_2-); IR (neat): 3364.2 (-OH gr.), 1716.4 cm-1 (-COOH gr.); UV spectrum, λ_{max} (MeOH): 226 and 280 nm. EIMS data: *m/z* (%) 266 [M]$^+$ (not appeared), 203 (2.1) [M$^+$ - (H_2O + CO_2)], 189 (5.5), 176 (7.2), 165 (11.5), 152 (67.5), 137 (100, base peak), 123 (4.5), 110 (4.3), 91(2.5), 81 (8.3), 69 (8.5).

Anti-proliferative activity of TFA reaction products on different cancer cell lines by using Sulfo-rhodamine B (SRB) assay

The evaluation of anti-proliferative activity of products obtained from trifluoro acetylation reaction of naturally occurring phenols has been performed against six different types of human cancer cell lines such as urinary bladder (HT-1376), HT-29 (colon), MDAT-32 (thyroid), BDCM (leukaemia), MCF-7 (breast) and ovarian (A-2780) cancer cell lines and were used to carry out the bioassay for cell cytotoxicity using sulfo-rhodamine B (SRB) assay at College of Pharmacy, The Ohio State University, Ohio, Columbus, USA. [26-28] The sulfo-rhodamine B (SRB) cell cytotoxicity assay is one of the most widely used methods to detect cell viability. This assay is independent of cell metabolic activity. The incorporated dye released from stained cells after washing is directly proportional to the cell biomass and can be measured at 460 nm (Table 1).

Sample preparation. Test samples and control (paclitaxel) were dissolved in 100% DMSO to prepare stock solutions of 10 mg/ml. Dilutions were prepared using 10 % DMSO in water and 100 % water.

Cell culture. urinary bladder (HT-1376), HT-29 (colon), MDAT-32) thyroid, BDCM (leukemia), MCF-7 (breast) and ovarian (A-2780) cancer cell lines were obtained from American Type Culture Collection, Manassas, VA, USA. Monolayer cells were cultured using T75 tissue culture flasks in Roswell Park Memorial Institute medium (RPMI) or Dulbecco's Modified Eagle Medium (DMEM), containing 10 % fetal bovine serum and 1 % anti-biotic-anti-mycotic from Gibco. Cells were kept at 37 °C and in an atmosphere with 5% of CO_2. *Anti-proliferative assays*. Anti-proliferative activity of test samples was evaluated in triplicate on cancer cells, using the SRB assay as reported previously in three independent experiments (Table 1).

CONCLUSION AND SUMMARY OF WORK

Isolated naturally occurring phenols from the fruit rind of *Myristica malabarica* have been used as subrostrate for TFA reaction. These phenols undergo de-acylation followed by trifluoro-acetylation with TFA to yield dihydroxy trifluoro-acetyl benzenes and respective fatty acids. When malabaricones are used as substrates for TFA reaction, trifluoro acetylation occurred at ortho position to one of the hydroxy groups of malabaricones to yield compound (**1**) as major product (2, 4-dihydroxy trifluoro-acetyl benzene) along with trace amount *ipso* product and respective fatty acids. But in the case of acyl phenol (**AP**) or 2, 6-dihydroxy benzene in association with acyl group at C-1 position is used as substrate for trifluoro-acetylation reaction under similar reaction condition, only product (**1**) has been formed as sole product (2, 4-dihydroxy trifluoro-acetyl benzene) along with respective fatty acid. It is a *regio* selective trifluoro acetylation of 2, 6-dihydroxy acetophenone or its related compounds like malabaricones and acyl phenol. The cell cytoxicity of these purified reaction products was screened against various human cancer cell lines in comparison with paclitaxel as control. It was found that compound **1** (2, 4-dihydroxy trifluoro acetyl benzene) exhibited anti-proliferative activity at 1.9±0.5, 1.9±0.5, 3.2±0.5 µM against different human cancer cell lines such as colon (HT), leukemia (BDCM) and ovarian (A2780) cancer cell lines.

Table 1: Anti-proliferative activity of compounds 1-2 and respective fatty acids 3(a-e) from TFA reaction products of naturally occurring phenols isolated from *Myristica malabarica* against different human cancer cell lines using SRB assay.

Samples	Anti-proliferative activity of TFA reaction products on different cancer cell lines using sulfo-rhodamine B (SRB) assay											
	HT-1376 Urinary bladder		HT-29 Colon		MDAT32 Thyroid		BDCM Leukemia		MCF-7 Breast		A2780 Ovarian	
	% Inhi.	IC_{50}±SE	% Inhi.	IC_{50}±SE	% Inhi.	IC_{50}±SE	% Inhi.	IC_{50}±SE	% Inhi.	IC_{50}±SE	% Inhi.	IC_{50}±SE
1	<50	-	**76.4**	**1.9 ± 0.5**	<50	-	**62.0**	**10.9 ±1.4**	<50	-	**3.9±0.1**	**3.9 ± 0.1**
2	<50	-	<50	-	<50	-	<50	-	<50	-	<50	-
3a	<50	-	<50	-	<50	-	<50	-	<50	-	<50	-
3b	<50	-	<50	-	<50	-	<50	-	<50	-	<50	-
3c	<50	-	<50	-	<50	-	<50	-	<50	-	-	-
3d	<50	-	<50	-	<50	-	<50	-	<50	-	<50	-
3e	<50	-	<50	-	<50	-	<50	-	<50	-	<50	-
Ester of **3(a-e)**	NT	-	NT	-	NT	-	NT	-	NT	-	NT	-
C14-acid	NT	-	NT	-	NT	-	NT	-	NT	-	NT	-
Paclitaxel	**-**	**13.17**	**-**	**0.051**		**0.69**		**0.028**		**0.028**		**0.037**

SUPPLIMENTARY INFORMATION

Supplementary information for this paper is available in ANNEXURE 1.

ACKNOWLEDGEMENTS

We express our sincere gratitude to Dr. David G. I. Kingston, Department of Chemistry, Virginia Tech, Blacksburg, Virginia 24061, USA to record ^{19}F NMR spectrum and for fostering to collaborate with Prof. Esperanza J. Carcache de Blanco, College of Pharmacy, The Ohio State University, Ohio, Columbus, USA. We acknowledge Dr. Dmitriy Uchenik, Dr. Deepa Krishnan, OSU College of Pharmacy instrumentation facility, for allowing acquisition of MS data and Mrs. Mamata V. Joshi for her excellent effort to acquire 2D-NMR data by using National Instrumental Facility, Tata Institute of Fundamental Research (TIFR) Centre, Colaba, Mumbai. Authors are very much grateful to Head of Division, Bio-Organic Division and Group Director of Bio-science Group for their continuous encouragement and ethical support.

AUTHOR CONTRIBUTION STATEMENT

AKB performed isolation, structural characterization, total experimental design, work and analyses and drafted manuscript. IC and ESA contributed anti-proliferative assay on different carcinoma cell lines. SF contributed analysis tools and analysed the XRD data of crystals of substrates used in trifluoro-acetyl reaction, structure analysis and computation. EJCB supervised biological experimental, analysed anti-proliferative assay data, performed final revision of the manuscript, and manage acquiring HRESI-MS and LR ESI-MS data with the assist of IC and ESA.

CONFLICT OF INTEREST

The authors declare that there is no conflict of interest regarding the publication of this article.

ADDITIONAL INFORMATION

For any information or query about this experiment, it is requested to contact in mail address abauri@rediffmail.com

COMPETING FINANCIAL INTEREST

The author declares no competing financial interest.

REFERENCES

1. R. Wolf. Process Research on the Preparation of 1-(3-Trimethylsilylphenyl)-2, 2, 2-trifluoroethanone by a Friedel-Crafts Acylation Reaction. *Organic Process Research Development*, 2008; 12: 23-29. https://doi.org/10.1021/op700199p

2. H. Maekawa, T. Ozaki, D. Zulkeflee, T. Murakami, S. Kihara, and I. Nishiguchi. Abnormal & Direct *para*-Trifluoro-acetylation of Branched Alkyl Phenyl Ketones by Magnesium-Promoted Reductive Aromatic Substitution. *Synlett.*, 2012; 23: 40-404. doi: 10.1055/s-0031-1290325
3. T. Furuya, A. S. Kamlet and T. Ritter. Catalysis for Fluorination and Trifluoromethylation. *Nature*, 2011; 473: 470-477. doi:10.1038/nature10108
4. H. Morimoto, T. Tsubogo, N. D. Litvinas and J. F. Hartwig. A Broadly Applicable Copper Reagent for Trifluoromethylations and Perfluoroalkylations of Aryl Iodides and Bromides. *Angew. Chem. Int. Ed.*, 2011; 50: 3793-3798. doi:10.1002/ange.201100633
5. M. Huiban, M. Tredwell, S. Mizuta, Z. Wan, X. Zhang, T. L. Collier, V. Gouverneur and J. Passchier. A broadly applicable [^{18}F] trifluoromethylation of the aryl and heteroaryl iodides for PET imaging. *Nature*, 2013; 5: 941-944. http://www.nature.com/naturechemistry
6. G. Shi, C. Shao, S. Pan, J. Yu and Y. Zhang. Silver-Catalyzed C-H Trifluoromethylation of Arenes Using Trifluoracetic acid as the Trifluoro methylating reagent. *Org. Lett.*, 2015; 17: 34-41. dx.doi.org/10.1021/ol503189j
7. J-J. Dai, C. Fang, B. Xiao, J. Yi, J. Xu, Z-J. Liu, X. Lu, L. Liu and Y. Fu. Copper Promoted Sandmeyer Trifluoromethylation Reaction. *J. Am. Chem. Soc.*, 2013; 135: 8436-8439. https://doi.org/10.1021/ja404217t
8. I. S. R. Stenhagen, A. K. Kirjavainen, S. J. Forsback, C. G. Jorgensen, E. G. Robins, S. K. Luthra, O. Solin and V. Gouverneur. [^{18}F] Fluorination of an aryl boronic ester using [^{18}F] selecfluor bis (triflate): application to 6-[^{18}F] fluoro-L-DOPA. *Chem. Com.*, 2013; 49: 1386-1388. doi: 10.1039/c2cc38646a
9. K. Muller, C. Faeh and F. Diederich. Fluorine in Pharmaceuticals: Looking beyond Institution. *Science*, 2007; 317: 1881-1886. https://doi.org/10.1126/science.1131943
10. P. Jeschke. The unique role of fluorine in the design of active ingredients for modern crop production. *Chem Bio Chem.*, 2004; 5: 570-589. https://doi.org/10.1002/cbic.200300833
11. Q. He, Y. Wang, I. Alfeazi and S. Sadeghi. Electrochemical Nucleophilic Synthesis of di-*tert*-butyl-(4-[^{18}F] fluoro-1,2-phenylene)-dicarbonate. *Applied Radiation and Isotopes*, 2014; 92: 52-57. https://doi.org/10.1016/j.apradiso.2014.06.013
12. E. Lee, A. S. Kamlet, D. C. Powers, C. N. Neumann, G. B. Boursalian, T. Furuya, D. C. Choi, J. M. Hooker and T. A Ritter. Fluoride-Derived Electrophilic Late-Stage Fluorination Reagent for PET Imaging. *Science*, 2011; 334: 639-641. doi: 10.1038/NCHEM.1756
13. M. Huiban, M. Tredwell, S. Mizuta, Z. Wan, X. Zhang, T. L. Collier, V. Gouverneur and J. Passchier. A broadly applicable [^{18}F] trifluoromethylation of the aryl and heteroaryl iodides for PET imaging. *Nature*, 2013; 5: 941-944. http://www.nature.com/doifinder/10.1038/nchem.1756
14. J. A. Ma, D. Cahard. Strategies for nucleophilic, electrophilic and radical trifluoromethylation. *J. Fluorine Chemistry*, 2007; 128: 975-996. https://doi.org/10.1016/j.jfluchem.2007.04.026
15. M. H. Hung, W. B. Farnham, A. E. Feiring and S. Rozen. Functional Fluoropolymers and Fluoropolymers 1: Synthesis (edited by G. Hougham, P. E. Cassidy, K. Johns and T. Davidson). 2002; chapter 4: 51-56. https://doi.org/10.1007/0-306-46918-9_4
16. K. K. Purushothaman, A. Sarada, J. D. Connolly, 'Malabaricones A-D, novel diarylnonanoids from *Myristica malabarica* Lam (*Myristicaceae*). *J. Chem. Soc., Perkin Trans. 1*, 1977; 587-588. https://doi.org/10.1039/P19770000587
17. B. S. Patro, A. K. Bauri, S. Mishra, S. Chattopadhyay. Anti-oxidant activity of *M. malabarica* Extracts and their constituents. *Agri. & Food Chem.*, 2005; 53: 6912-6918. doi: 10.1021/jf050861
18. A. Manna, P. Saha, A. Sarkar, D. Mukhopadhyay, A. K. Bauri, D. Kumar, P. Das S. Chattopadhyay, M. Chatterjee. Malabaricone-A Induces A redox Imbalance That Mediates Apoptosis in U937 Cell Line. *PLOS ONE*, 2012; 7: e36938. https://doi.org/10.1371/journal.pone.0036938
19. M. Tyagi, A. K. Bauri, B. S. Patro, S. Chattopadhyay, 'Mechanism of the malabaricone C induced toxicity to the MCF cell line. *Free Rad. Res.*, 2014; 48: 446-477. https://doi.org/10.3109/10715762.2014.886328
20. M. Tyagi, B. Maity, B. Saha, A. K. Bauri, M. Subramaniam, S. Chattopadhyay, B. Patro. The spice derived phenolic, malabaricone B induces mitochondrial damage in lung cancer (A549) cells via p53-independent pathway. *Food & Function*, 2018; *14:9*(11): 5715-5727. https://doi.org/10.1039/C8FO00624E
21. M. Tyagi, R. Bhattacharyya, A. K. Bauri, B. S. Patro, S. Chattopadhyay. DNA damage dependent activation of checkpoint kinase 1 and mitogen activated protein kinase p38 are required in malabaricone-C induced mitochondrial cell death. *Biochim. Biophys. Acta*, 2014; 1840: 1014-1027. https://doi.org/10.1016/j.bbagen.2013.11.020
22. M. Tyagi, A. K. Bauri, S. Chattopadhyay, B. S. Patro. Thiol anti-oxidants sensitize Malabaricone C induce cancer cell death via reprogramming redox p53 and NF-kB proteins in *vitro* and *vivo*. *Free Rad. Biol. Med.*, 2020; 148: 182-199. https://doi.org/10.1016/j.freeradbiomed.2020.01.011
23. A. K. Bauri, Y. Du, P. J. Brodie, S. Foro, D. G. I. Kingston. Anti-proliferative Acyl Phenol and Arylnonanoids from the Fruit Rind of *Myristica malabarica*. *Chem. & Biodiver.*, 2022; e202200343. https://doi.org/10.1002/cbdv.202200343

24. A. K. Bauri, I. C. Diomicio, E. S. Arellano, S. Foro and E. J. Carcache de Blanco. Study of anti-proliferative activity of phenols from the fruit rind of *Myristica malabarica. Eur. J. Biomed. Pharma. Sci.*, 2024; 11: 253-288. www.ejbps.com
25. A. K. Bauri, I. C. Diomicio, E. S. Arellano, S. Foro and E. J. Carcache de Blanco. Regio-selective bromination of phenols from Myristica malabarica and their anti-proliferative activity. *Eur. J. Biomed. Pharma. Sci*., 2024; 11: 158-187. www.ejbps.com
26. G. D. Anaya-Eugenio, C. Y. Tan, L. H. Rakotondraibe, E. J. Carcache de Blanco. Tumor suppressor p53 independent apoptosis in HT-29 cells by auransterol from *Penicillium aurantiacobrunneum*. *Biomed. Pharmacother*., 2020; 127: 110124. https://doi.org/10.1016/j.biopha.2020.110124
27. V. Vichai, K. Kirtikara. Sulfo-rhodamin B colorimetric assay for cytotoxicity screening. *Nat. Protoc*., 2006; 1: 1112-1116. doi: 10.1038/nprot.2006.179
28. G. D. Anaya-Eugenio, E. M. Addo, N. Ezzone, M. Henkin, T. N. Ninh, Y. Ren, D. D. Soejarto, A. D. Kinghorn, Car cache de Blanco. Caspase-dependent apoptosis in prostate cancer cells and zebrafish by corchorusoside C from *Streptocaulon juventas*. *J. Nat. Prod.*, 2019; 82: 1645-1655. https://doi.org/10.1021/acs.jnatprod.9b00140

ANNXURE
SUPPLIMENTARY INFORMATION
FOR AFORESAID MANUSCRIPT

Entry No.	Legendary tittle
Figure S1	^{1}H NMR spectrum (CD_3COCD_3, 200 MHz) of compound **1** (2, 4-dihydroxy trifluoro-acetophenone)
Figure S2	^{13}C NMR spectrum (CD_3COCD_3, 50 MHz) of compound **1** (2, 6-dihydroxy trifluoro-acetophenone)
Figure S3	^{19}F NMR spectrum ($CDCl_3$, 470 MHz) of compound **1** (2, 6-dihydroxy trifluoro-acetophenone
Figure S4	UV spectrum (MeOH) of compound **1** (2, 4-dihyroxy trifluoro-acetophenone)
Figure S5	IR spectrum (KBr) spectrum of compound **1** (2, 4-dihyroxy trifluoro-acetophenone)
Figure S6	EIMS of compound **1** (2, 4-dihyroxy trifluoro-acetophenone)
Figure S7	^{1}H NMR spectrum (CD_3COCD_3, 200 MHz) of compound **2** very trace amount (2, 6-dihydroxy trifluoro-acetophenone)
Figure S8	Expansion of ^{1}H NMR spectrum (CD_3COCD_3, 200 MHz) of compound **2** (2, 6-dihydroxy trifluoro-acetophenone)
Figure S9	^{13}C NMR spectrum (CD_3COCD_3, 50 MHz) of compound **2** (2, 6-dihydroxy trifluoro-acetophenone)
Figure S10	^{19}F NMR spectrum (CD_3COCD_3, 125 MHz) of compound **2** (2, 6-dihyroxy trifluoro-acetophenone)
Figure S11	UV spectrum (MeOH) of compound **1** (2, 4-dihyroxy trifluoro-acetophenone)
Figure S12	IR spectrum (KBr) spectrum of compound **2** (2, 6-dihyroxy trifluoro-acetophenone)
Figure S13	Mass spectrum of compound **2** (2, 4-dihyroxy trifluoro-acetophenone)
Figure S14	^{1}H NMR spectrum (CD_3COCD_3, 500 MHz) of compound **3a** (phenyl nonanoic acid)
Figure S15	^{1}H NMR spectrum (CD_3COCD_3, 500 MHz) of compound **3a** (phenyl nonanoic acid)
Figure S16	^{13}C NMR spectrum ($CDCl_3$, 500 MHz) of compound **3a** (phenyl nonanoic acid)
Figure S17	IR spectrum (KBr) spectrum of compound **3a** (phenyl nonanoic acid)
Figure S18	UV spectrum (MeOH) of compound **3a** (phenyl nonanoic acid)
Figure S19	Mass spectrum of compound **3a** (phenyl nonanoic acid)
Figure S20	^{1}H NMR spectrum (CD_3COCD_3, 500 MHz) of compound **3b** [9(3-hydroxy phenyl) nonanoic acid)
Figure S21	^{13}C NMR spectrum (CD_3COCD_3, 50 MHz) of compound **3b** [9(3-hydroxy phenyl) nonanoic acid]
Figure S22	UV spectrum (MeOH) of compound **3b** [9(3-hydroxy phenyl) nonanoic acid]
Figure S23	IR spectrum (KBr) spectrum of compound **3b** [9(3-hydroxy phenyl) nonanoic acid]
Figure S24	EIMS spectrum of compound **3b** [9(3-hydroxy phenyl) nonanoic acid]
Figure S25	^{1}H NMR spectrum ($CDCl_3$, 50 MHz) methyl ester of compound **3b** [9(3-hydroxy phenyl) nonanoic acid]
Figure S26	UV spectrum (MeOH) methyl ester of compound **3b** [9(3-hydroxy phenyl) nonanoic acid]
Figure S27	IR spectrum (KBr) spectrum of methyl ester of compound **3b** [9(3-hydroxy phenyl) nonanoic acid]
Figure S28	EIMS spectrum of compound **3b** [9 (3-hydroxy phenyl) nonanoic acid]
Figure S29	^{1}H NMR spectrum ($CDCl_3$, 500 MHz) of compound **3c** [9(3, 4-dihydoxy phenyl) nonanoic acid]
Figure S30	Expansion of ^{1}H NMR spectrum (CD_3COCD_3, 500 MHz) of compound **3c** [9(3, 4-dihydroxy phenyl) nonanoic acid]
Figure S31	Expansion of ^{1}H NMR spectrum (CD_3COCD_3, 500 MHz) of compound **3c** [9(3, 4-dihydoxy phenyl) nonanoic acid]
Figure S32	^{13}C NMR spectrum (CD_3COCD_3, 125 MHz) of compound **3c** [9(3, 4-dihydoxy phenyl) nonanoic acid]
Figure S33	UV spectrum (MeOH) of methyl ester of compound **3c** [9(3, 4-dihydroxy phenyl) nonanoic acid]
Figure S34	UV spectrum (in MeOH) methyl ester of compound **3c** [9(3, 4-dihydroxy phenyl) nonanoic acid]
Figure S35	EIMS of methyl ester of compound **3c** [9(3, 4-dihydroxy phenyl) nonanoic acid]
Figure S36	^{1}H NMR spectrum of methyl ester of compound **3c** [9 (3, 4-dihydroxy phenyl) nonanoic acid]
Figure S37	UV MeOH) spectrum of methyl ester of compound **3c** [9(3, 4-dihydroxy phenyl) nonanoic]

Figure S38	IR spectrum (KBr) of methyl ester of compound **3c** [9(3, 4-dihydroxy phenyl) nonanoic acid]
Figure S39	^{1}H NMR spectrum (CD_3COCD_3, 500 MHz) of compound **3d** [9(3, 4-dihydroxy phenyl) nonanoic acid]
Figure S40	^{13}C NMR spectrum (CD_3COCD_3, 50 MHz) of compound **3d** [9(3, 4-dihydroxy phenyl) nonanoic acid]
Figure S41	UV spectrum (MeOH) of methyl ester of compound **3e** [9(3, 4-dihydroxy phenyl) nonanoic acid]
Figure S42	^{1}H NMR spectrum of compound **3e** (nonanoic acid)
Figure S43	EIMS spectrum of methyl ester of compound **3d** [9(3, 4-dihydroxy phenyl) nonanoic acid]
Figure S44	^{13}C NMR ($CDCl_3$, 50 MHz) spectrum of compound **3e** (nonanoic acid)
Figure S45	^{1}H NMR spectrum (CD_3COCD_3, 500 MHz) of malabaricone D cleaved with TFA acid
Figure S46	^{1}H NMR spectrum (CD_3COCD_3, 500 MHz) of malabaricone D cleaved with TFA acid
Figure S47	^{1}H NMR spectrum (CD_3COCD_3, 500 MHz) of malabaricone C cleaved with TFA acid
Figure S48	^{1}H NMR spectrum of methyl ester of compound **3e** (nonanoic acid)
Figure S49	^{13}C NMR ($CDCl_3$, 50 MHz) spectrum of compound **3e** (nonanoic acid)
Figure S50	UV spectrum (MeOH) of compound **3e** (nonanoic acid)
Figure S5	IR spectrum (KBr) of compound **3e** (nonanoic acid
Figure S52	EIMS spectrum of methyl ester of compound **3e** (nonanoic acid)
Figure S53	^{1}H NMR spectrum (CD_3COCD_3, 500 MHz) of malabaricone B and its crude TFA reaction products
Figure S54	Stacking plot of ^{1}H NMR spectra of malabaricone B ($CDCl_3$, 500 MHz) and its TFA reaction products in crude form (CD_3COCD_3, 500 MHz)
Figure S55	Expansion of stacking plot of ^{1}H NMR spectra of malabaricone B ($CDCl_3$, 500 MHz) and its TFA reaction products in crude form (CD_3COCD_3, 500 MHz)
Figure S56	Expansion of stacking plot of ^{1}H NMR spectra of malabaricone B ($CDCl_3$, 500 MHz) and its TFA reaction products in crude form (CD_3COCD_3, 500 MHz)
Figure S57	Expansion of stacking plot of ^{1}H NMR spectra of malabaricone B ($CDCl_3$, 125 MHz) and its TFA reaction products (CD_3COCD_3, 125 MHz)
Figure S58	Expansion of stacking plot of ^{1}H NMR spectra of malabaricone B ($CDCl_3$, 125 MHz) and its TFA reaction products (CD_3COCD_3, 125 MHz)
Figure S59	Stacking plot of ^{1}H NMR spectra of malabaricone B ($CDCl_3$, 500 MHz) and its TFA reaction products in crude form (CD_3COCD_3, 500 MHz)
Figure S60	Expansion ^{1}H NMR stacking plot of malabaricone C ($CDCl_3$, 500 MHz) and its crude TFA reaction products (CD_3COCD_3, 500 MHz)
Figure S61	Expansion ^{1}H NMR stacking plot of malabaricone C ($CDCl_3$, 500 MHz) and its crude TFA reaction products (CD_3COCD_3, 500 MHz)
Figure S62	^{1}H NMR spectra of stacking plot of malabaricone D ($CDCl_3$, 500 MHz) and its crude TFA reaction products (CD_3COCD_3, 500 MHz)
Figure S63	Expansion of ^{1}H NMR spectra of stacking plot of malabaricone D ($CDCl_3$, 500 MHz) and its crude TFA reaction products (CD_3COCD_3, 500 MHz)
Figure S64	Expansion of ^{1}H NMR spectra of stacking plot of malabaricone D ($CDCl_3$, 500 MHz) and its crude TFA reaction products (CD_3COCD_3, 500 MHz)
Figure S65	Stacking plot ^{1}H NMR spectra of crude TFA reaction products of malabaricone D (CD_3COCD_3, 500 MHz) and malabaricone D ($CDCl_3$, 500 MHz)
Figure S66	Expansion stacking plot ^{1}H NMR spectra of crude TFA reaction products of malabaricone D (CD_3COCD_3, 500 MHz) and malabaricone D ($CDCl_3$, 500 MHz)
Figure S67	Expansion of stacking plot ^{1}H NMR spectra of crude TFA reaction products of malabaricone D (CD_3COCD_3, 500 MHz) and malabaricone D ($CDCl_3$, 500 MHz)
Figure S68	Stacking plot of ^{1}H NMR spectrum of acyl phenol (CD_3COCD_3, 500 MHz) and its crude TFA reaction products (CD_3COCD_3, 500 MHz)
Figure S69	Expansion stacking plot of ^{1}H NMR spectrum of acyl phenol (CD_3COCD_3, 500 MHz) and its crude TFA reaction products (CD_3COCD_3, 500 MHz)
Figure S70	Stacking plot of ^{13}C NMR spectrum of acyl phenol (CD_3COCD_3, 125 MHz) and its crude TFA reaction products (CD_3COCD_3, 125 MHz)
Figure S71	Expansion of stacking plot of ^{13}C NMR spectrum of acyl phenol (CD_3COCD_3, 125 MHz) and its crude TFA reaction products (CD_3COCD_3, 125 MHz)
Figure S72	Expansion of stacking plot of ^{13}C NMR spectrum of acyl phenol (CD_3COCD_3, 125 MHz) and its crude TFA reaction products (CD_3COCD_3, 125 MHz)
Figure S73	^{13}C NMR spectrum ($CDCl_3$, 125 MHz) of crude TFA reaction products of acyl phenol
Figure S74	Expansion of ^{13}C NMR spectrum ($CDCl_3$, 125 MHz) of crude TFA reaction products of acyl phenol
Figure S75	Expansion of ^{13}C NMR spectrum ($CDCl_3$, 125 MHz) of crude TFA reaction products of acyl phenol
Figure S76	^{1}H NMR spectrum ($CDCl_3$, 500 MHz) of crude TFA reaction products of acyl phenol

Figure S77	Expansion of ^{1}H NMR spectrum ($CDCl_3$, 500 MHz) of crude TFA reaction products of acyl phenol
Figure S78	Expansion of ^{1}H NMR spectrum ($CDCl_3$, 500 MHz) of crude TFA reaction products of acyl phenol
Figure S79	^{1}H NMR spectrum ($CDCl_3$, 500 MHz) of crude TFA reaction product of acyl phenol
Figure S80	^{13}C NMR spectrum ($CDCl_3$, 125 MHz) of crude TFA reaction product of acyl phenol
Figure S81	Expansion of ^{13}C NMR spectrum ($CDCl_3$, 125 MHz) of crude TFA reaction product of acyl phenol
Figure S82	^{1}H NMR spectrum ($CDCl_3$, 125 MHz) of crude TFA reaction product of acyl phenol
Figure S83	Expansion of ^{1}H NMR spectrum (CD_3COCD_3, 500 MHz) of crude TFA reaction products of malabaricone C
Figure S84	^{13}C NMR spectrum (CD_3COCD_3, 125 MHz) of 9(4-hydroxy phenyl) nonanoic acid
Figure S85	^{1}H NMR spectrum ($CDCl_3$, 500 MHz) of crude TFA reaction products of malabaricone C
Figure S86	Expansion of ^{1}H NMR spectrum (CD_3COCD_3, 500 MHz) of crude TFA reaction products of malabaricone C
Figure S87	Expansion of ^{1}H NMR spectrum (CD_3COCD_3, 500 MHz) of crude TFA reaction products of malabaricone C
Figure S88	Expansion of ^{1}H NMR spectrum (CD_3COCD_3, 500 MHz) of crude TFA reaction products of malabaricone C
Figure S89	Stacking plot of ^{1}H NMR spectrum (CD_3COCD_3, 500 MHz) of malabaricone C and its crude TFA reaction products
Figure S90	Expansion of stacking plot of ^{1}H NMR spectrum (CD_3COCD_3, 500 MHz) of malabaricone C and its crude TFA reaction products
Figure S91	Expansion of stacking plot of ^{1}H NMR spectrum (CD_3COCD_3, 500 MHz) of malabaricone C and its crude TFA reaction products
Figure S92	Stacking plot of ^{1}H NMR spectra ($CDCl_3$, 500 MHz) of malabaricone B and its TFA reaction products (CD_3COCD_3, 500 MHz)
Figure S93	Expansion of stacking plot of ^{1}H NMR spectra ($CDCl_3$, 500 MHz) of malabaricone B and its TFA reaction products (CD_3COCD_3, 500 MHz)
Figure S94	Expansion of stacking plot of ^{1}H NMR spectra ($CDCl_3$, 500 MHz) of malabaricone B and its TFA reaction products (CD_3COCD_3, 500 MHz)
Figure S95	Stacking plot of ^{1}H NMR spectra ($CDCl_3$, 500 MHz) of malabaricone C and its TFA reaction products (CD_3COCD_3, 500 MHz)
Figure S96	Expansion of stacking plot of ^{1}H NMR spectra ($CDCl_3$, 500 MHz) of malabaricone C and its TFA reaction products (CD_3COCD_3, 500 MHz)
Figure S97	Expansion of stacking plot of ^{1}H NMR spectra ($CDCl_3$, 500 MHz) of malabaricone C and its TFA reaction products (CD_3COCD_3, 500 MHz)
Figure S98	Stacking plot of ^{1}H NMR spectra ($CDCl_3$, 500 MHz) of malabaricone D and its TFA reaction products (CD_3COCD_3, 500 MHz)
Figure S99	Expansion of stacking plot of ^{1}H NMR spectra ($CDCl_3$, 500 MHz) of malabaricone D and its TFA reaction products (CD_3COCD_3, 500 MHz)
Figure S100	Graphical abstract

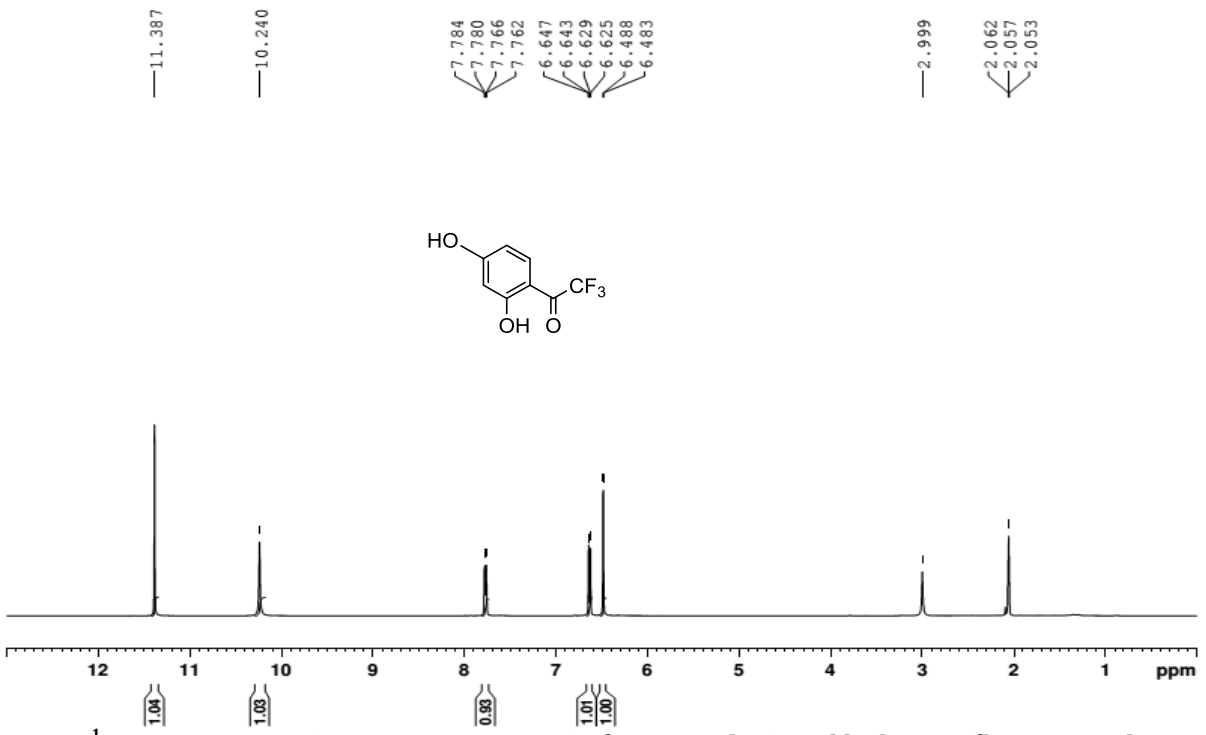

Figure S1: ^{1}H NMR spectrum (CD_3COCD_3, 200 MHz) of compound 1 (2, 4-dihydroxy trifluoro-acetophenone).

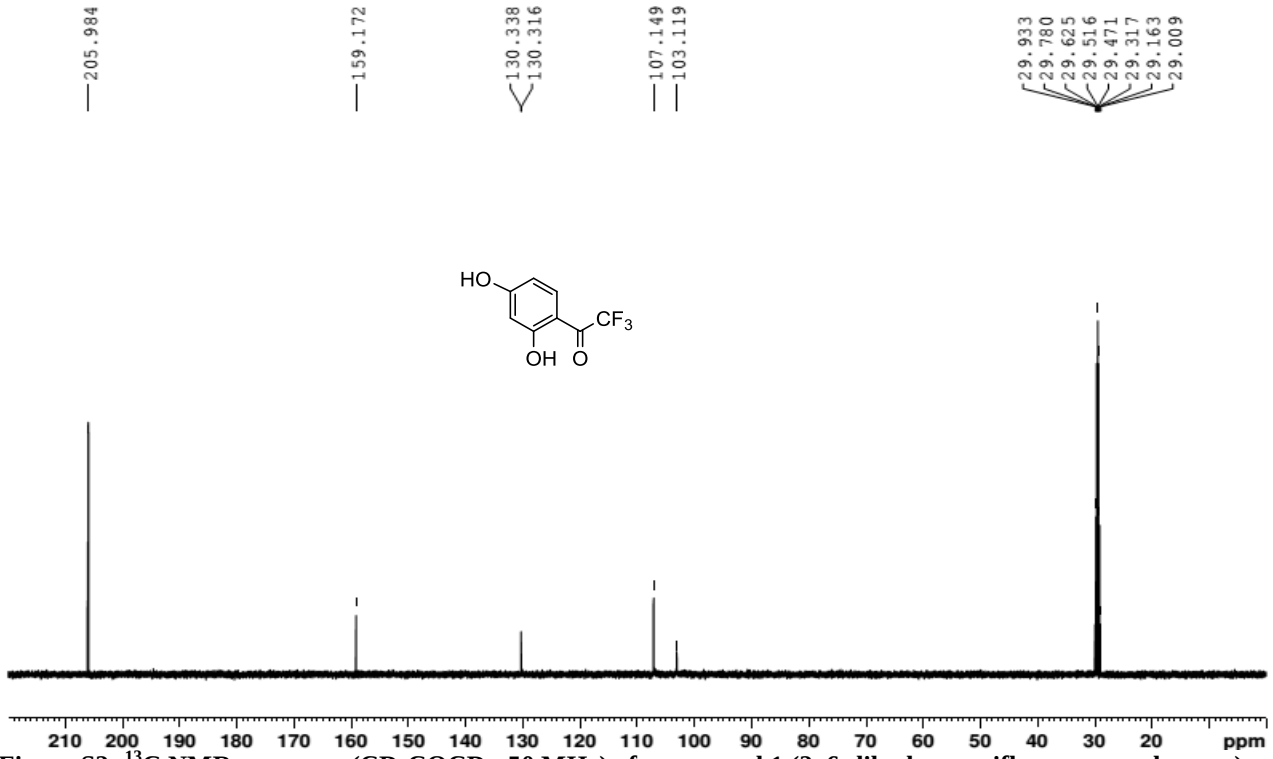

Figure S2: ^{13}C NMR spectrum (CD_3COCD_3, 50 MHz) of compound 1 (2, 6-dihydroxy trifluoro-acetophenone).

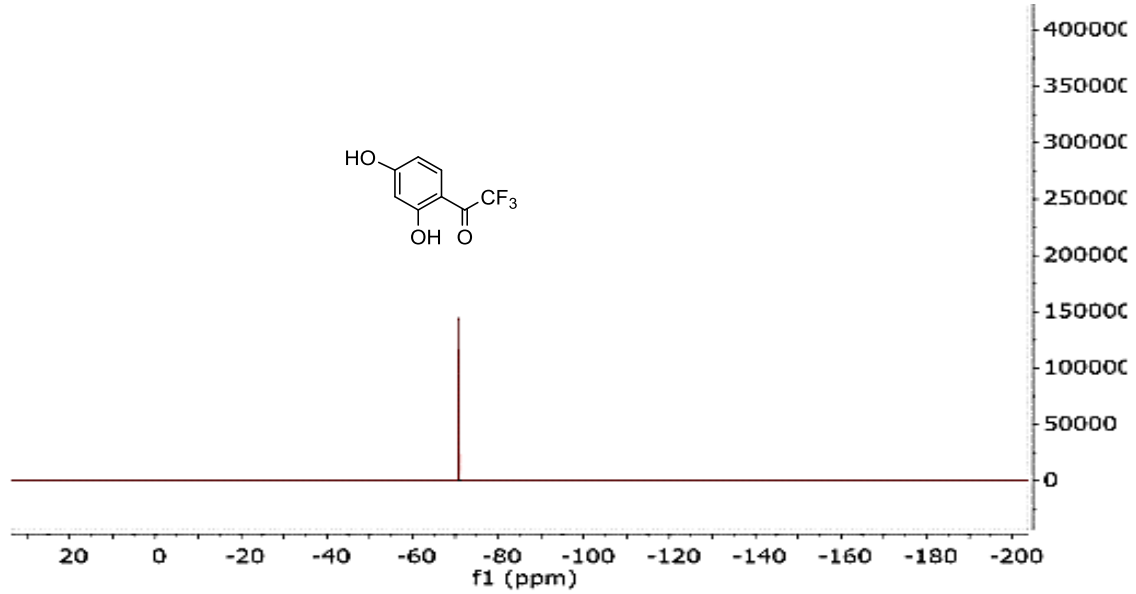

Figure S3: ^{19}F NMR spectrum ($CDCl_3$, 470 MHz) of compound 1 (2, 6-dihydroxy trifluoro-acetophenone.

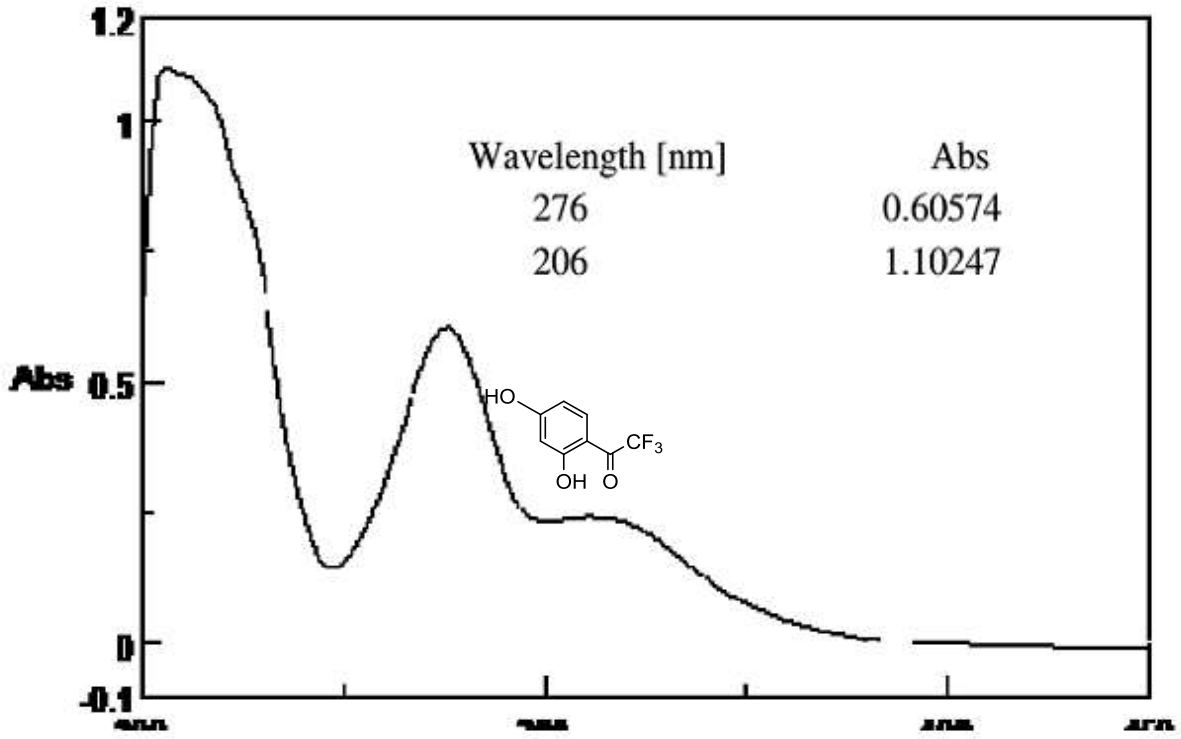

Figure S4: UV spectrum (MeOH) of compound 1 (2, 4-dihyroxy trifluoro-acetophenone).

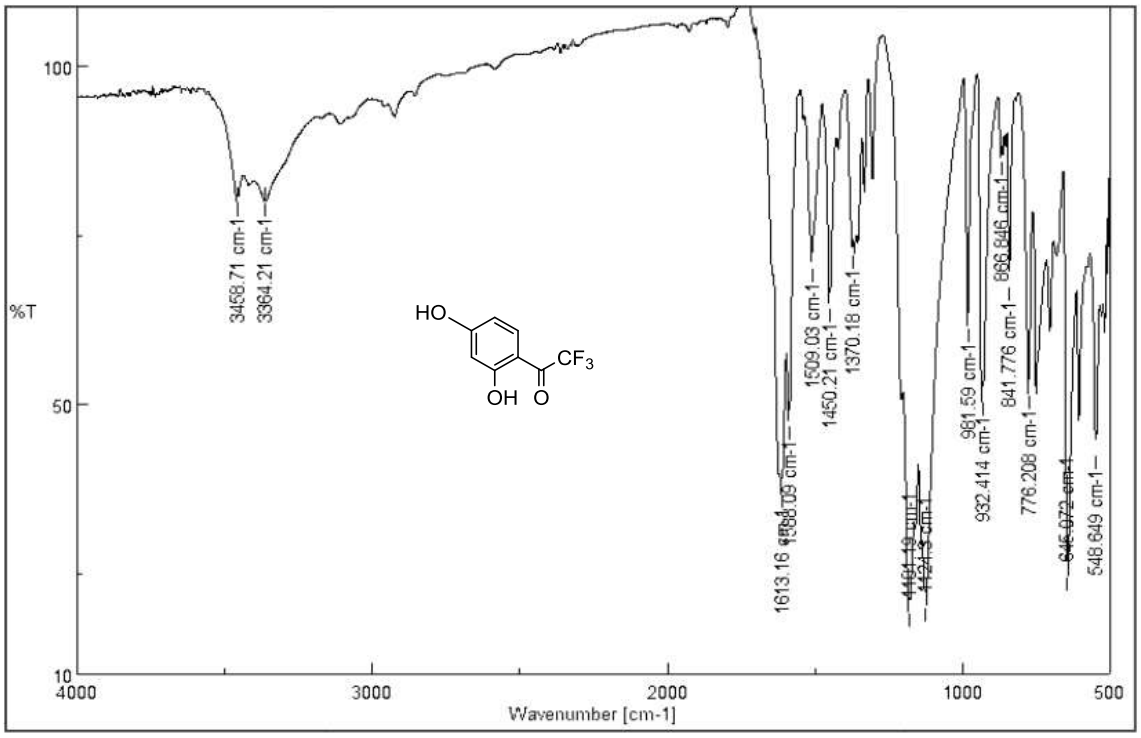

Figure S5: IR spectrum (KBr) spectrum of compound 1 (2, 4-dihyroxy trifluoro-acetophenone).

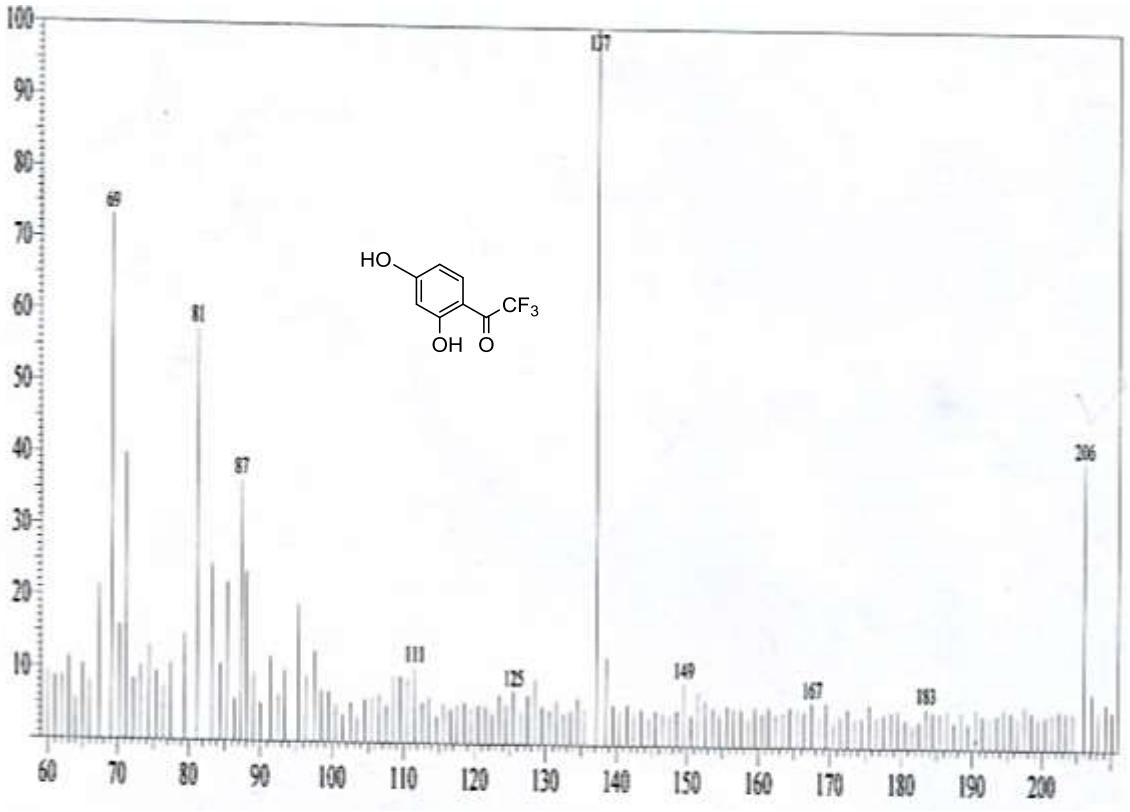

Figure S6: EIMS of compound 1 (2, 4-dihyroxy trifluoro-acetophenone).

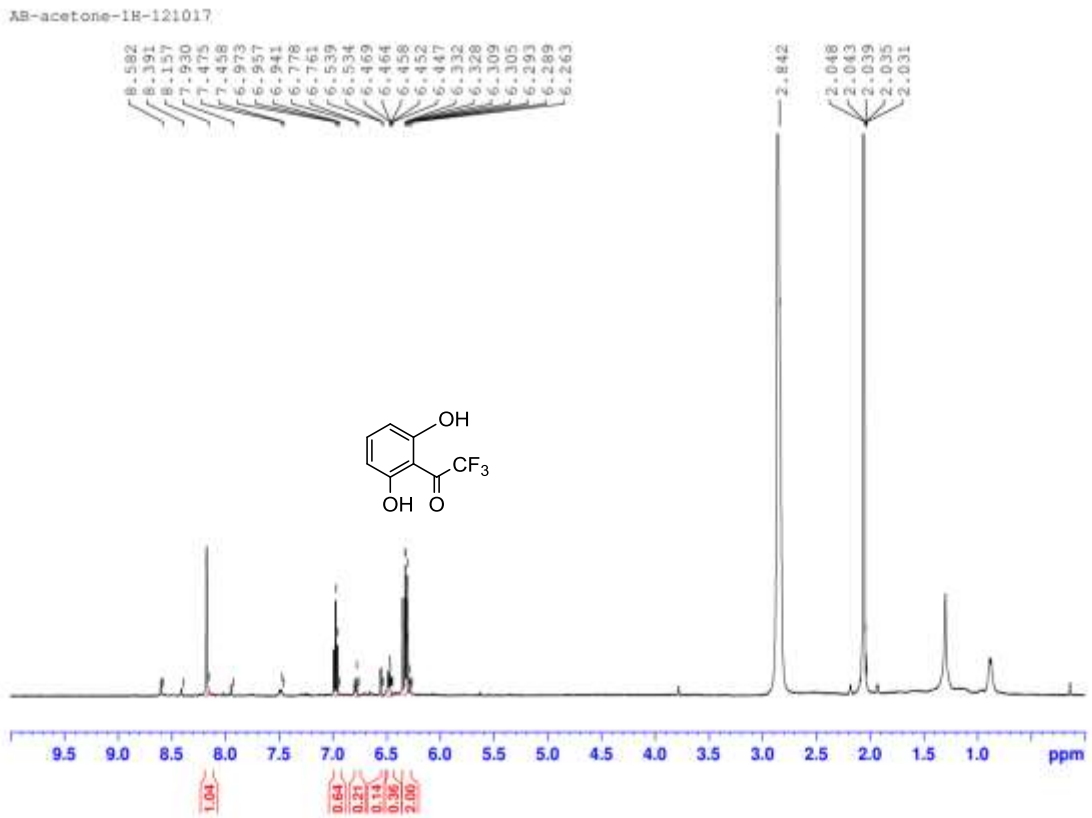

Figure S7: ^{1}H NMR spectrum (CD_3COCD_3, 200 MHz) of compound 2 very trace amount (2, 6-dihydroxy trifluoro-acetophenone).

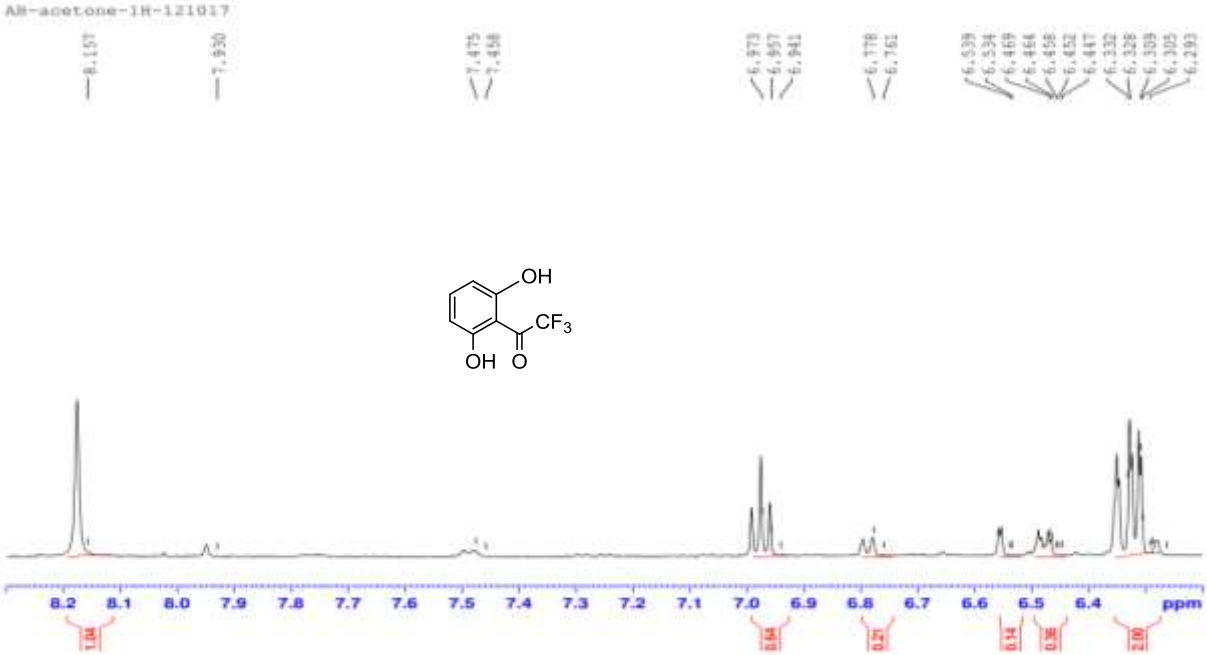

Figure S8: Expansion of ^{1}H NMR spectrum (CD_3COCD_3, 200 MHz) of compound 2 (2, 6-dihydroxy trifluoro-acetophenone).

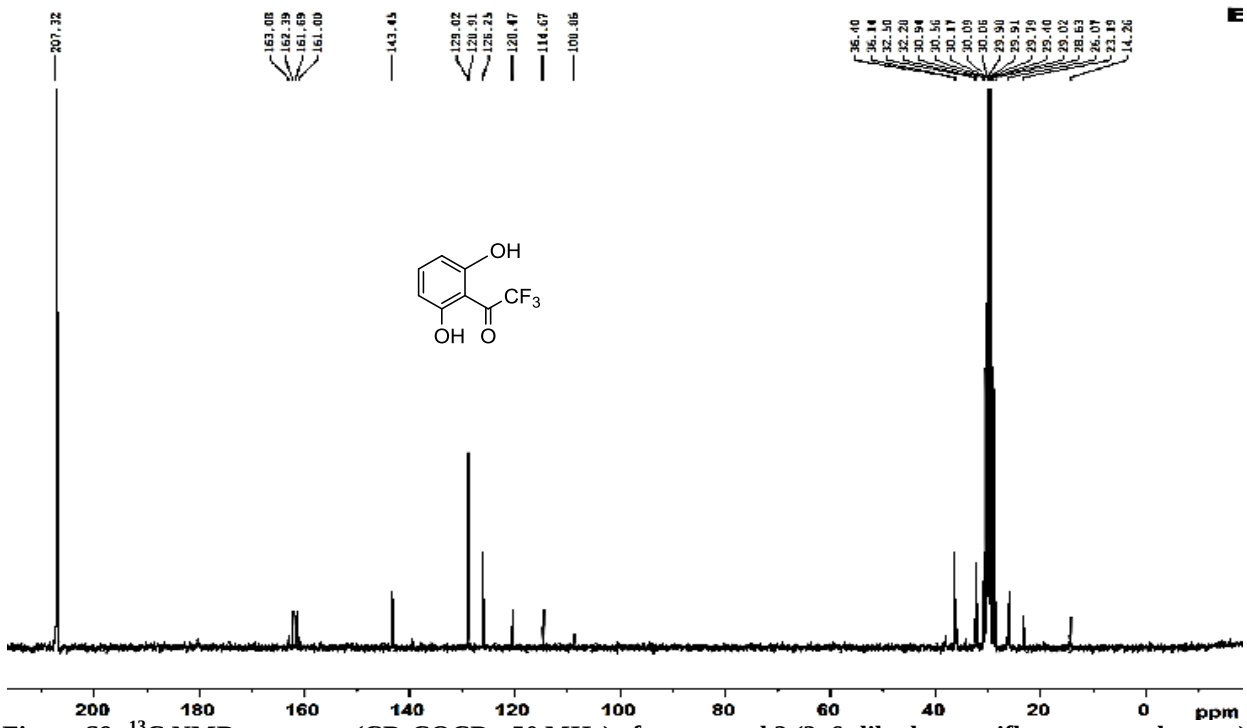

Figure S9: ^{13}C NMR spectrum (CD_3COCD_3, 50 MHz) of compound 2 (2, 6-dihydroxy trifluoro-acetophenone)

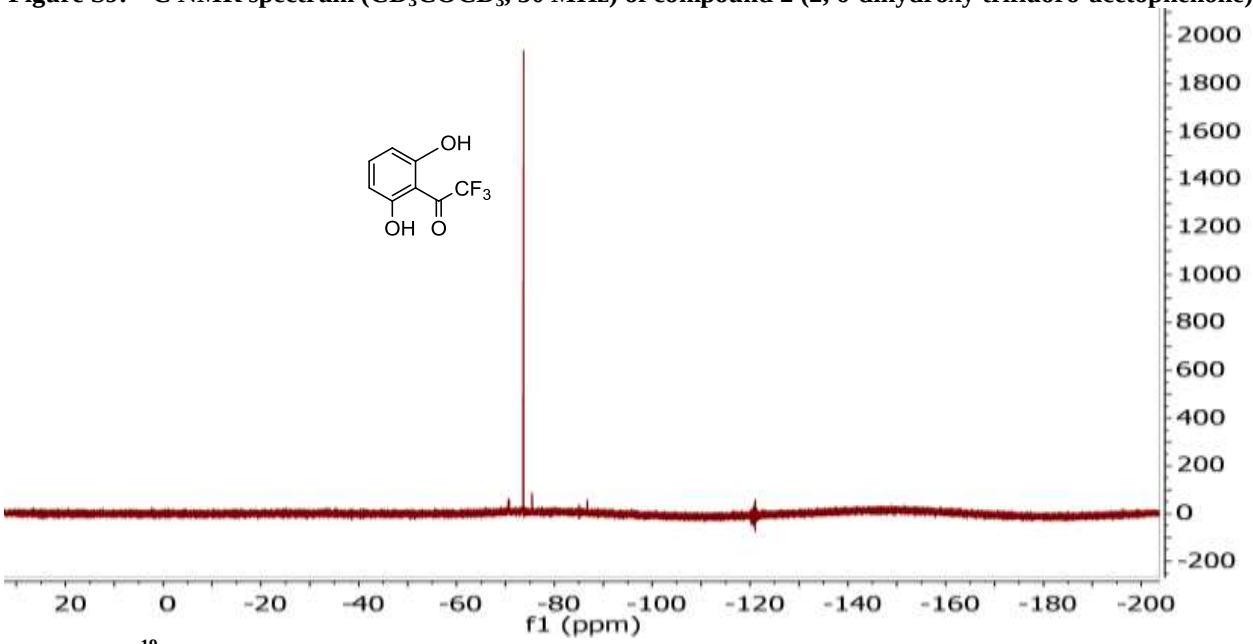

Figure S10: ^{19}F NMR spectrum (CD_3COCD_3, 125 MHz) of compound 2 (2, 6-dihyroxy trifluoro-acetophenone).

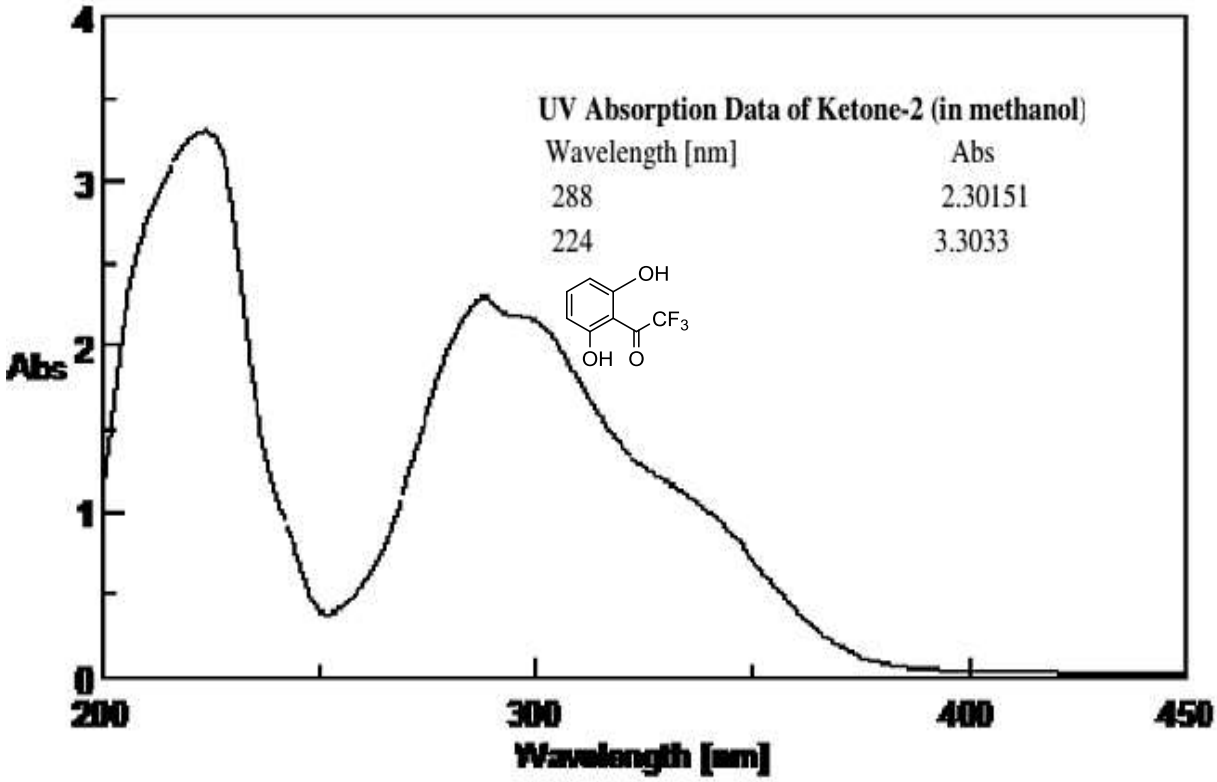

Figure S11: UV spectrum (MeOH) of compound 1 (2, 4-dihyroxy trifluoro-acetophenone).

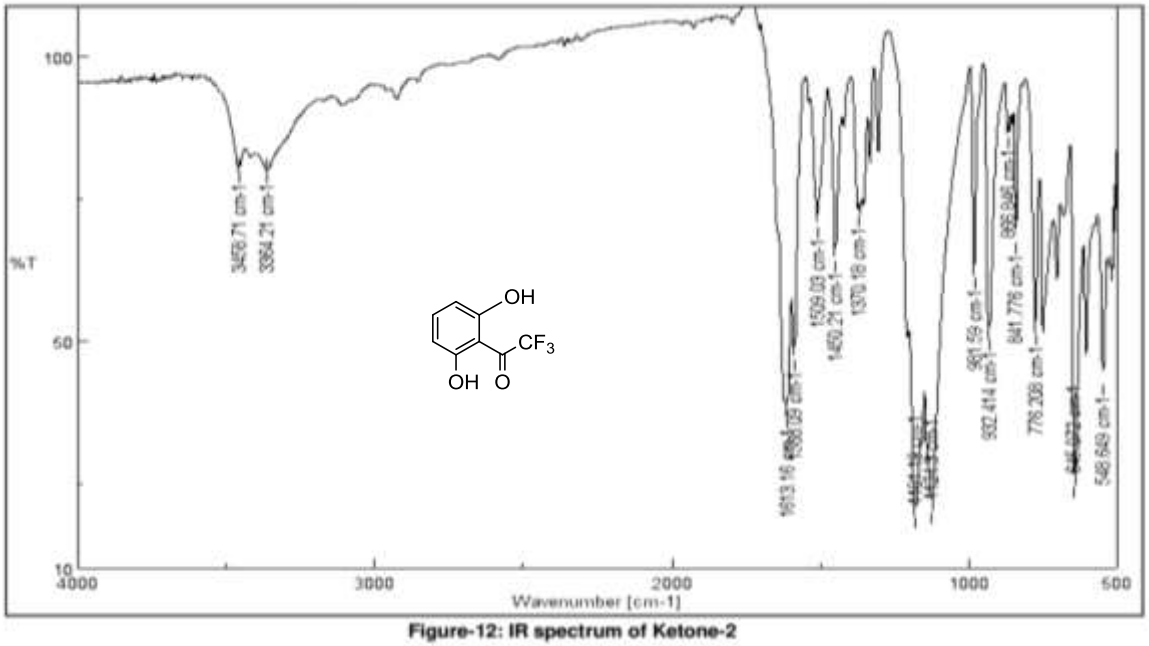

Figure-12: IR spectrum of Ketone-2

Figure S12: IR spectrum (KBr) spectrum of compound 2 (2, 6-dihyroxy trifluoro-acetophenone).

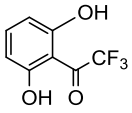

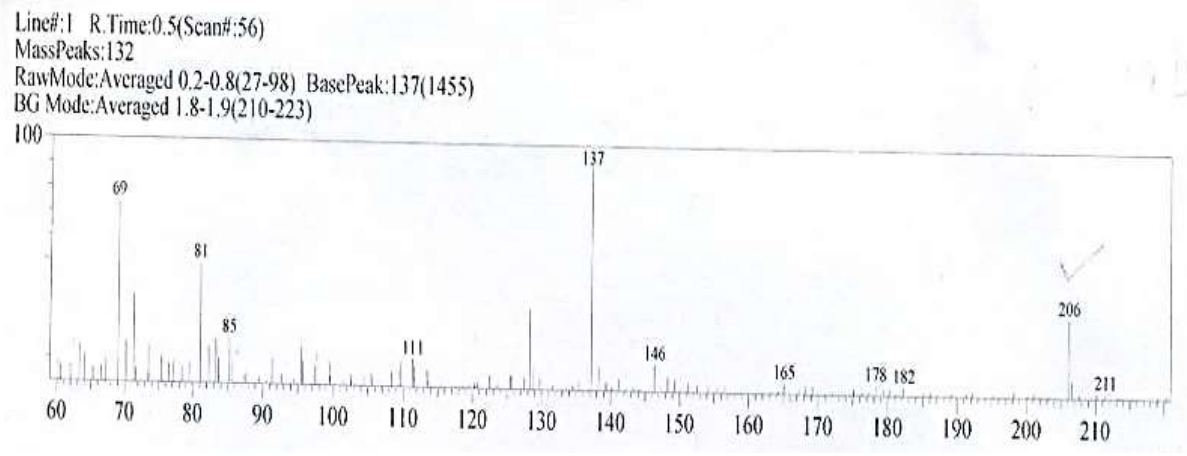

Figure S13: Mass spectrum of compound 2 (2, 4-dihyroxy trifluoro-acetophenone).

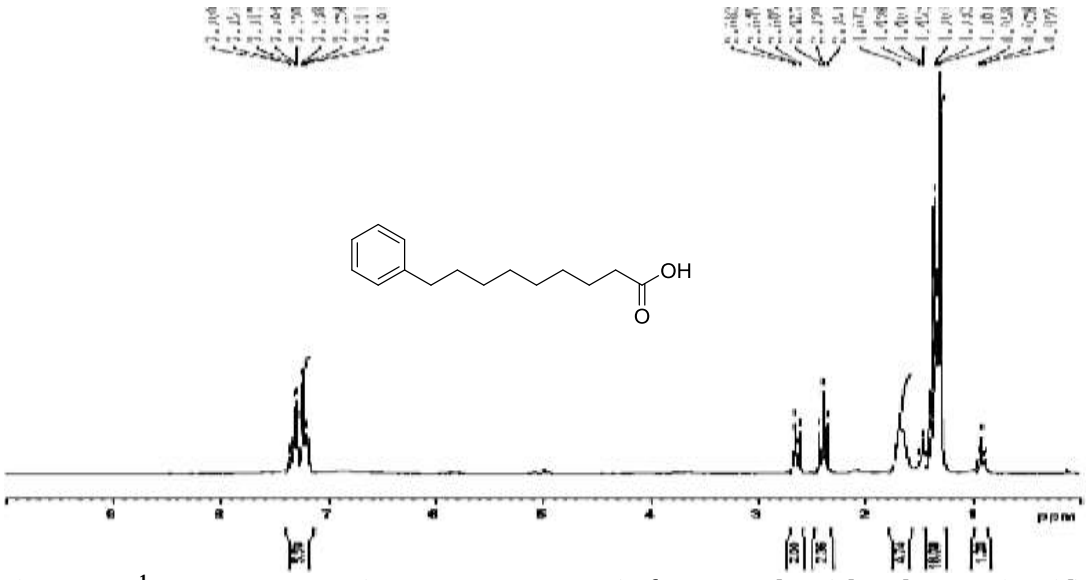

Figure S14: ^{1}H NMR spectrum (CD_3COCD_3, 500 MHz) of compound 3a (phenyl nonanoic acid).

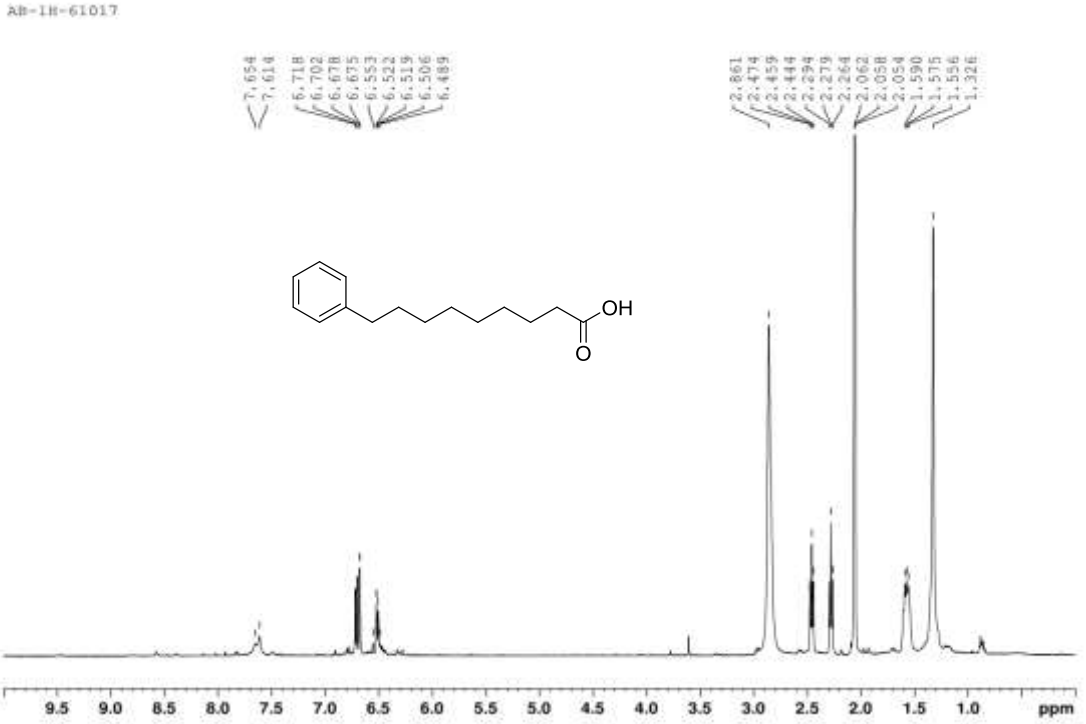

Figure S15: ^{1}H NMR spectrum (CD_3COCD_3, 500 MHz) of compound 3a (phenyl nonanoic acid).

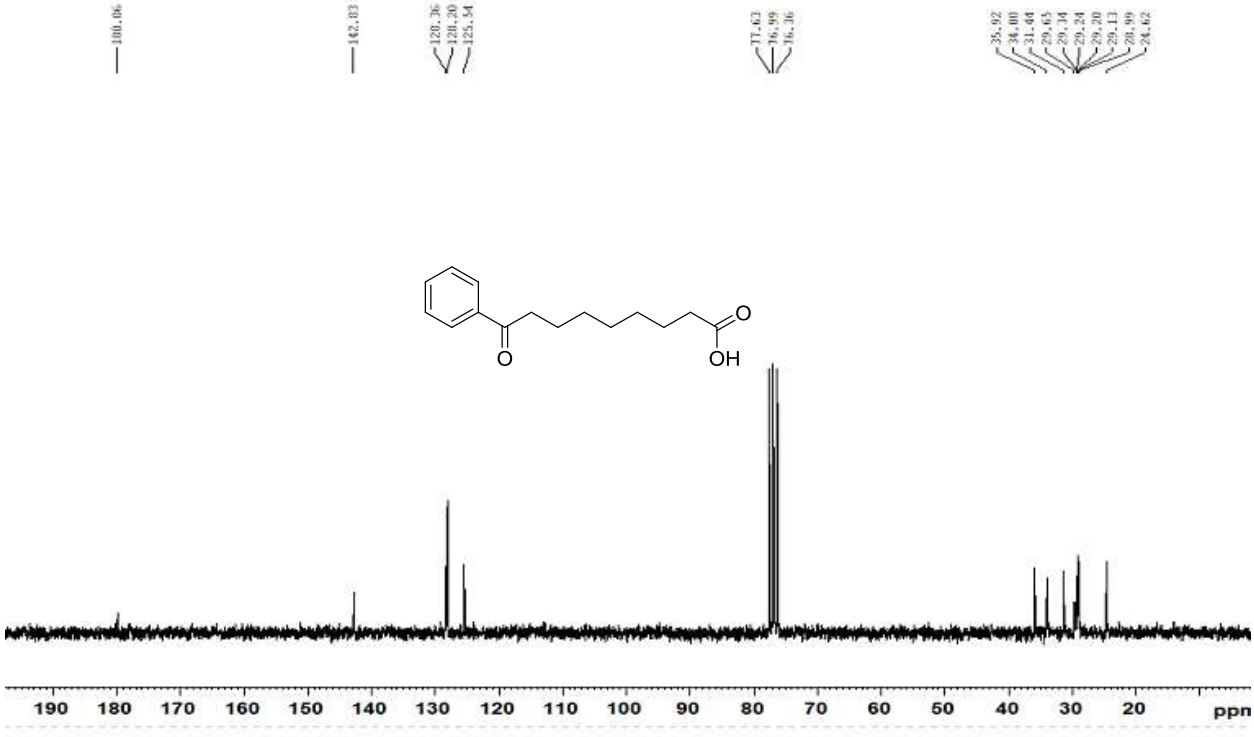

Figure S16: ^{13}C NMR spectrum ($CDCl_3$, 500 MHz) of compound 3a (phenyl nonanoic acid).

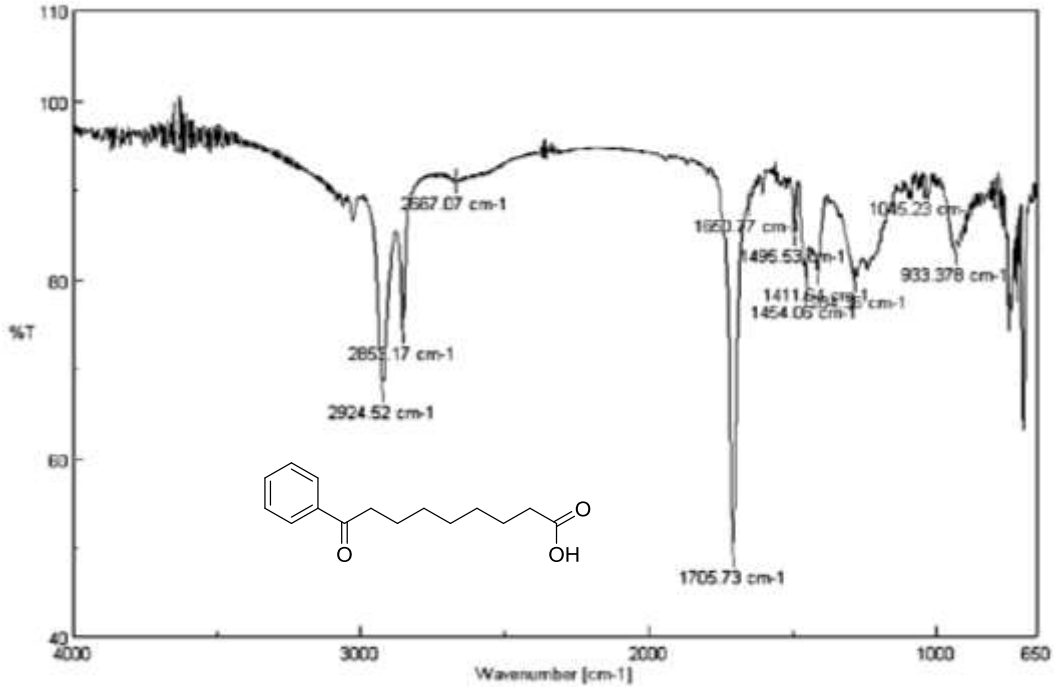

Figure S17: IR spectrum (KBr) spectrum of compound 3a (phenyl nonanoic acid).

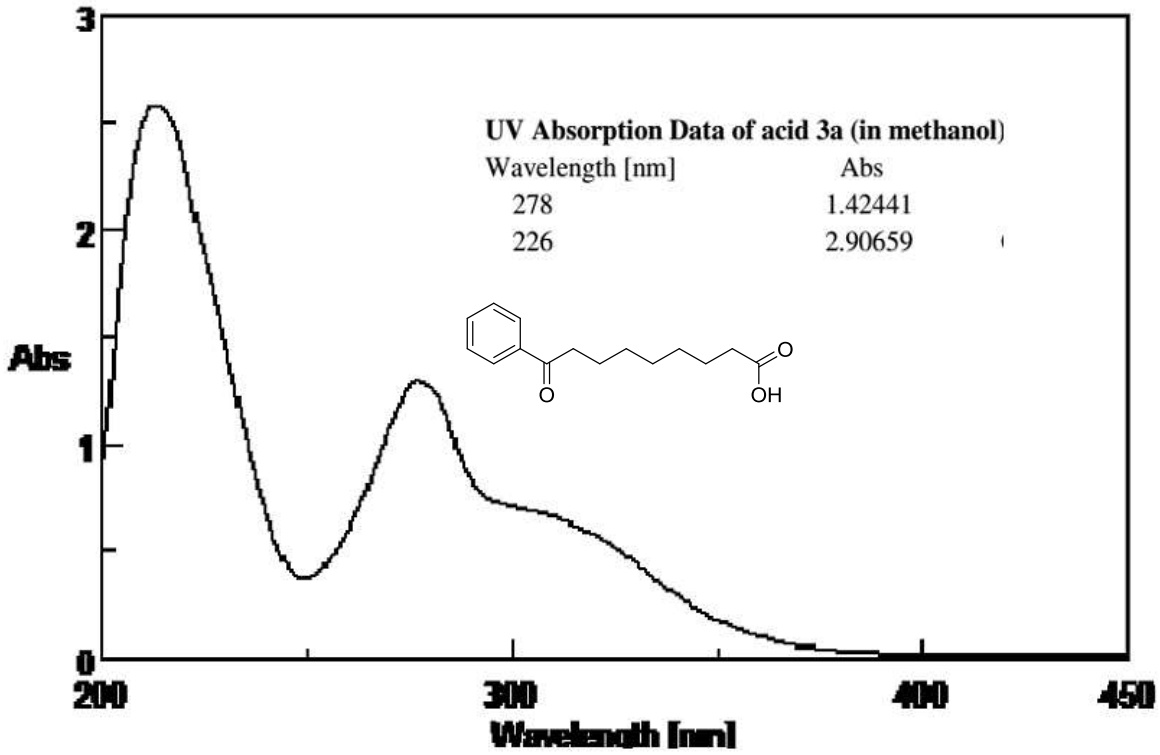

Figure S18: UV spectrum (MeOH) of compound 3a (phenyl nonanoic acid).

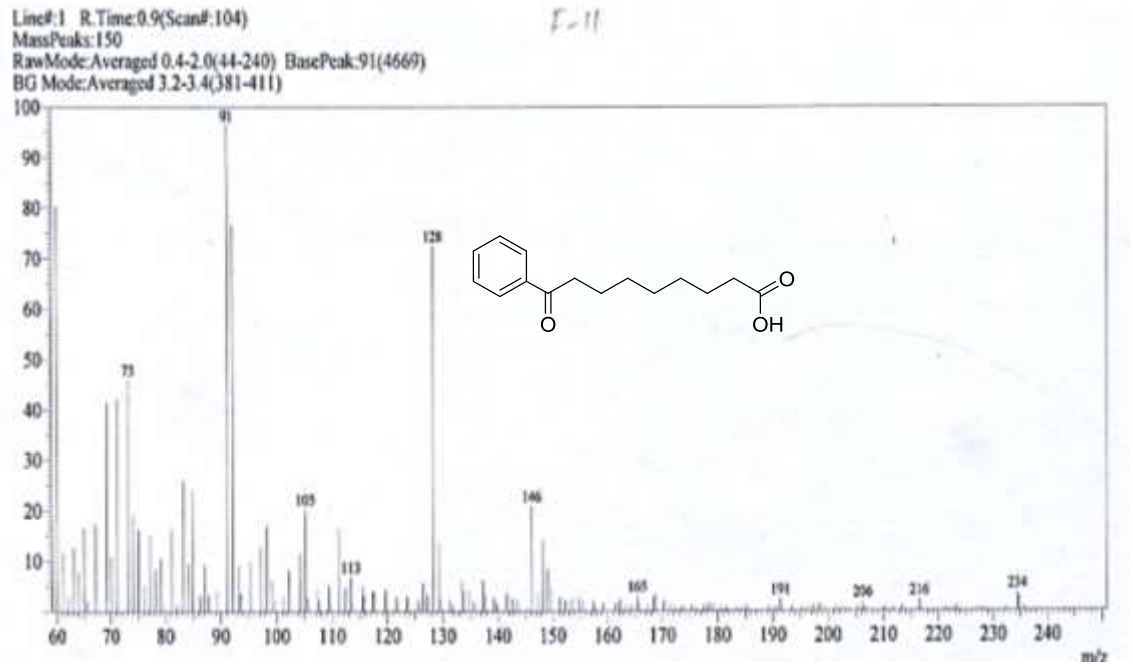

Figure S19: Mass spectrum of compound 3a (phenyl nonanoic acid).

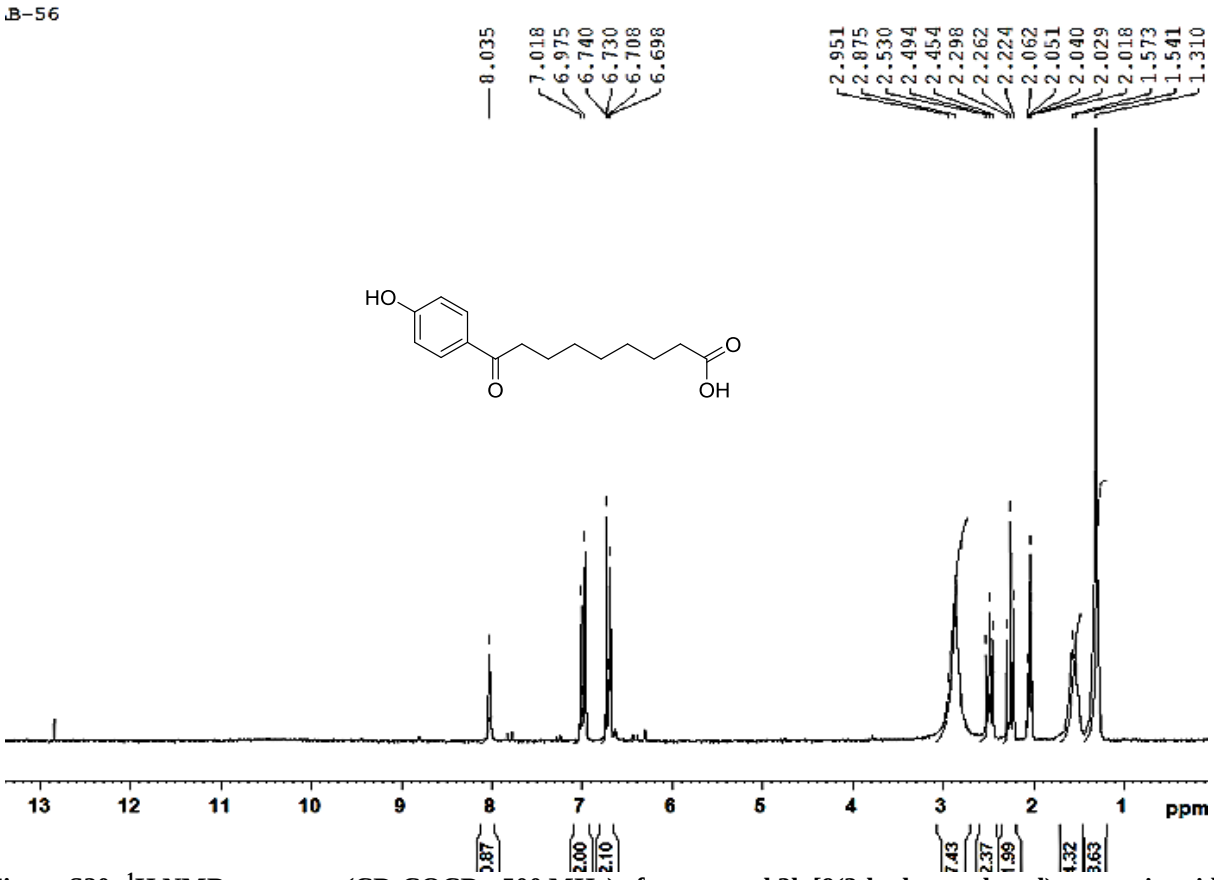

Figure S20: ^{1}H NMR spectrum (CD_3COCD_3, 500 MHz) of compound 3b [9(3-hydroxy phenyl) nonanoic acid]

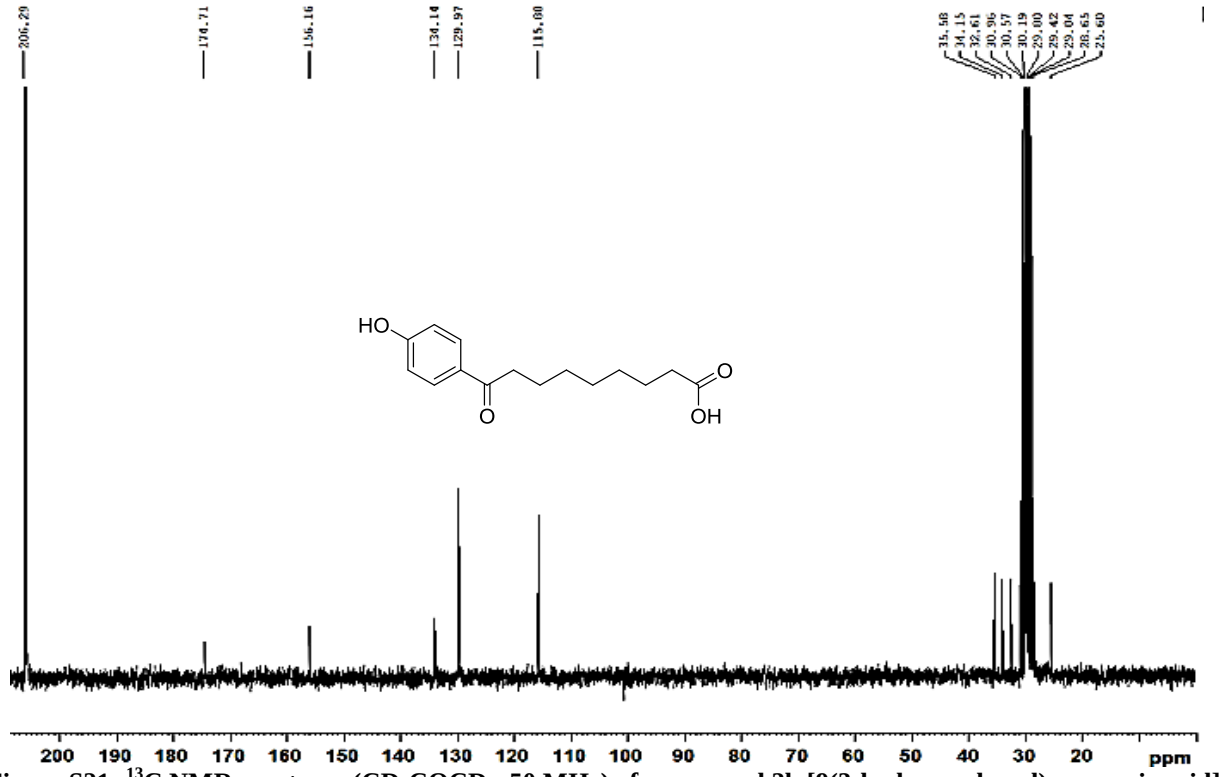

Figure S21: ^{13}C NMR spectrum (CD_3COCD_3, 50 MHz) of compound 3b [9(3-hydroxy phenyl) nonanoic acid].

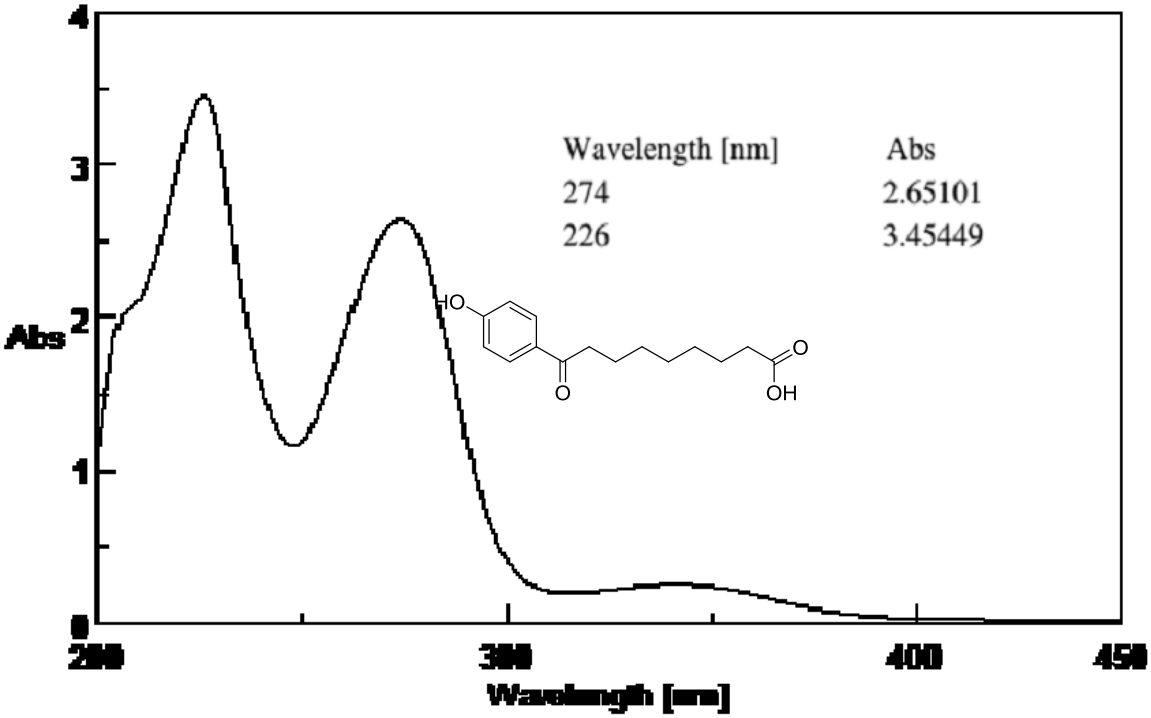

Figure S22: UV spectrum (MeOH) of compound 3b [9(3-hydroxy phenyl) nonanoic acid].

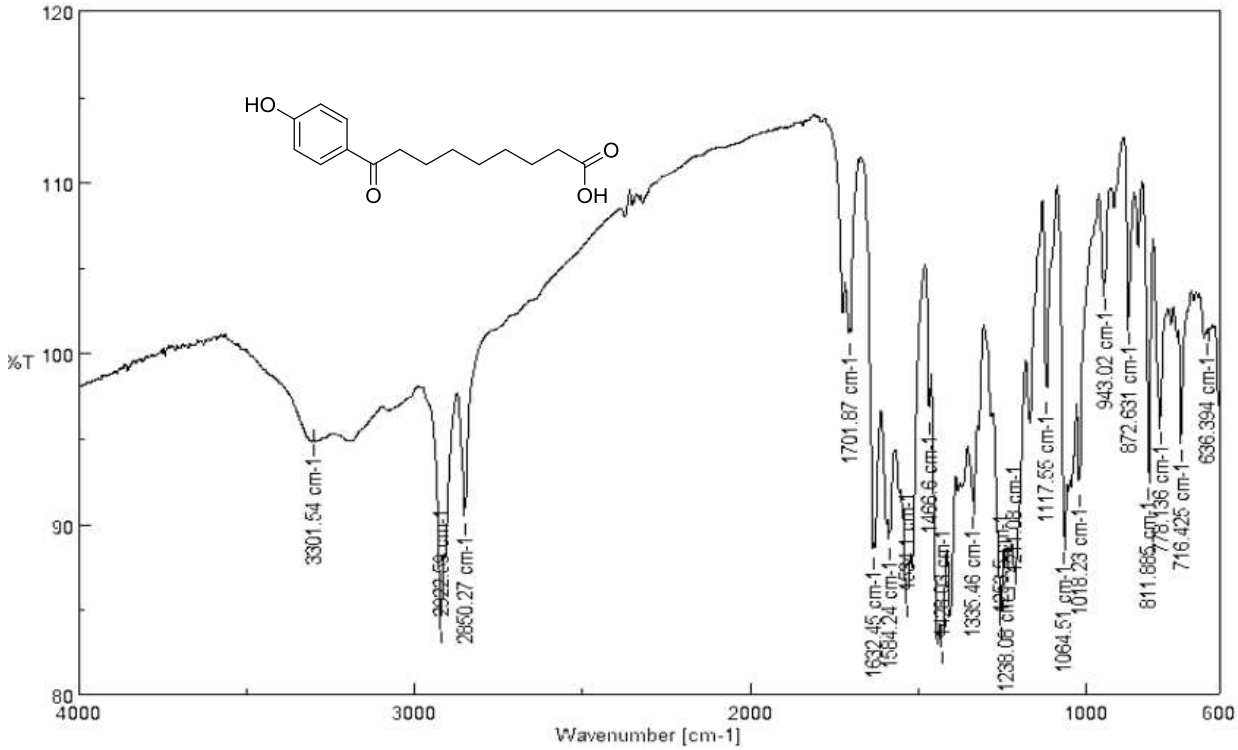

Figure S23: IR spectrum (KBr) spectrum of compound 3b [9(3-hydroxy phenyl) nonanoic acid].

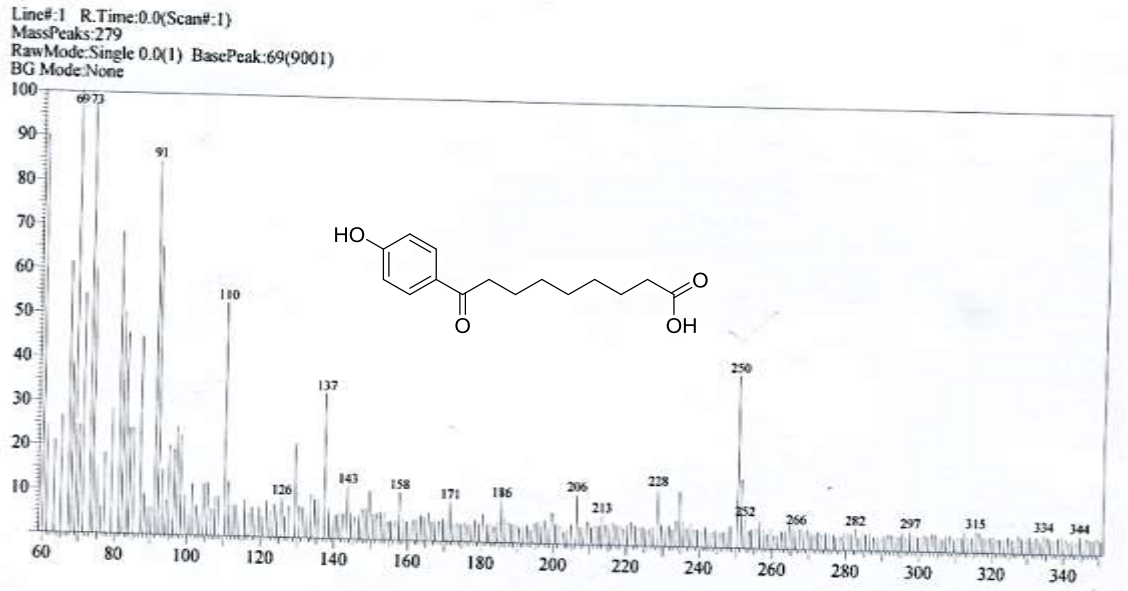

Figure S24: EIMS spectrum of compound 3b [9(3-hydroxy phenyl) nonanoic acid].

Figure S25: ^{1}H NMR spectrum ($CDCl_3$, 50 MHz) methyl ester of compound 3b [9(3-hydroxy phenyl) nonanoic acid].

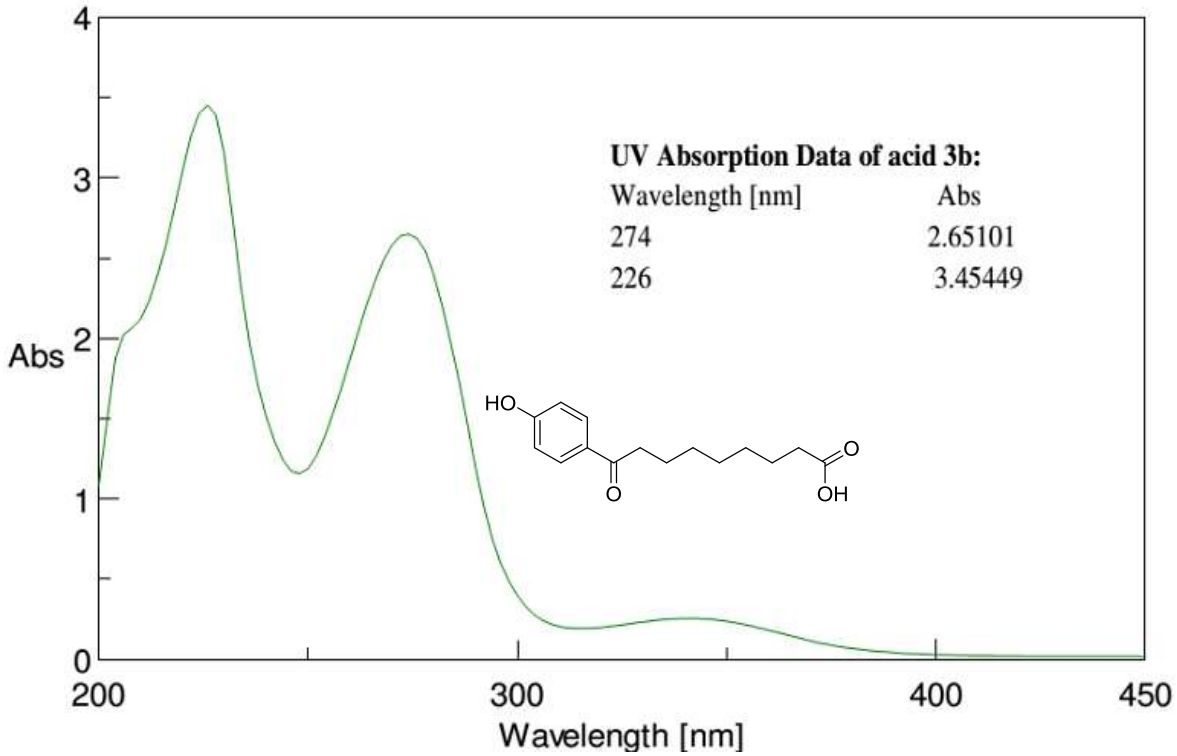

Figure S26: UV spectrum (MeOH) methyl ester of compound 3b [9(3-hydroxy phenyl) nonanoic acid].

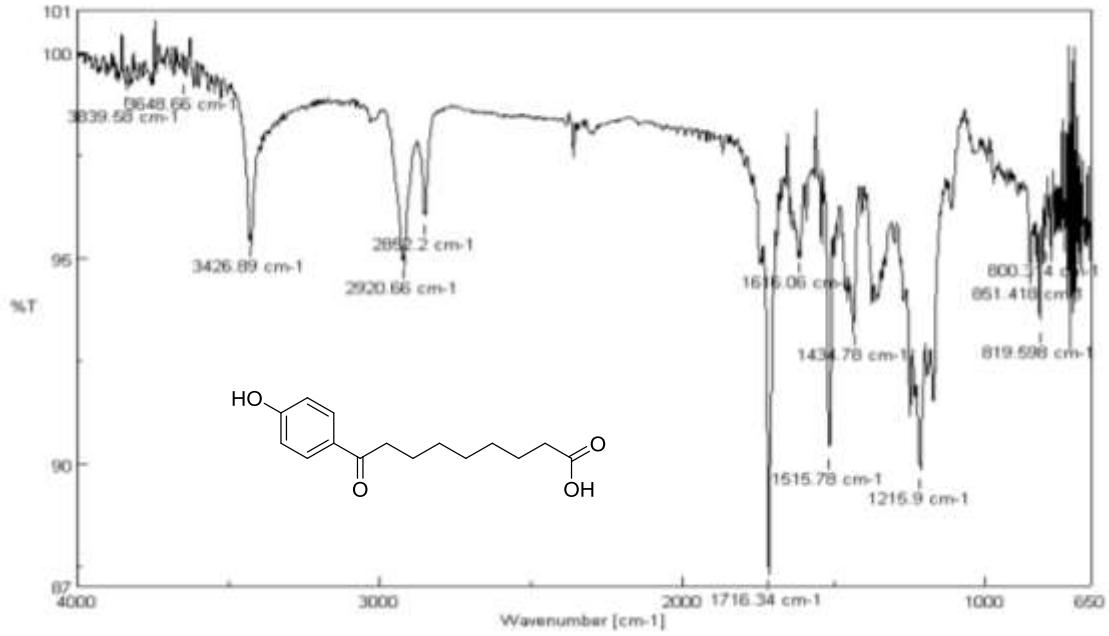

Figure S27: IR spectrum (KBr) spectrum of methyl ester of compound 3b [9(3-hydoxy phenyl) nonanoic acid].

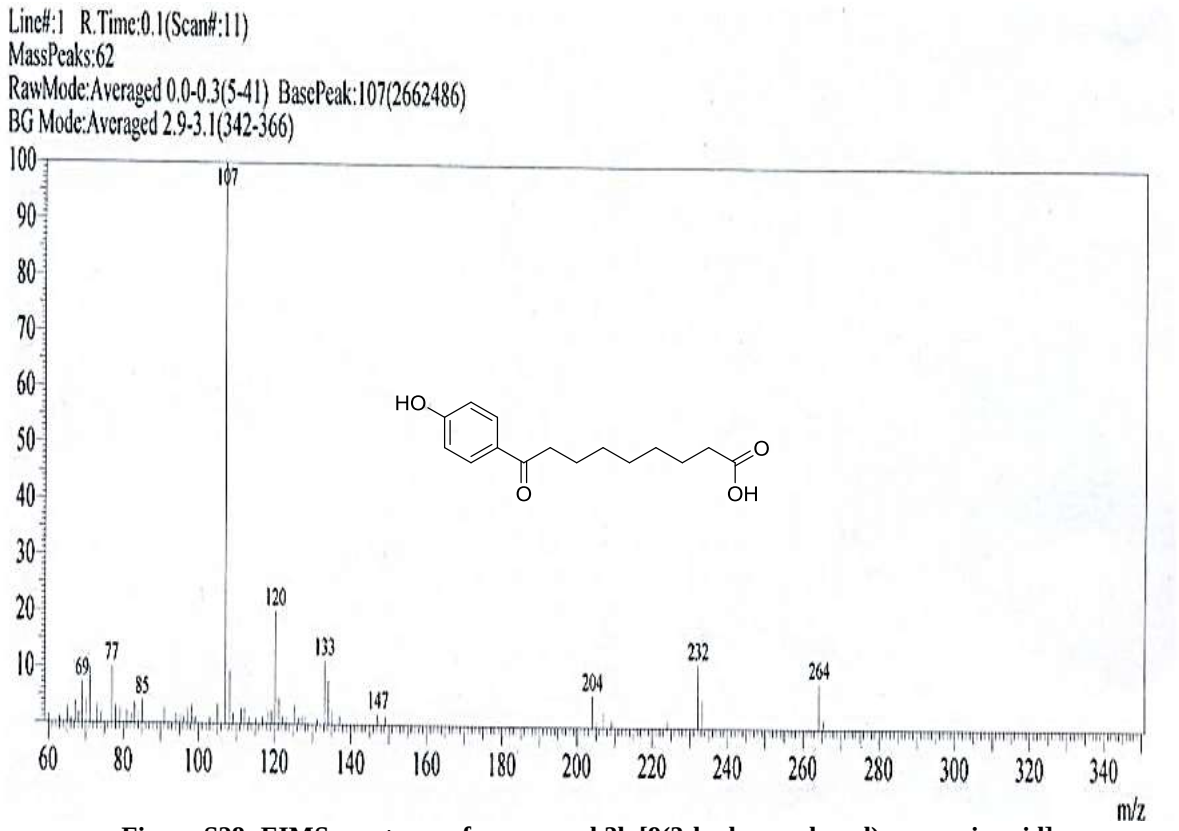

Figure S28: EIMS spectrum of compound 3b [9(3-hydroxy phenyl) nonanoic acid].

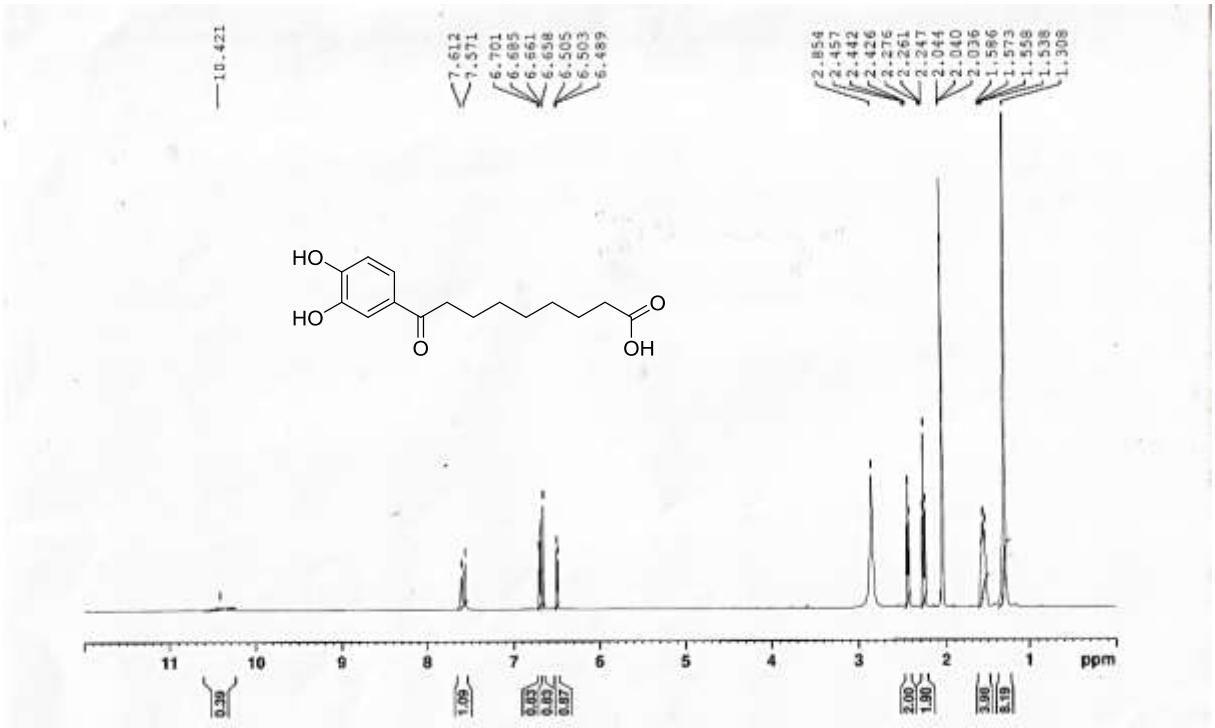

Figure S29: ^{1}H NMR spectrum ($CDCl_3$, 500 MHz) of compound 3c [9(3, 4-dihydoxy phenyl) nonanoic acid].

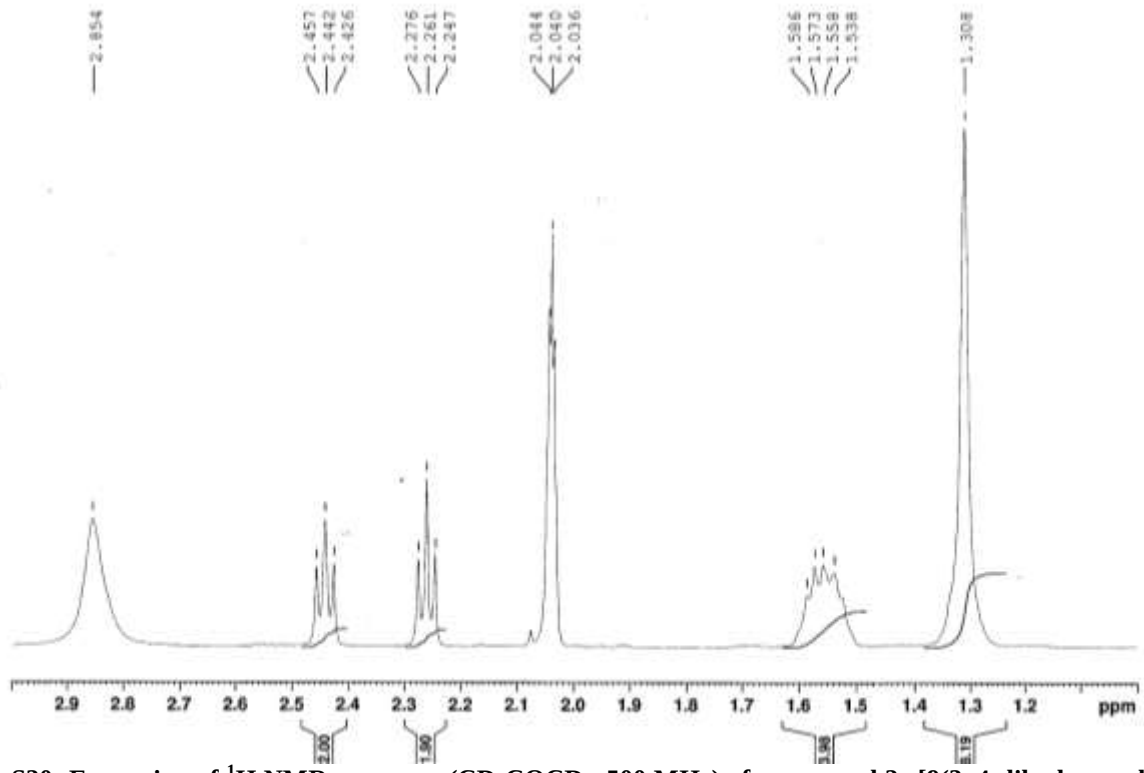

Figure S30: Expansion of ^{1}H NMR spectrum (CD_3COCD_3, 500 MHz) of compound 3c [9(3, 4-dihydroxy phenyl) nonanoic acid].

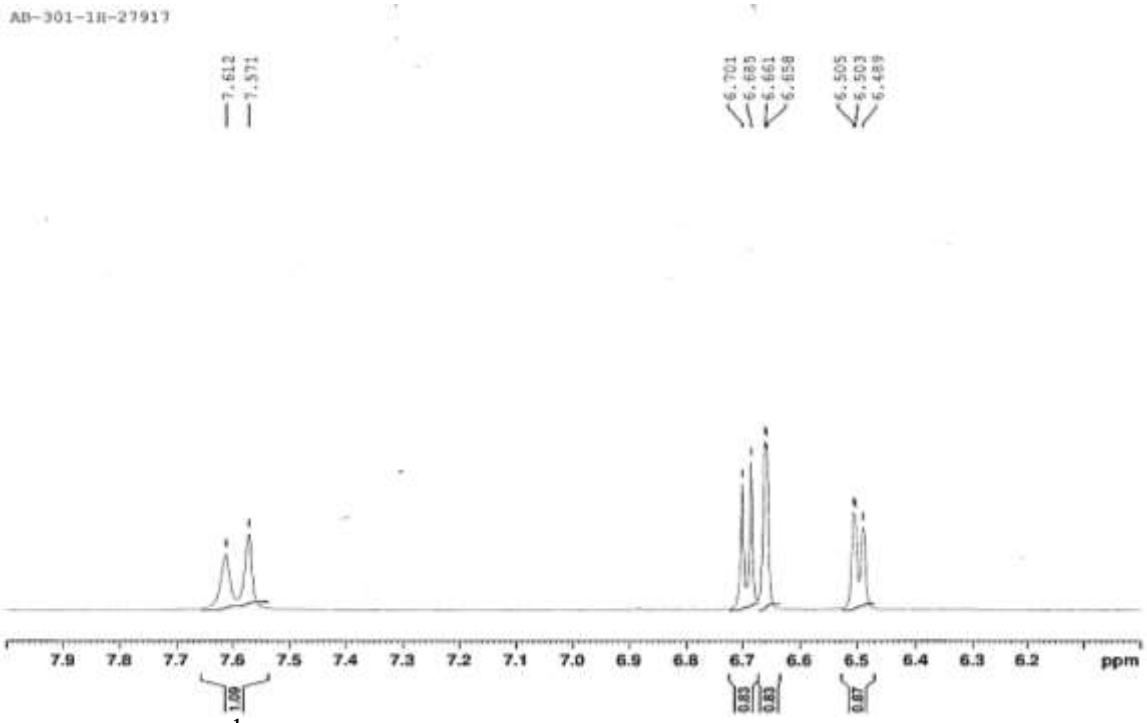

Figure S31: Expansion of ^{1}H NMR spectrum (CD_3COCD_3, 500 MHz) of compound 3c [9(3, 4-dihydoxy phenyl) nonanoic acid].

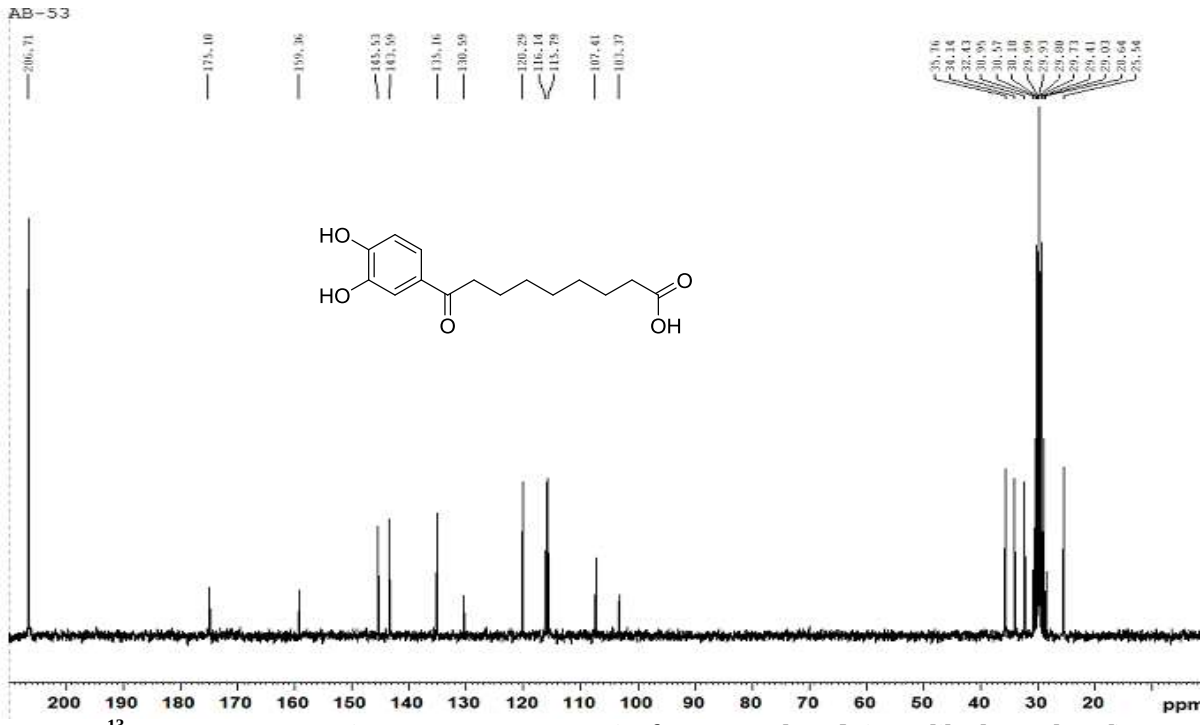

Figure S32: ^{13}C NMR spectrum (CD_3COCD_3, 500 MHz) of compound 3c [9(3, 4-dihydoxy phenyl) nonanoic acid].

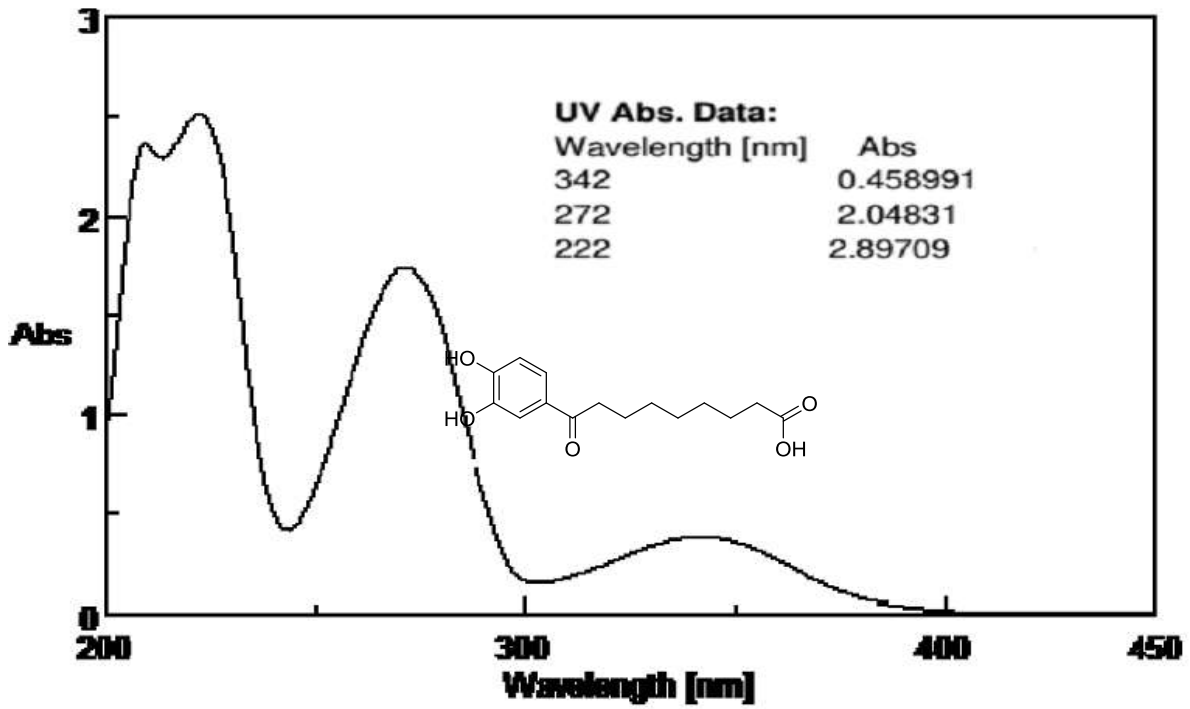

Figure S33: UV spectrum (MeOH) of methyl ester of compound 3c [9(3, 4-dihydroxy phenyl) nonanoic acid].

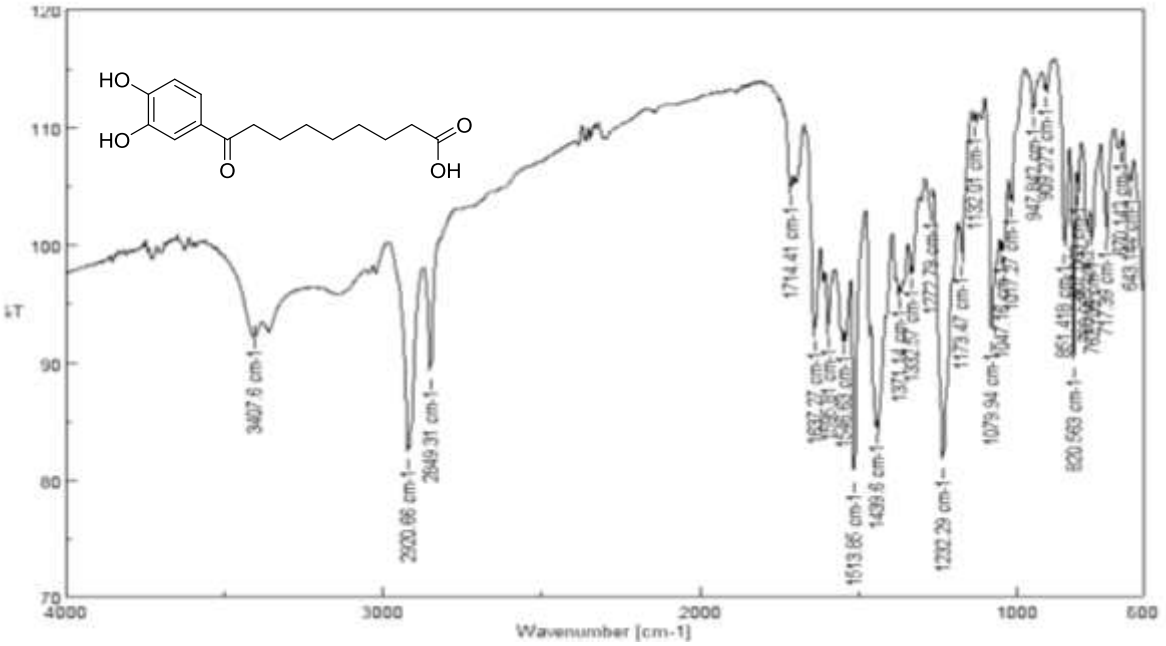

Figure S34: UV spectrum (in MeOH) methyl ester of compound 3c [9(3, 4-dihydroxy phenyl) nonanoic acid].

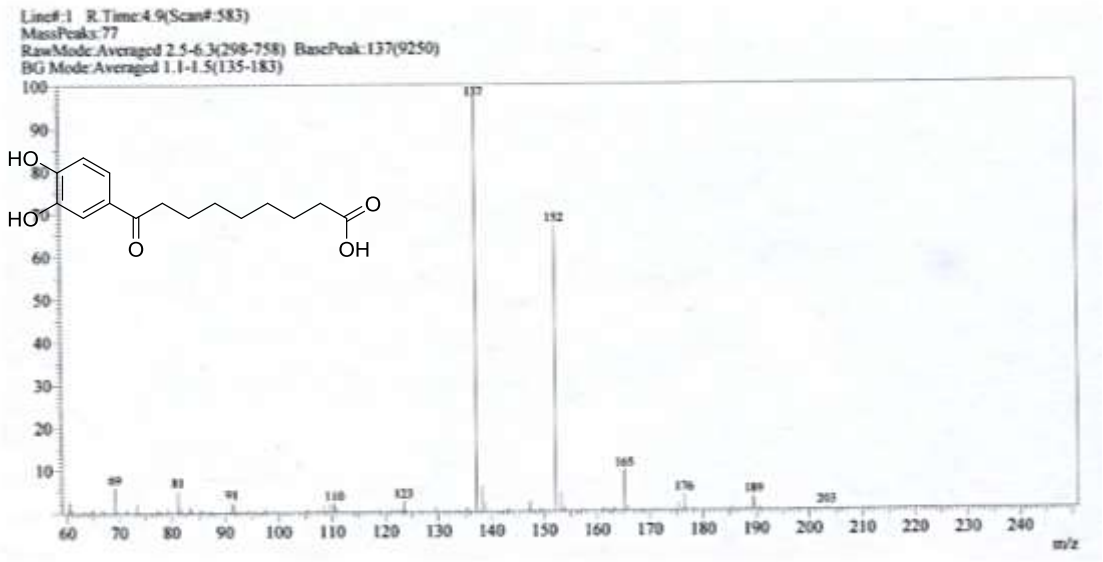

Figure S35: EIMS of methyl ester of compound 3c [9(3, 4-dihydroxy phenyl) nonanoic acid].

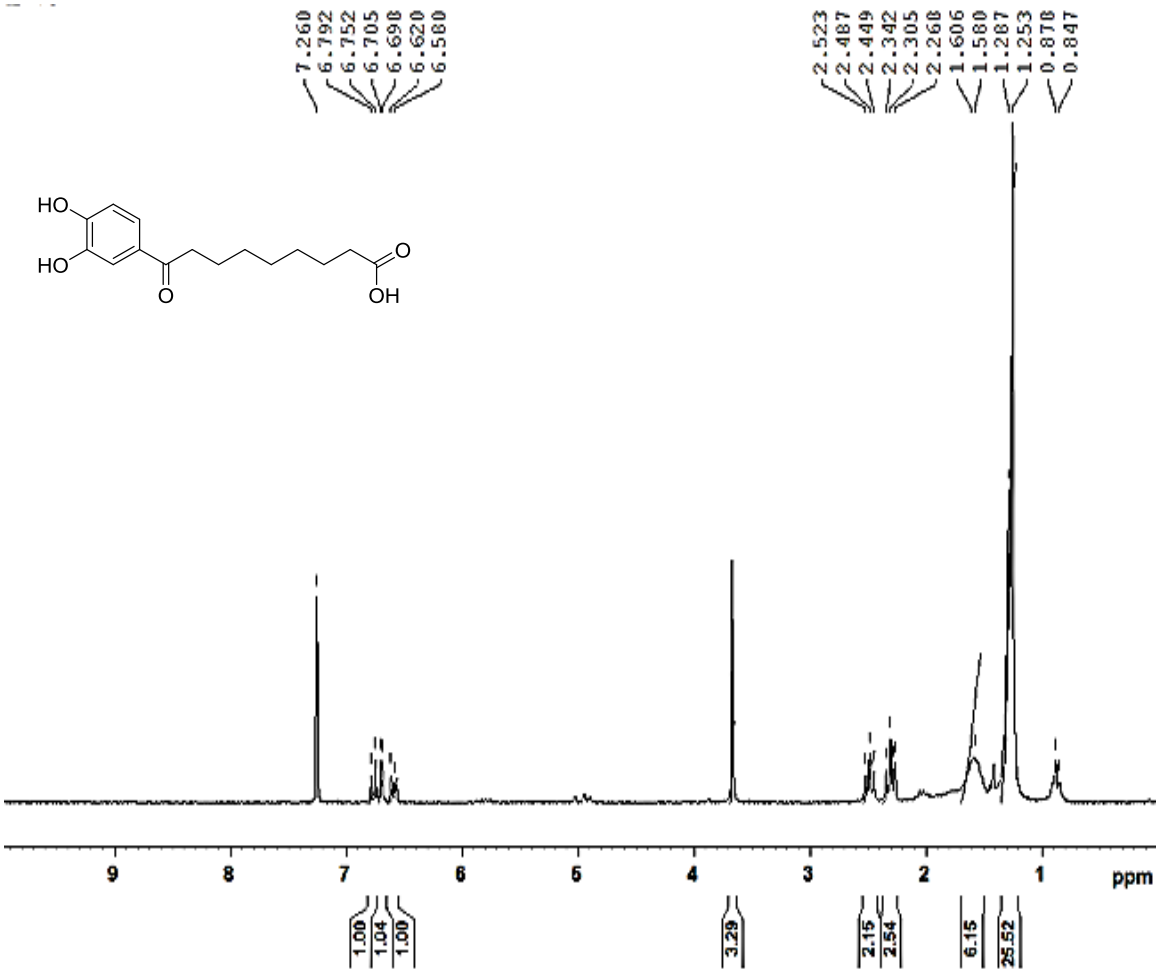

Figure S36: ^{1}H NMR spectrum of methyl ester of compound 3c [9(3, 4-dihydroxy phenyl) nonanoic acid].

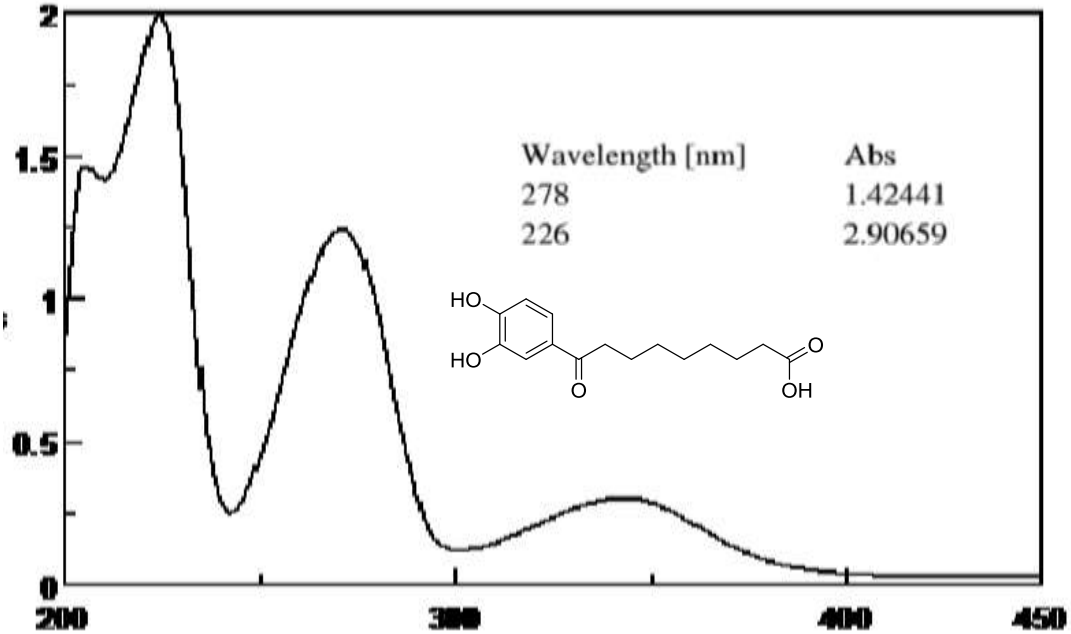

Figure S37: UV MeOH) spectrum of methyl ester of compound 3c [9(3, 4-dihydroxy phenyl) nonanoic].

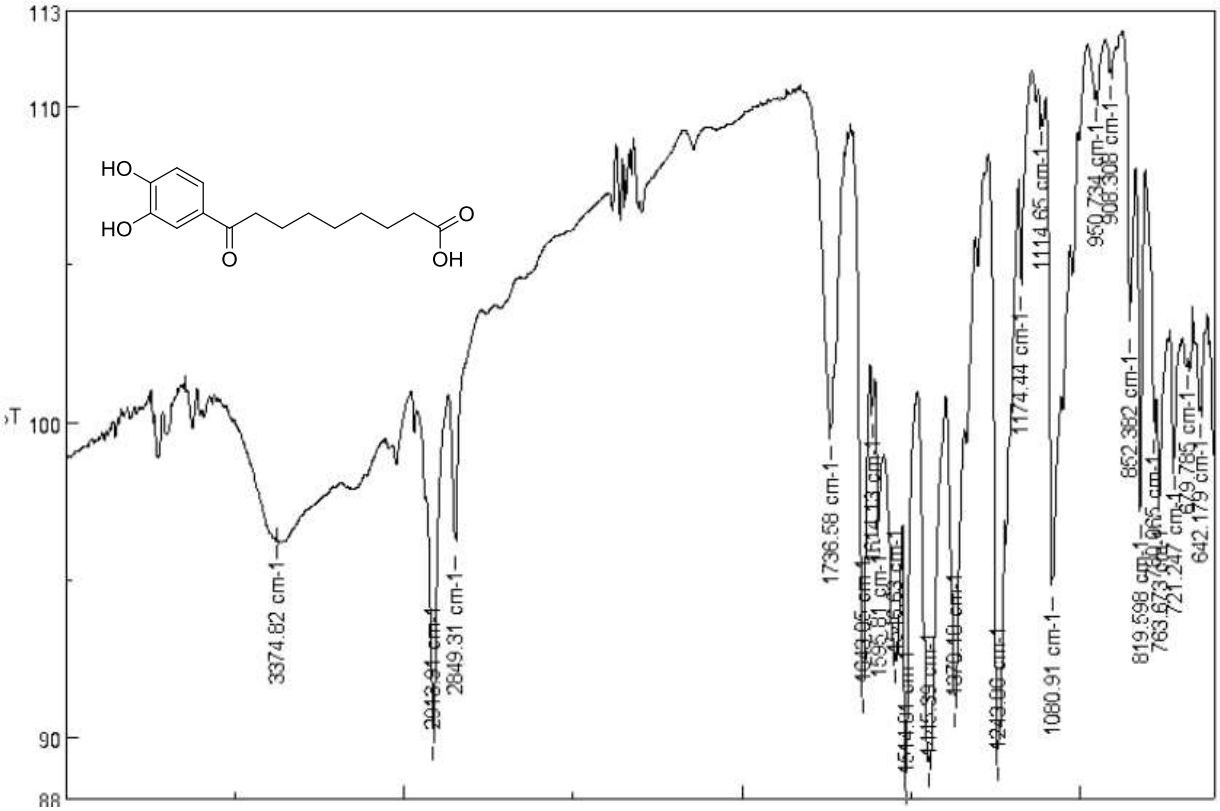

Figure S38: IR spectrum (KBr) of methyl ester of compound 3c [9(3, 4-dihydroxy phenyl) nonanoic acid].

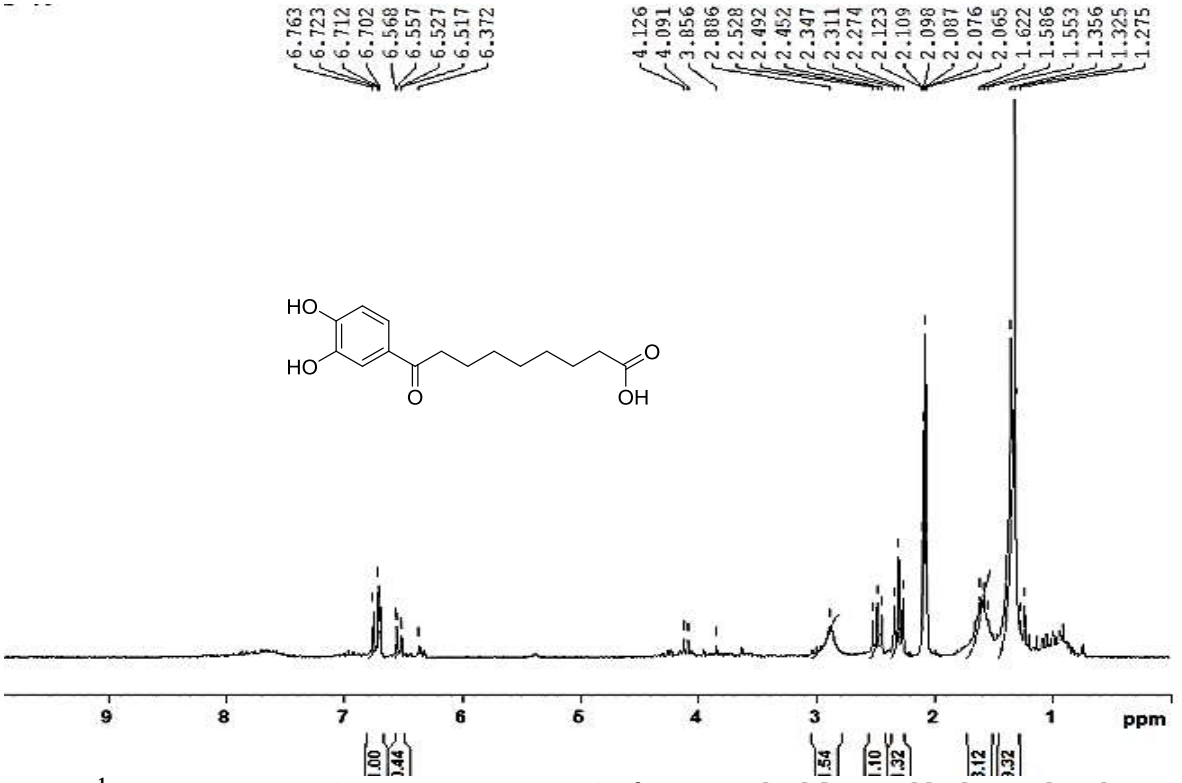

Figure S39: ^{1}H NMR spectrum (CD_3COCD_3, 500 MHz) of compound 3d [9(3, 4-dihydroxy phenyl) nonanoic acid].

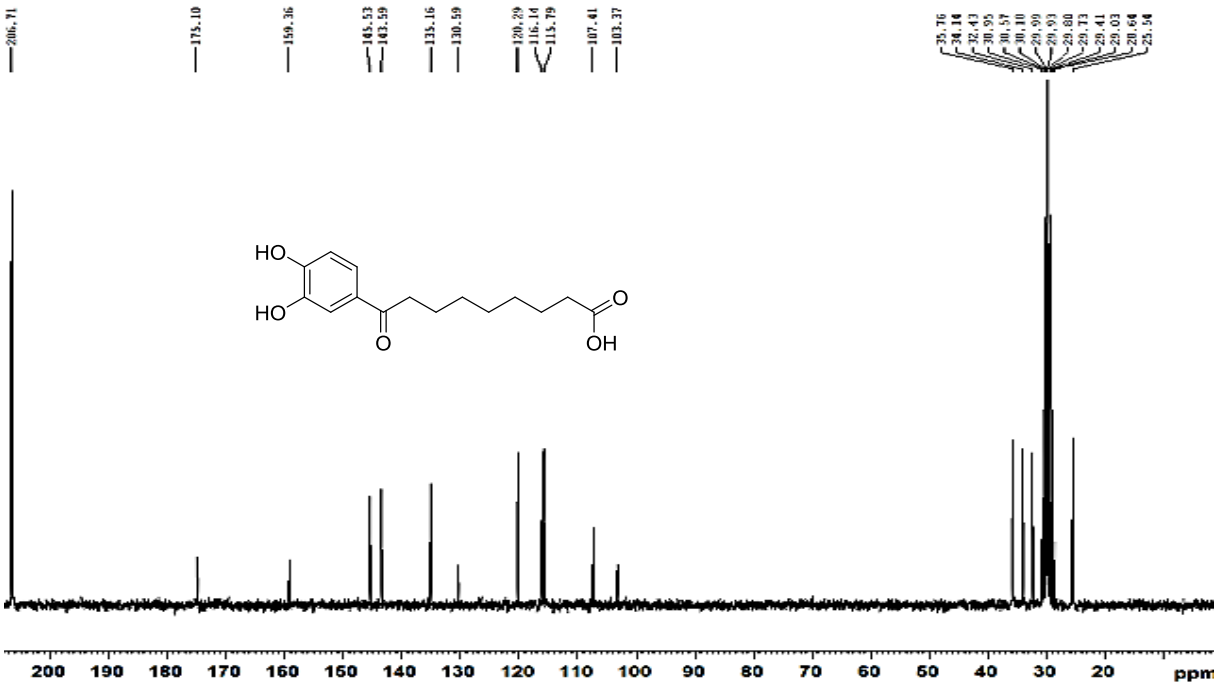

Figure S40: ^{13}C NMR spectrum (CD_3COCD_3, 50 MHz) of compound 3d [9(3, 4-dihydroxy phenyl) nonanoic acid].

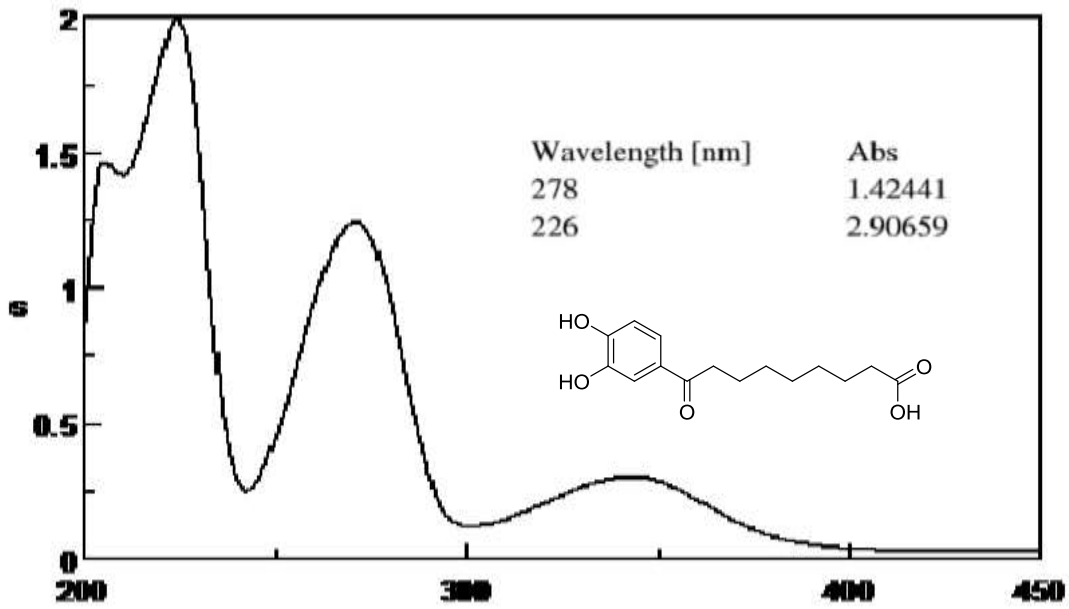

Figure S41: UV spectrum (MeOH) of methyl ester of compound 3e [9(3, 4-dihydroxy phenyl) nonanoic acid].

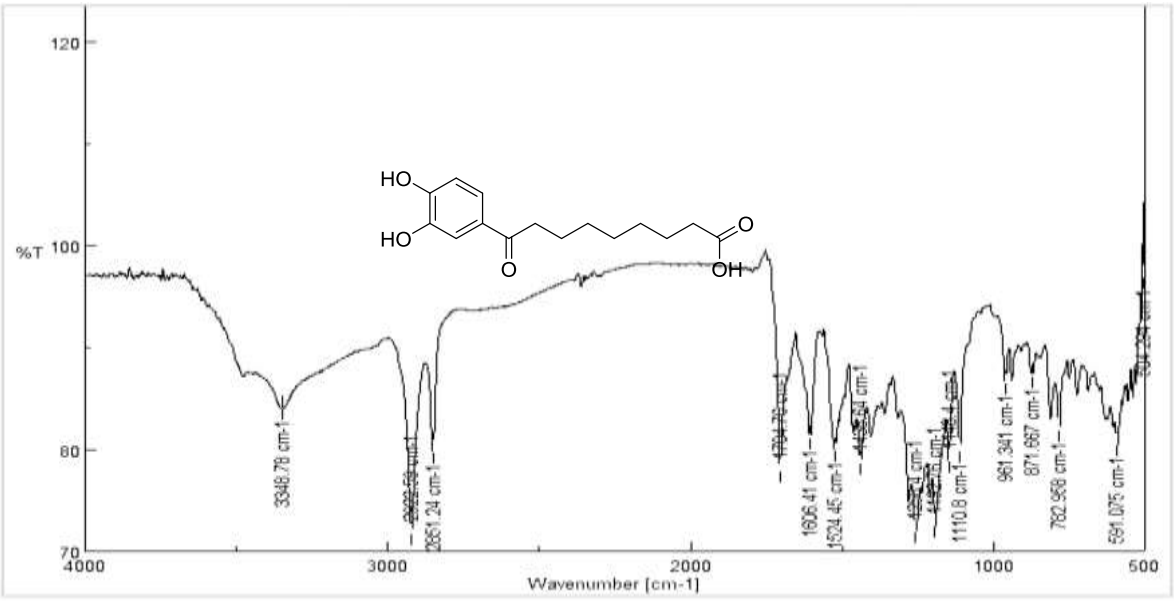

Figure S42: IR spectrum (KBr) of methyl ester of compound 3d [9(3, 4-dihydroxy phenyl) nonanoic].

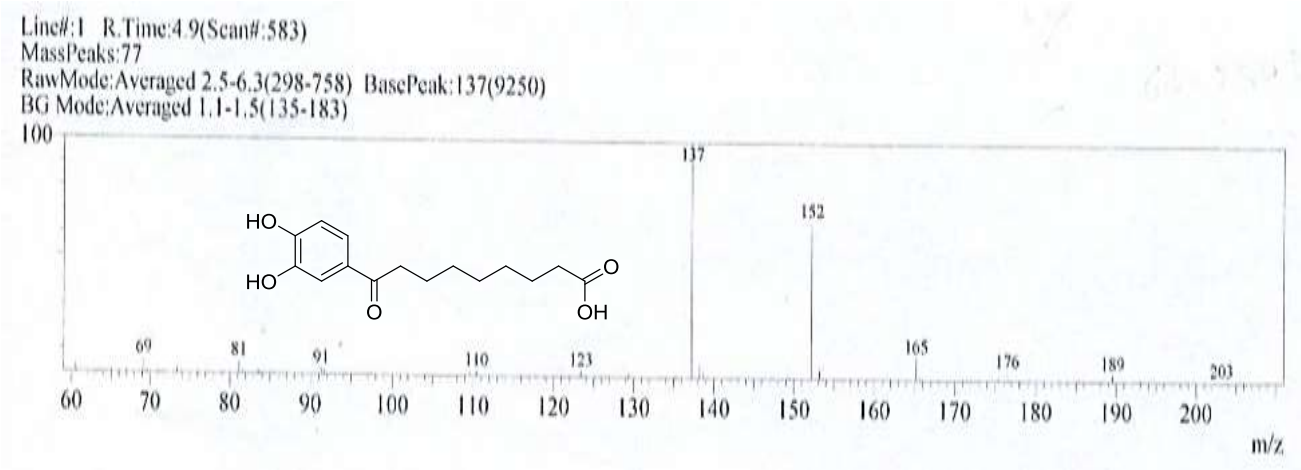

Figure S43: EIMS spectrum of methyl ester of compound 3d [9(3, 4-dihydroxy phenyl) nonanoic acid].

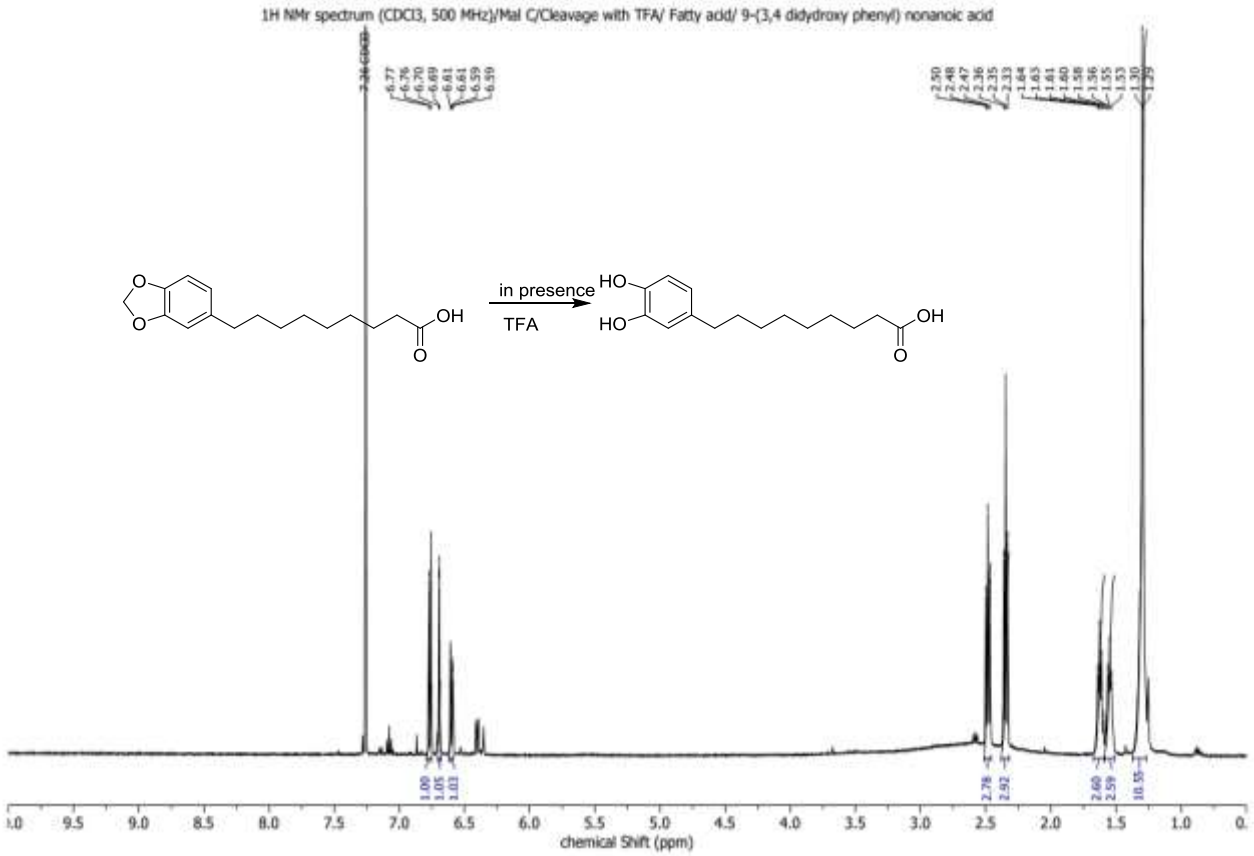

Figure S44: ^{1}H NMR spectrum ($CDCl_3$, 500 MHz) of malabaricone D cleaved with TFA acid.

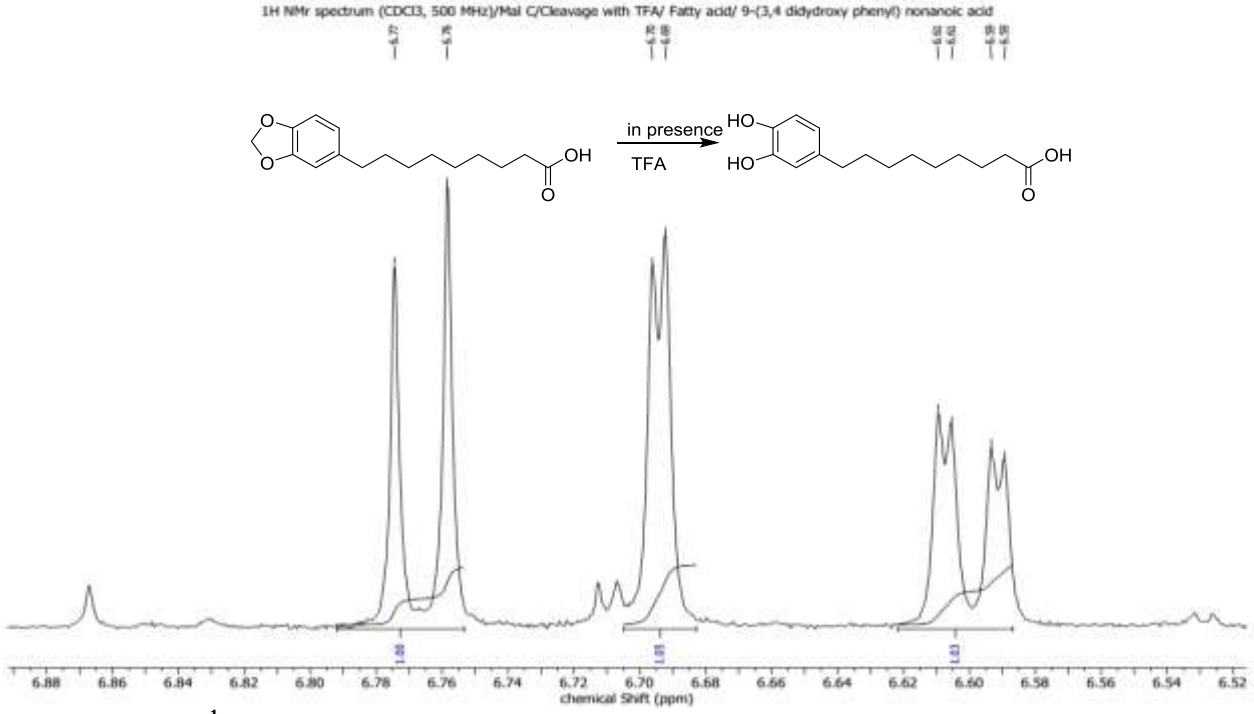

Figure S45: ^{1}H NMR spectrum (CD_3COCD_3, 500 MHz) of malabaricone D cleaved with TFA acid.

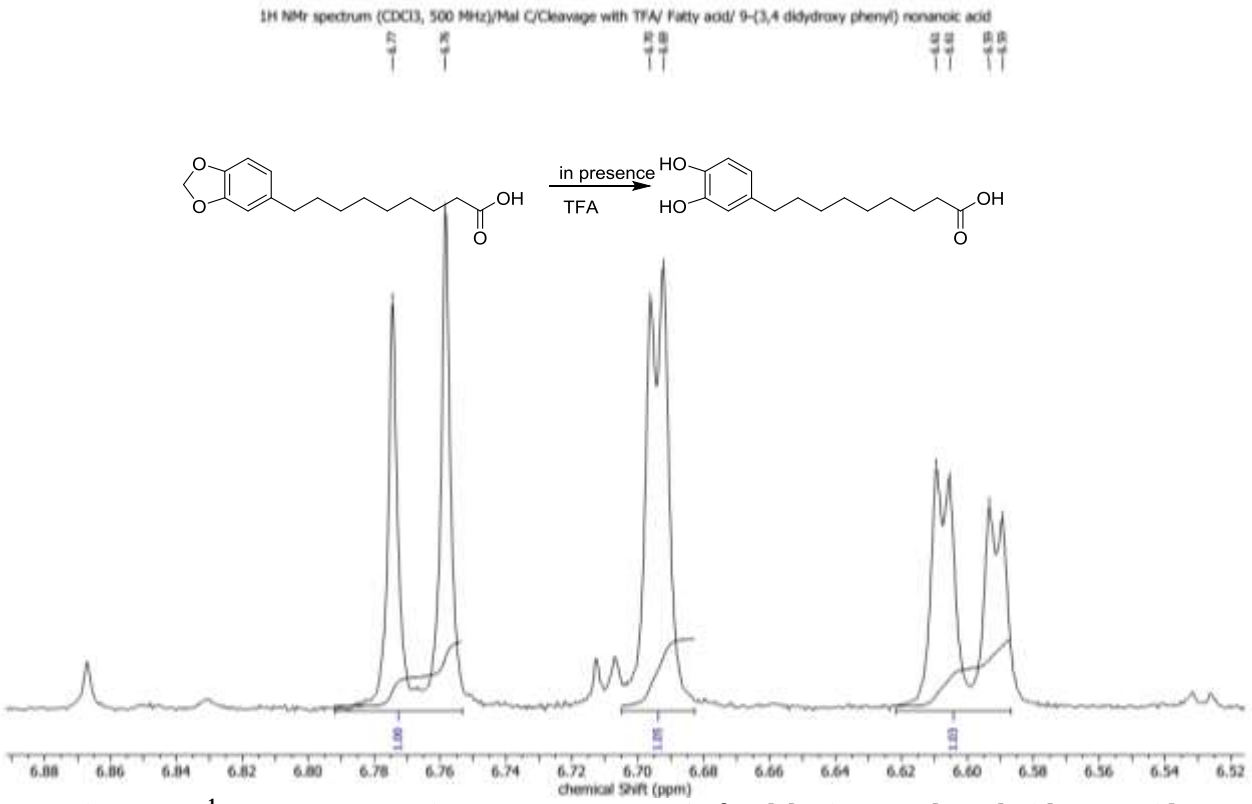

Figure S46: ^{1}H NMR spectrum (CD_3COCD_3, 500 MHz) of malabaricone D cleaved with TFA acid.

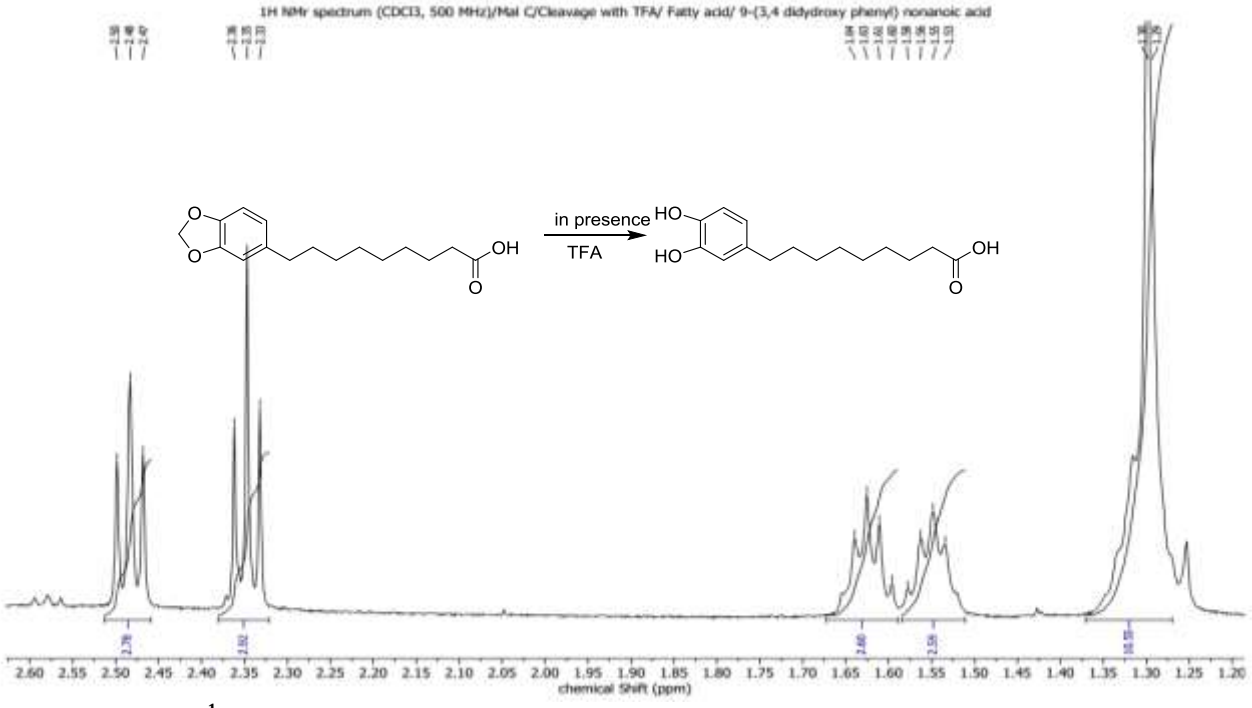

Figure S47: ^{1}H NMR spectrum (CD_3COCD_3, 500 MHz) of malabaricone C cleaved with TFA acid.

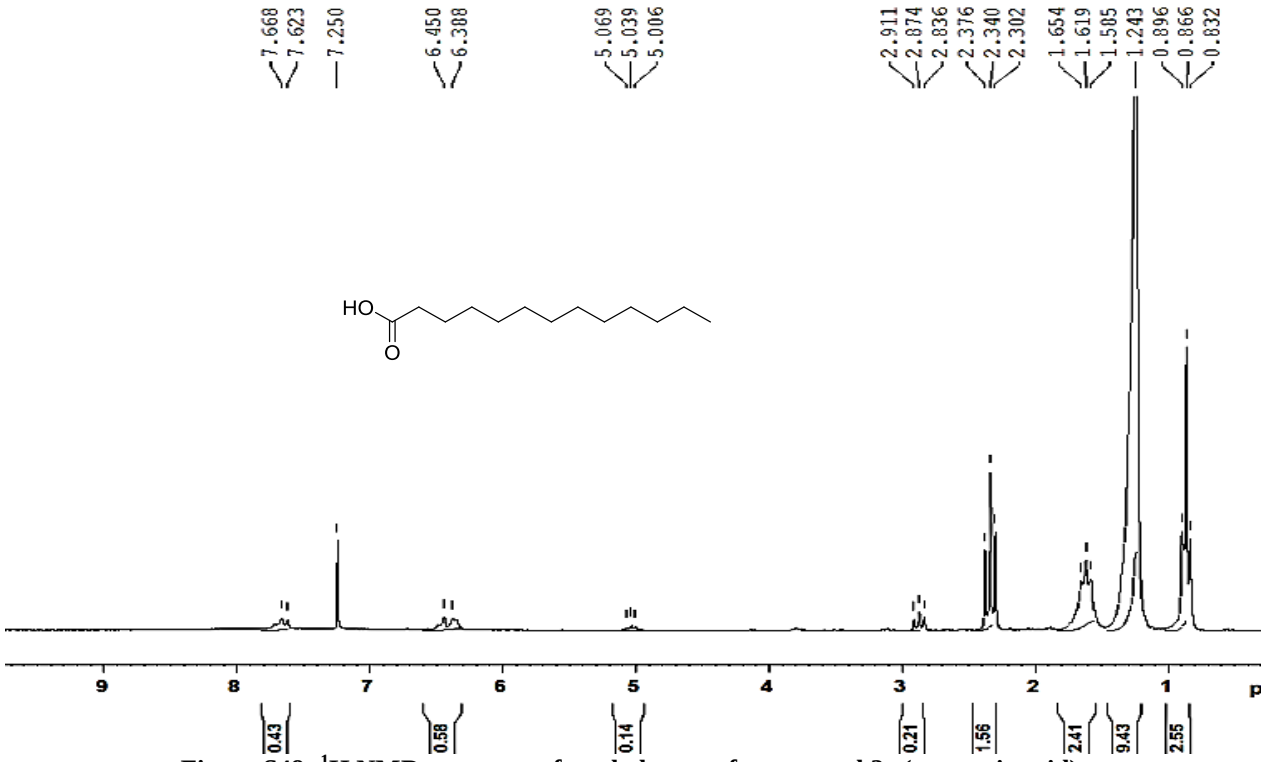

Figure S48: ^{1}H NMR spectrum of methyl ester of compound 3e (nonanoic acid).

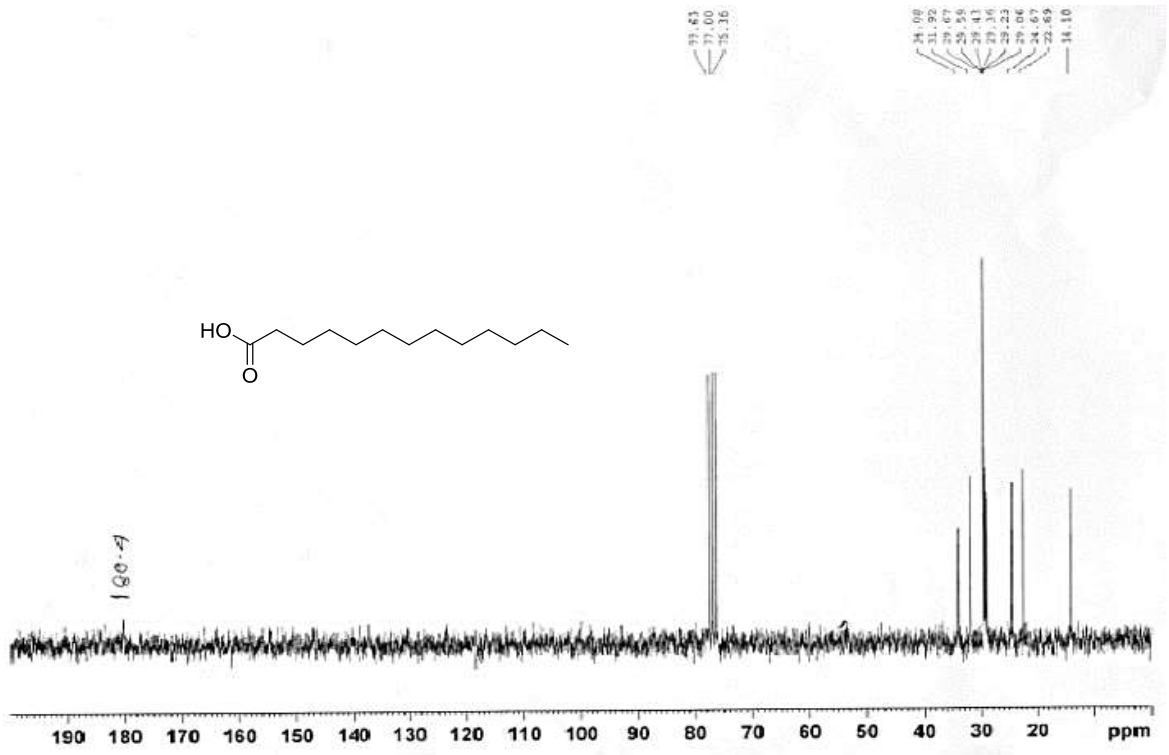

Figure S49: ^{13}C NMR ($CDCl_3$, 50 MHz) spectrum of compound 3e (nonanoic acid).

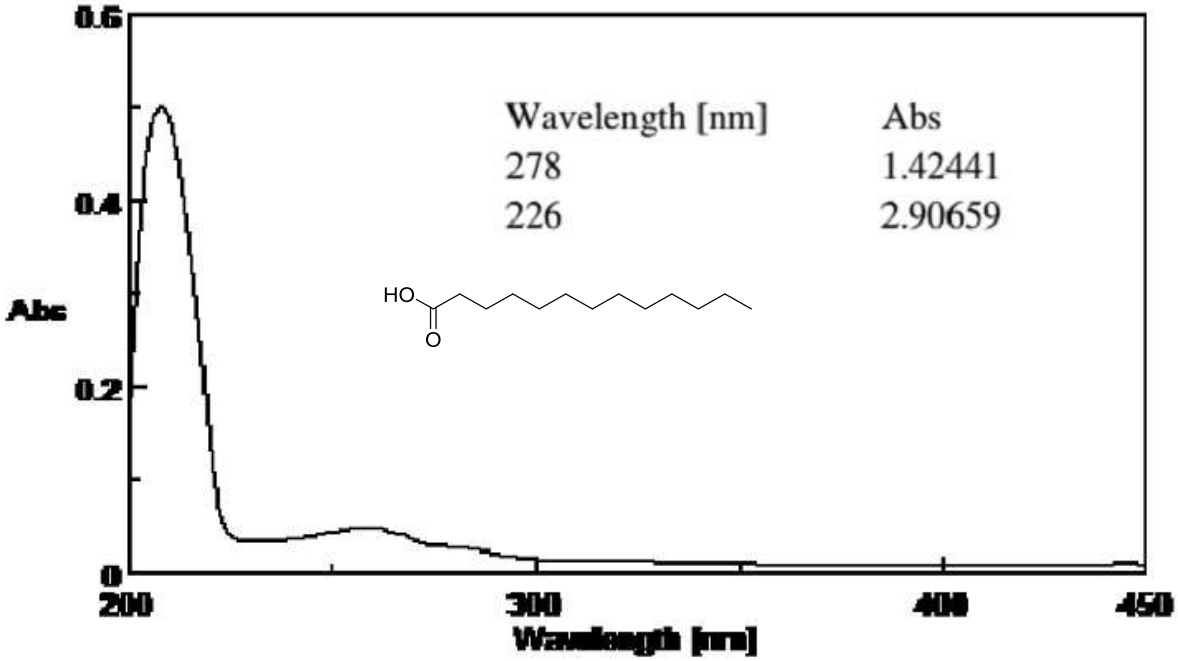

Figure S50: UV spectrum (MeOH) of compound 3e (nonanoic acid)

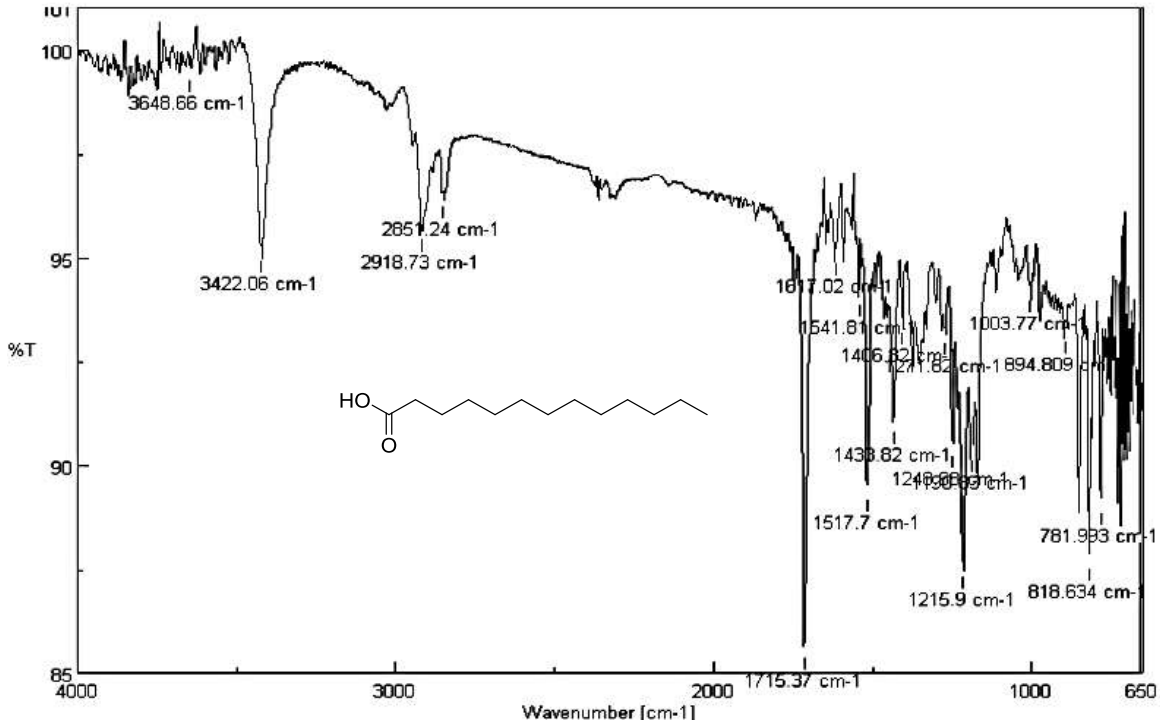

Figure S51: IR spectrum (KBr) of compound 3e (nonanoic acid).

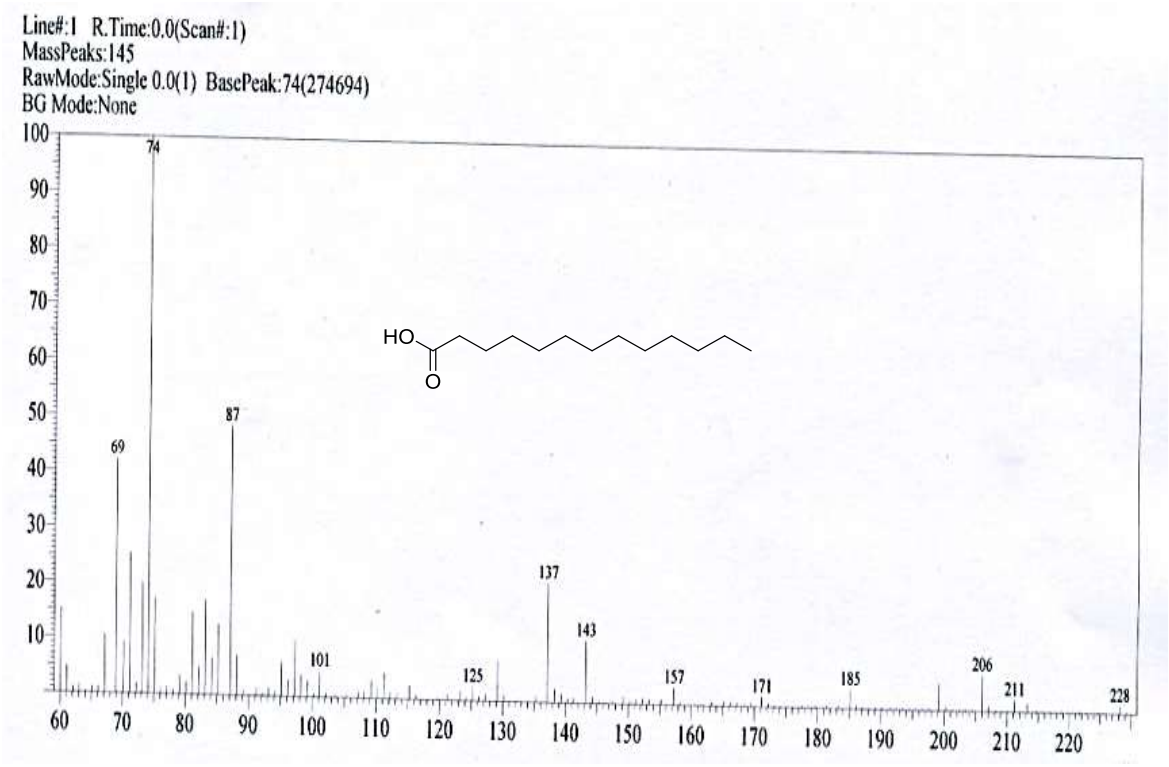

Figure S52: EIMS spectrum of methyl ester of compound 3e (nonanoic acid).

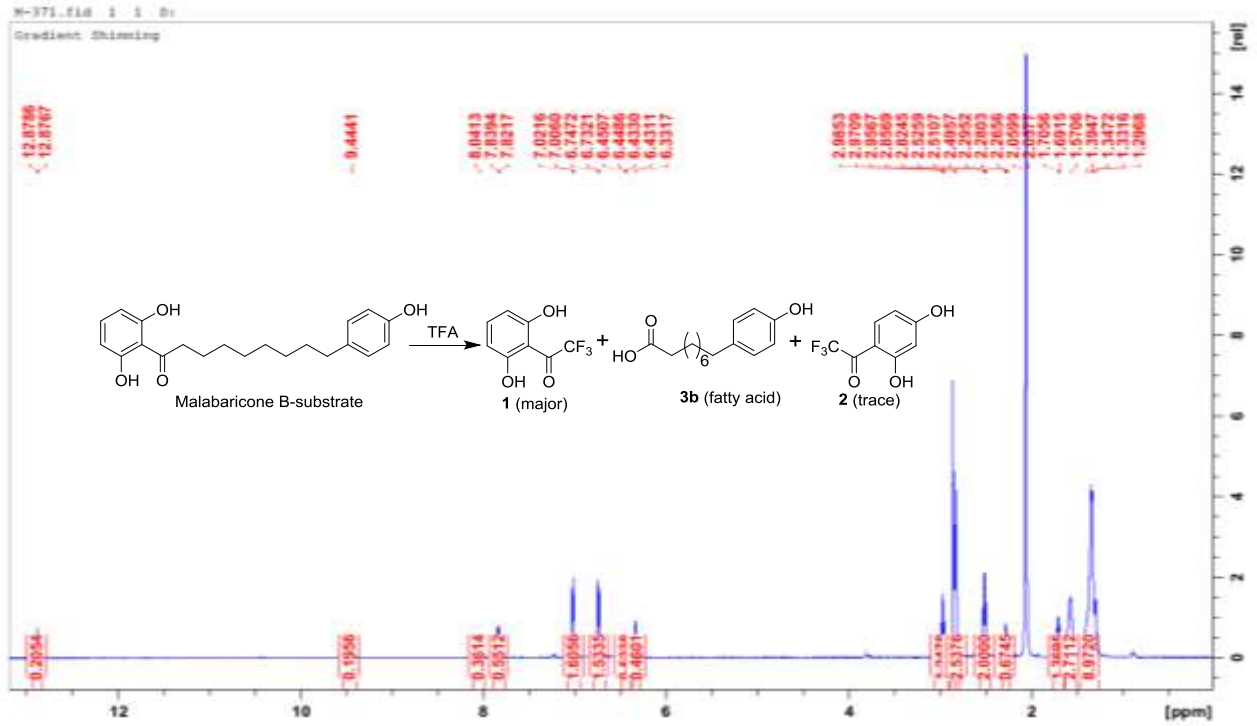

Figure S53: ^{1}H NMR spectrum (CD_3COCD_3, 500 MHz) of malabaricone B and its crude TFA reaction products.

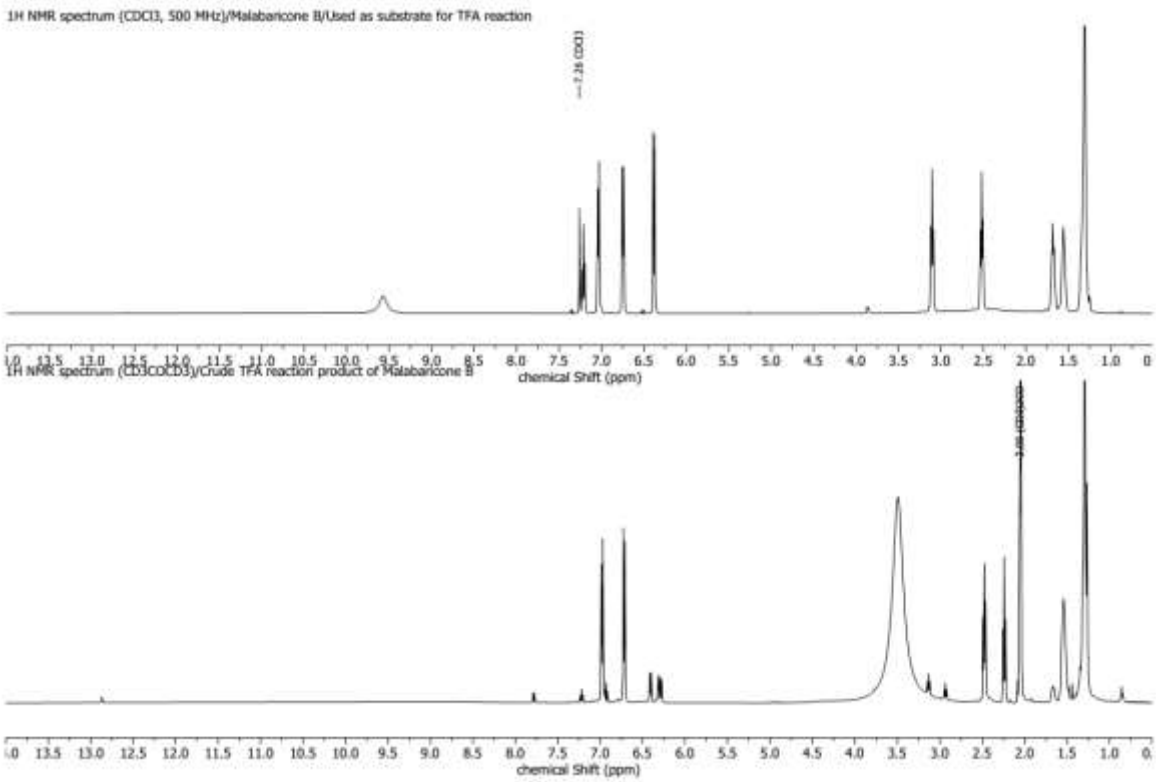

Figure S54: Stacking plot of ^{1}H NMR spectra of malabaricone B ($CDCl_3$, 500 MHz) and its TFA reaction products in crude form (CD_3COCD_3, 500 MHz),

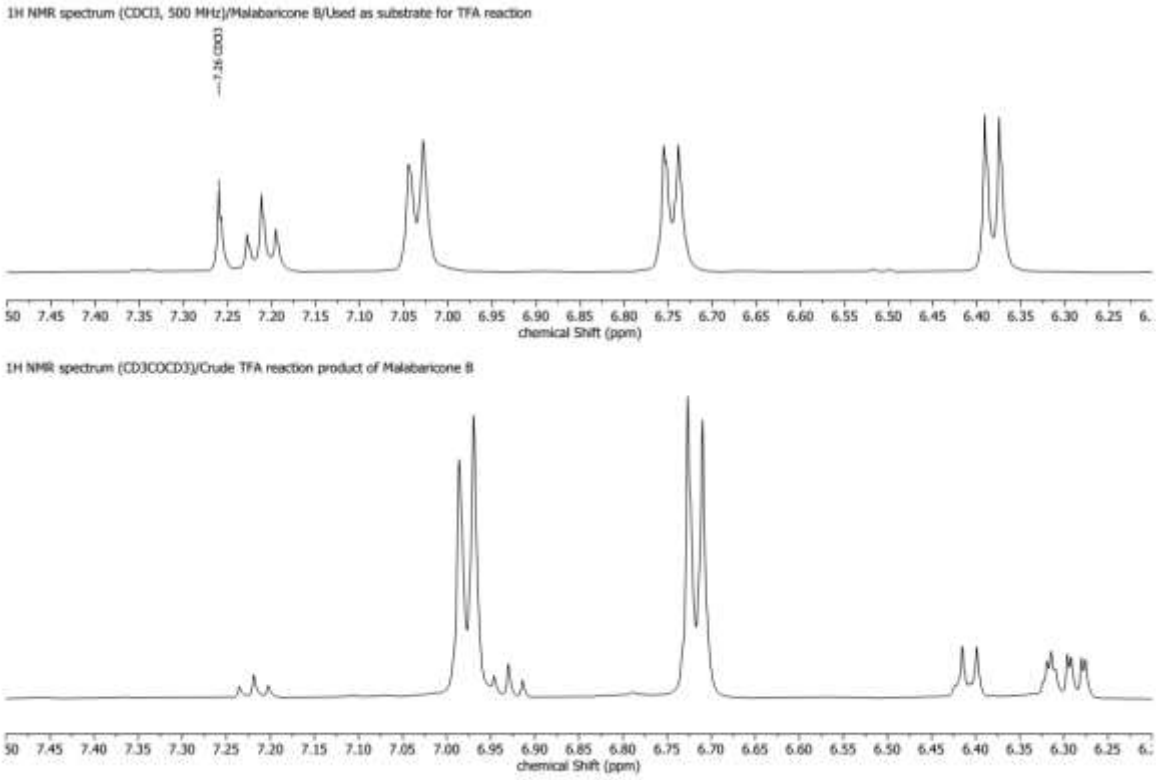

Figure S55: Expansion of stacking plot of ^{1}H NMR spectra of malabaricone B ($CDCl_3$, 500 MHz) and its TFA reaction products in crude form (CD_3COCD_3, 500 MHz).

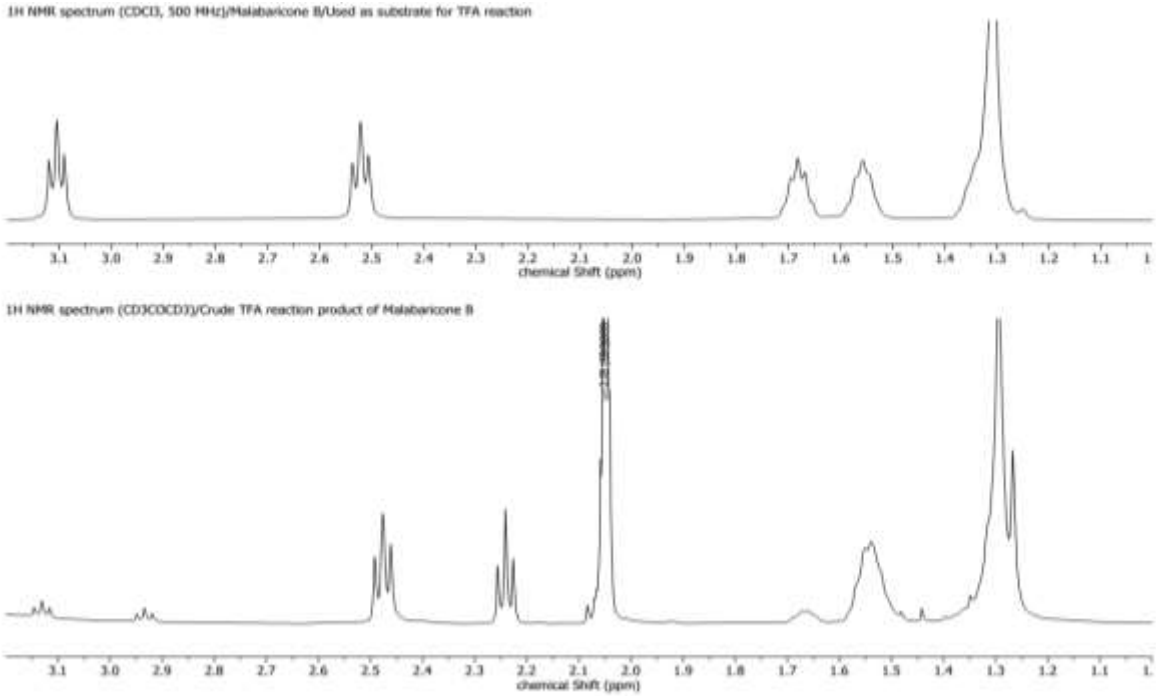

Figure S56: Expansion of stacking plot of ^{1}H NMR spectra of malabaricone B ($CDCl_3$, 500 MHz) and its TFA reaction products in crude form (CD_3COCD_3, 500 MHz).

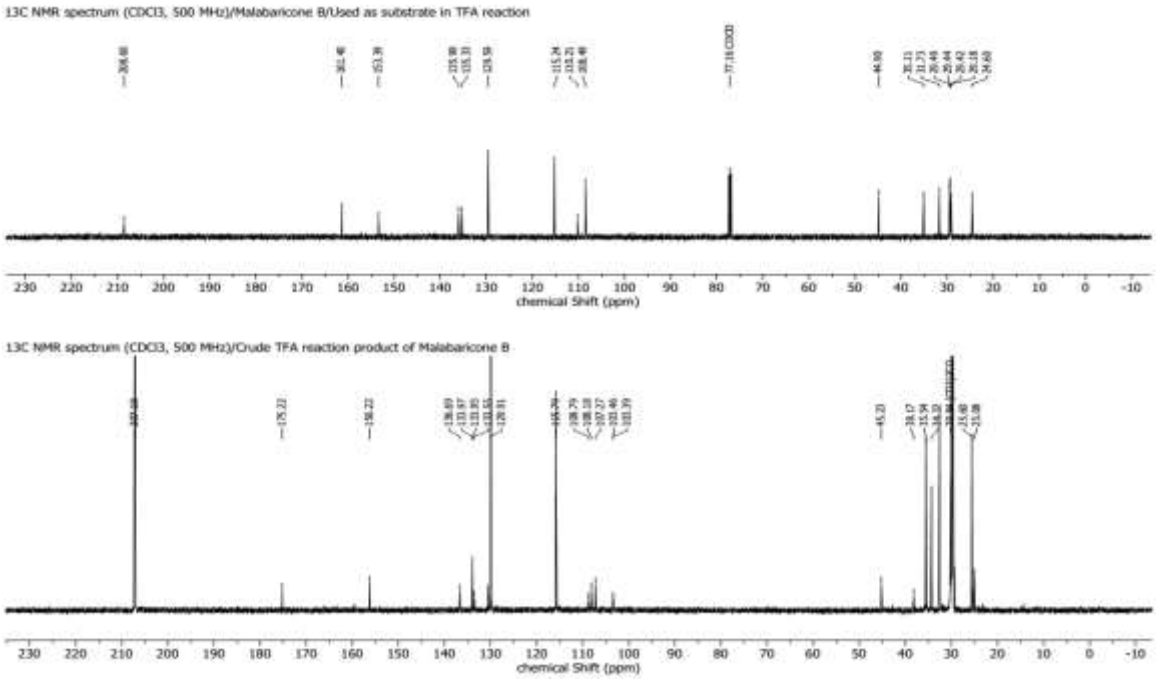

Figure S57: Stacking plot of ^{1}H NMR spectra of malabaricone B ($CDCl_3$, 125 MHz) and its TFA reaction products in crude form (CD_3COCD_3, 125 MHz).

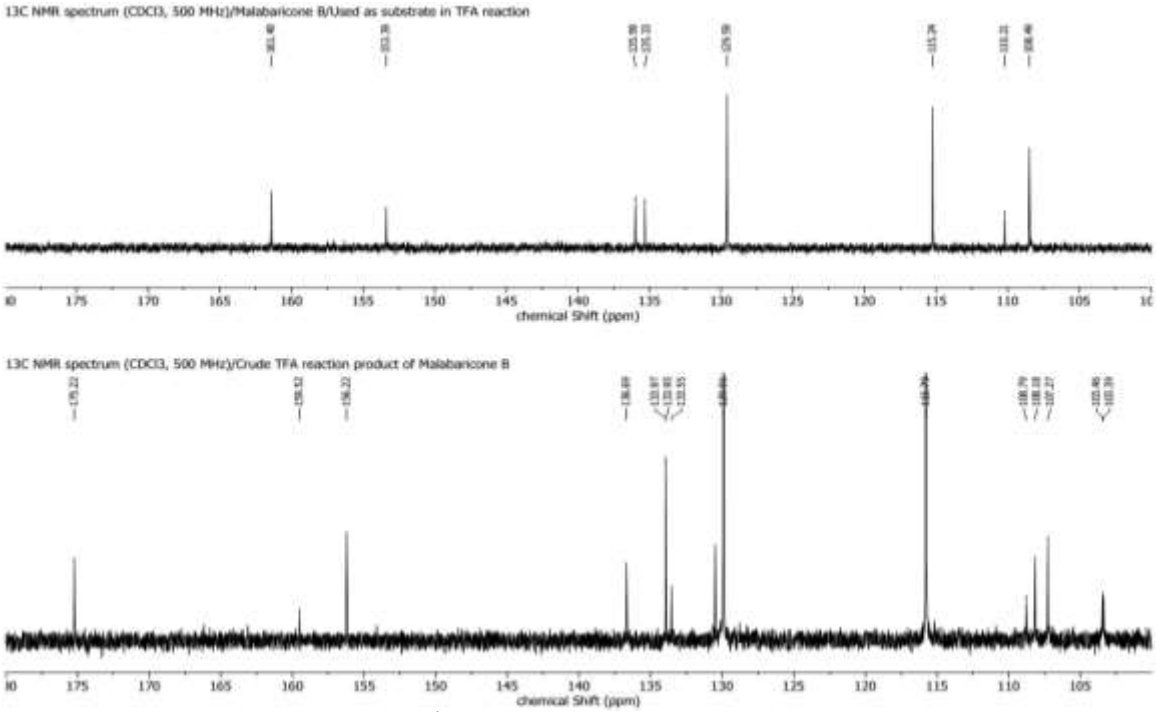

Figure S58: Expansion of stacking plot of ^{1}H NMR spectra of malabaricone B ($CDCl_3$, 125 MHz) and its TFA reaction products (CD_3COCD_3, 125 MHz).

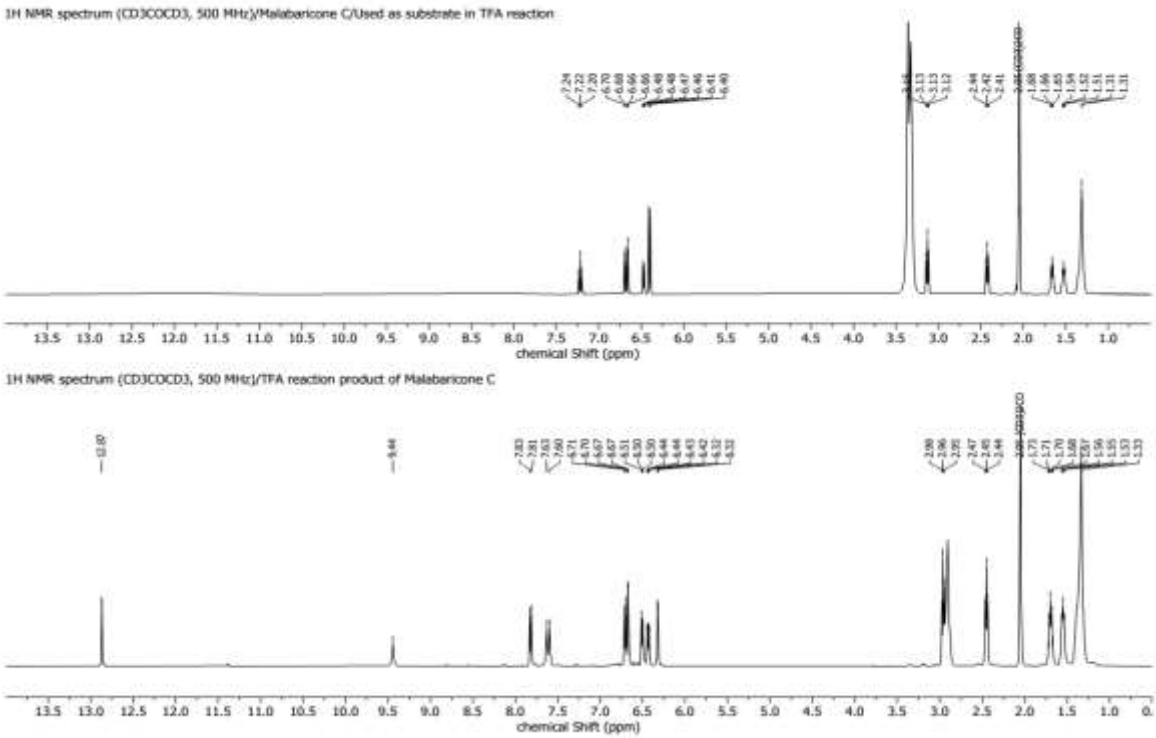

Figure S59: Stacking plot of ^{1}H NMR spectra of malabaricone B ($CDCl_3$, 500 MHz) and its TFA reaction products in crude form (CD_3COCD_3, 500 MHz).

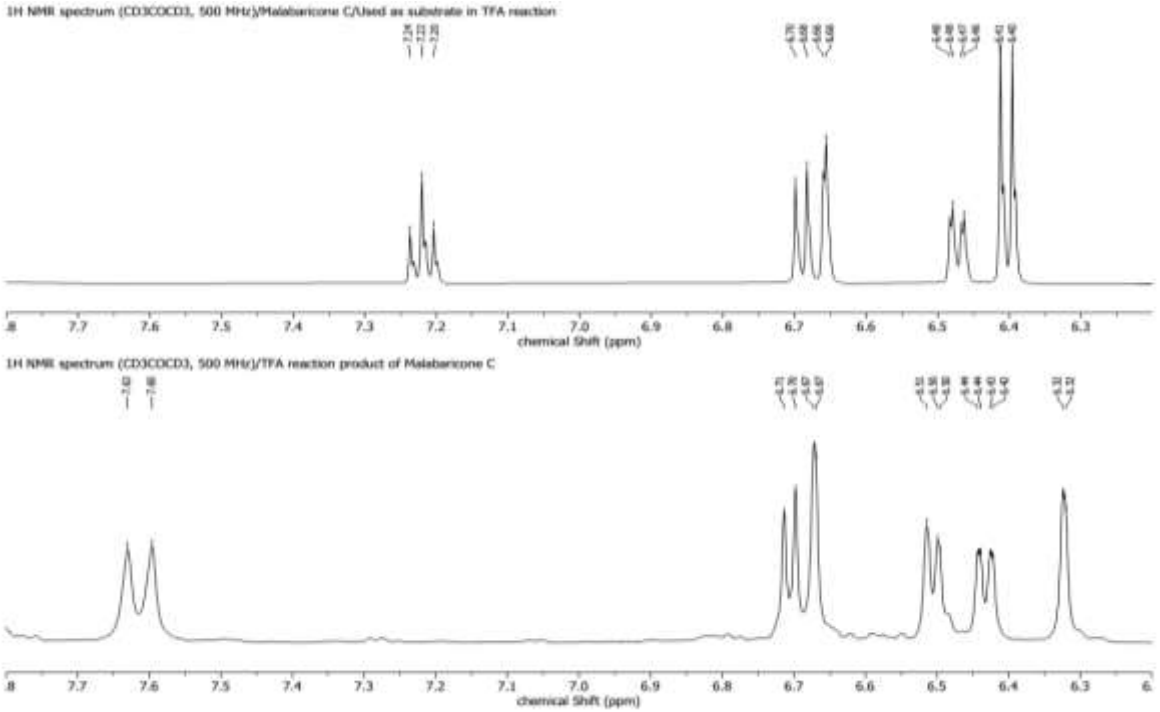

Figure S60: Expansion ^{1}H NMR stacking plot of malabaricone C ($CDCl_3$, 500 MHz) and its crude TFA reaction products (CD_3COCD_3, 500 MHz).

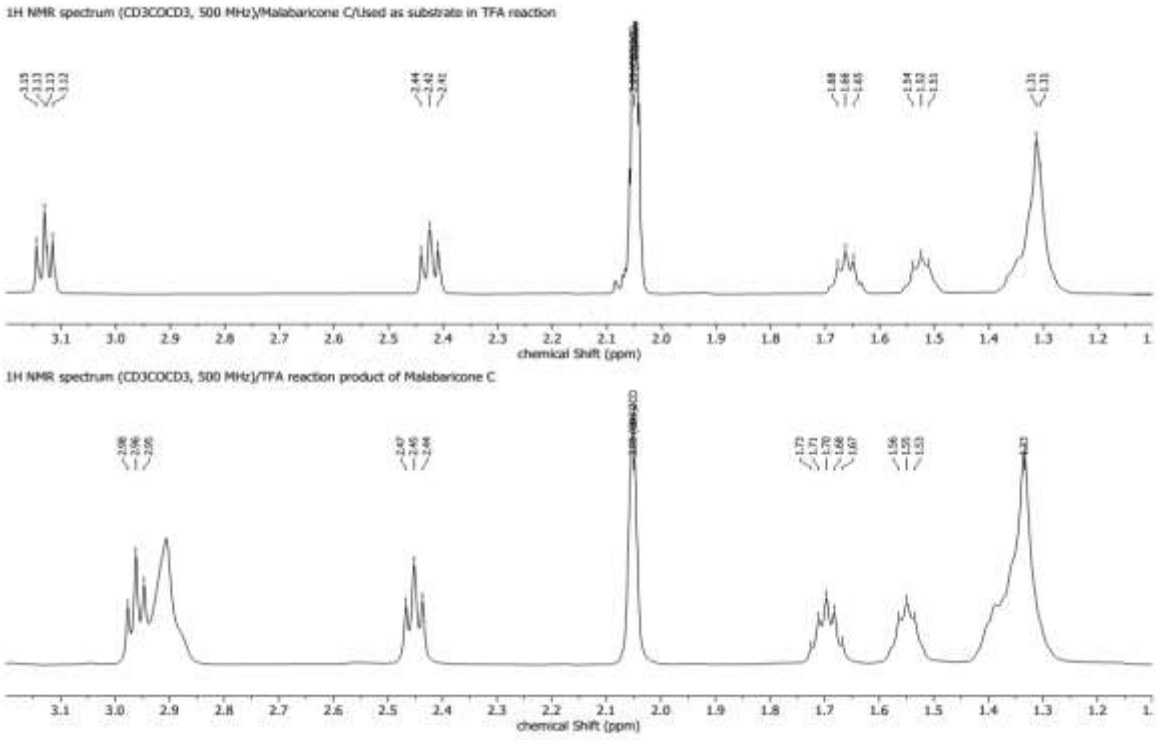

Figure S61: Expansion ^{1}H NMR stacking plot of malabaricone C ($CDCl_3$, 500 MHz) and its crude TFA reaction products (CD_3COCD_3, 500 MHz).

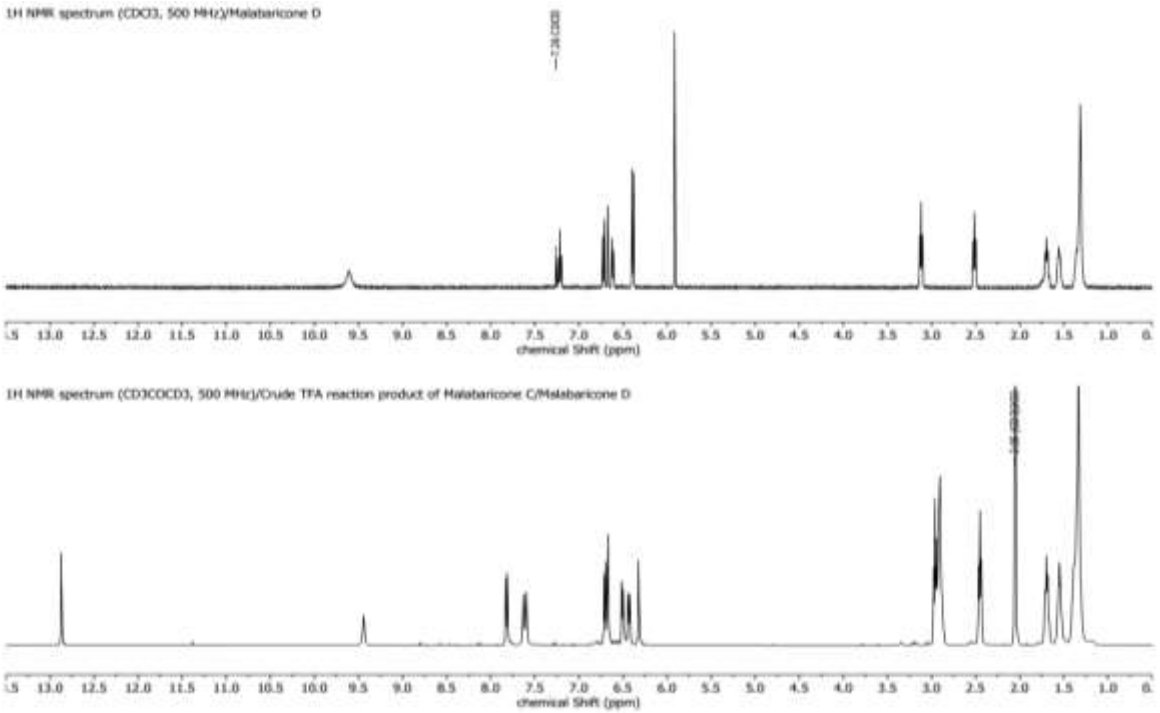

Figure S62: ^{1}H NMR spectra of stacking plot of malabaricone D ($CDCl_3$, 500 MHz) and its crude TFA reaction products (CD_3COCD_3, 500 MHz).

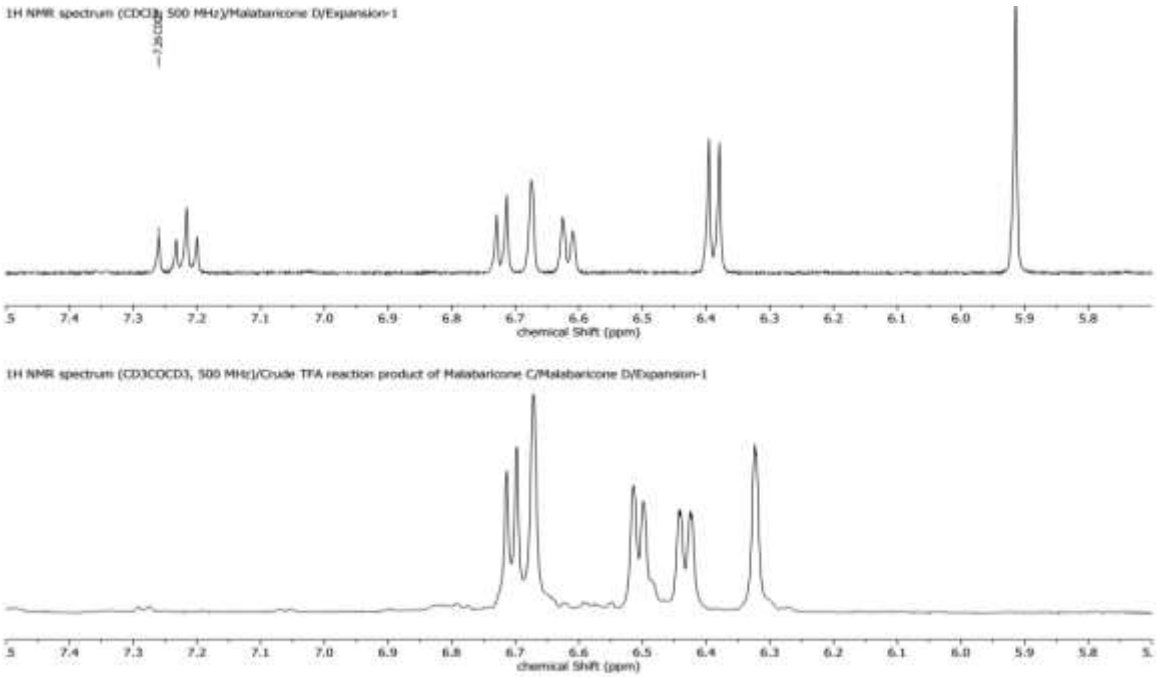

Figure S63: Expansion of ^{1}H NMR spectra of stacking plot of malabaricone D ($CDCl_3$, 500 MHz) and its crude TFA reaction products (CD_3COCD_3, 500 MHz).

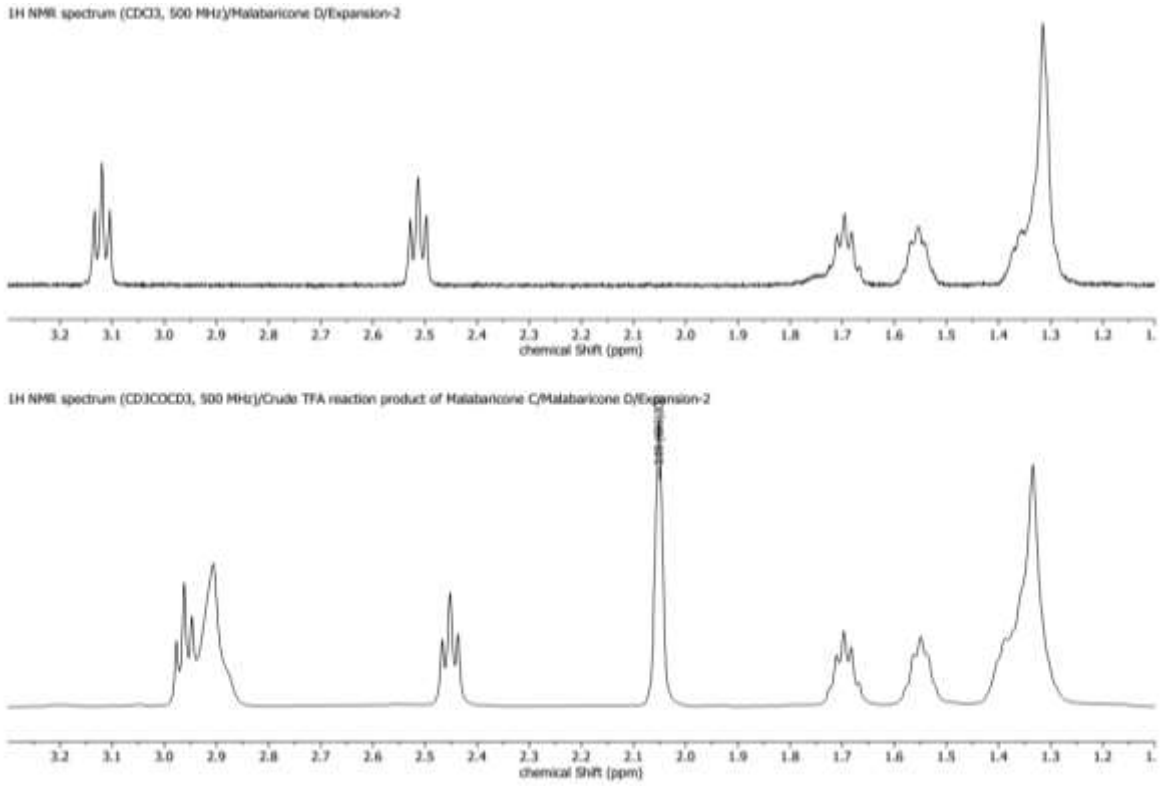

Figure S64: Expansion of ^{1}H NMR spectra of stacking plot of malabaricone D ($CDCl_3$, 500 MHz) and its crude TFA reaction products (CD_3COCD_3, 500 MHz).

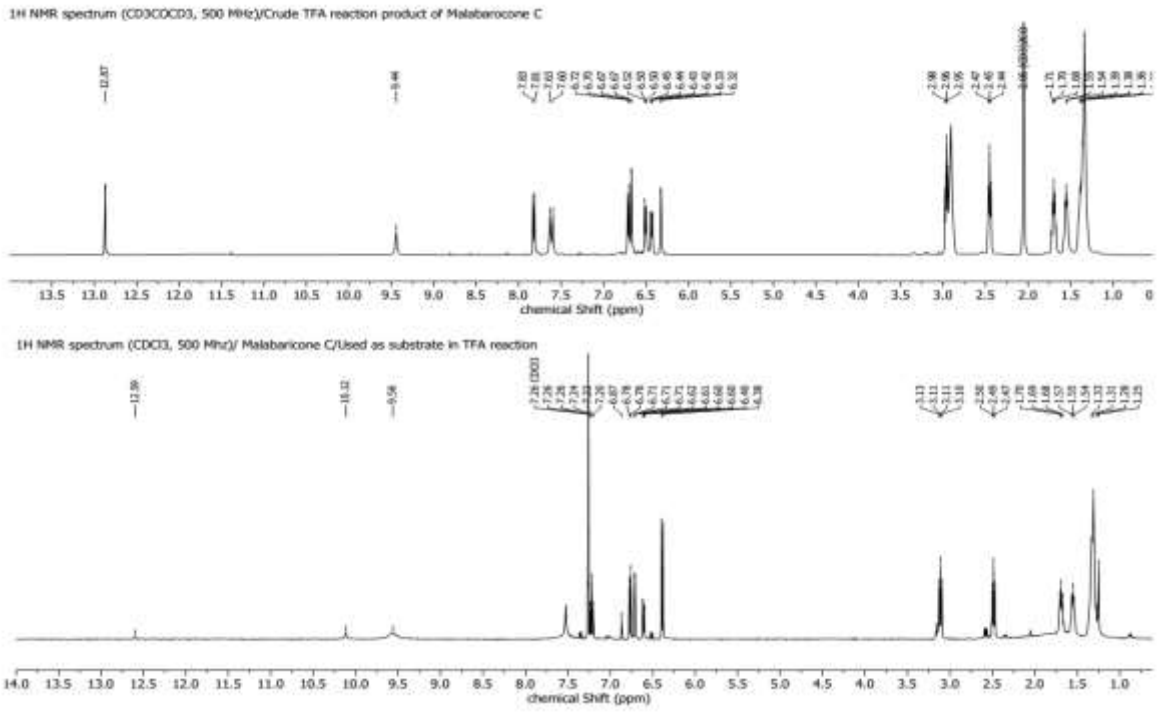

Figure S65: Stacking plot ^{1}H NMR spectra of crude TFA reaction products of malabaricone D (CD_3COCD_3, 500 MHz) and malabaricone D ($CDCl_3$, 500 MHz).

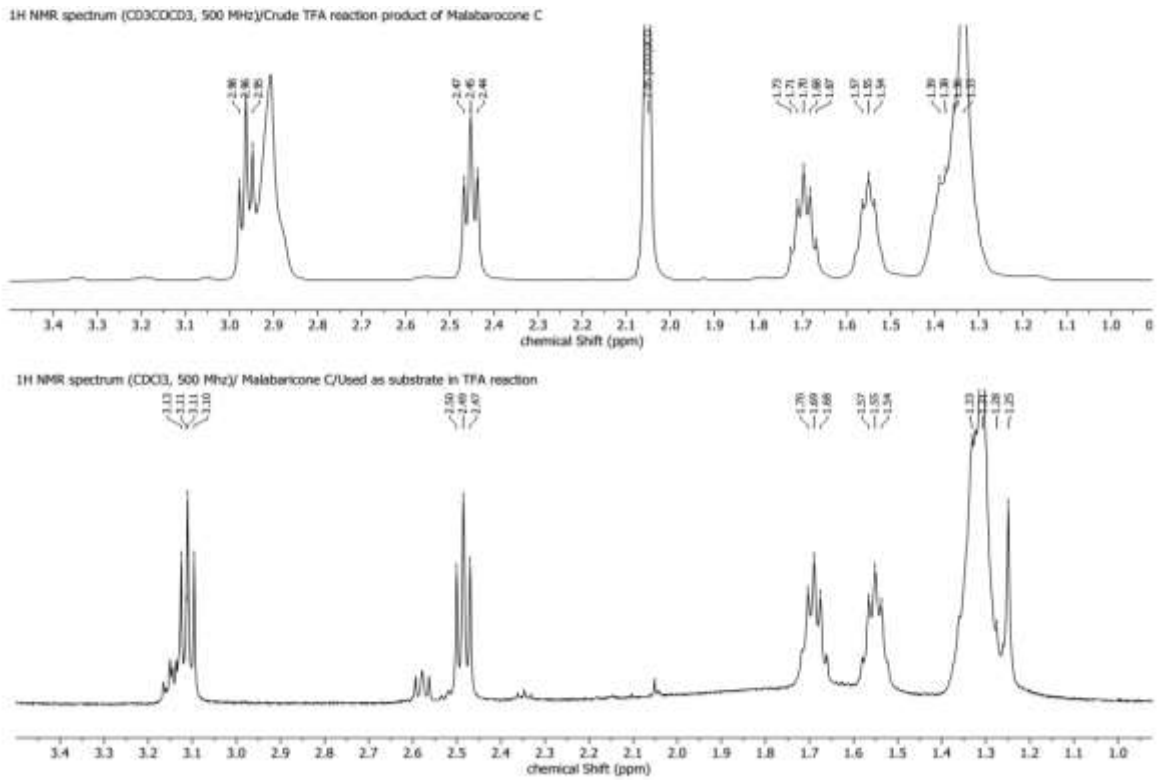

Figure S66: Expansion stacking plot ^{1}H NMR spectra of crude TFA reaction products of malabaricone D (CD_3COCD_3, 500 MHz) and malabaricone D ($CDCl_3$, 500 MHz).

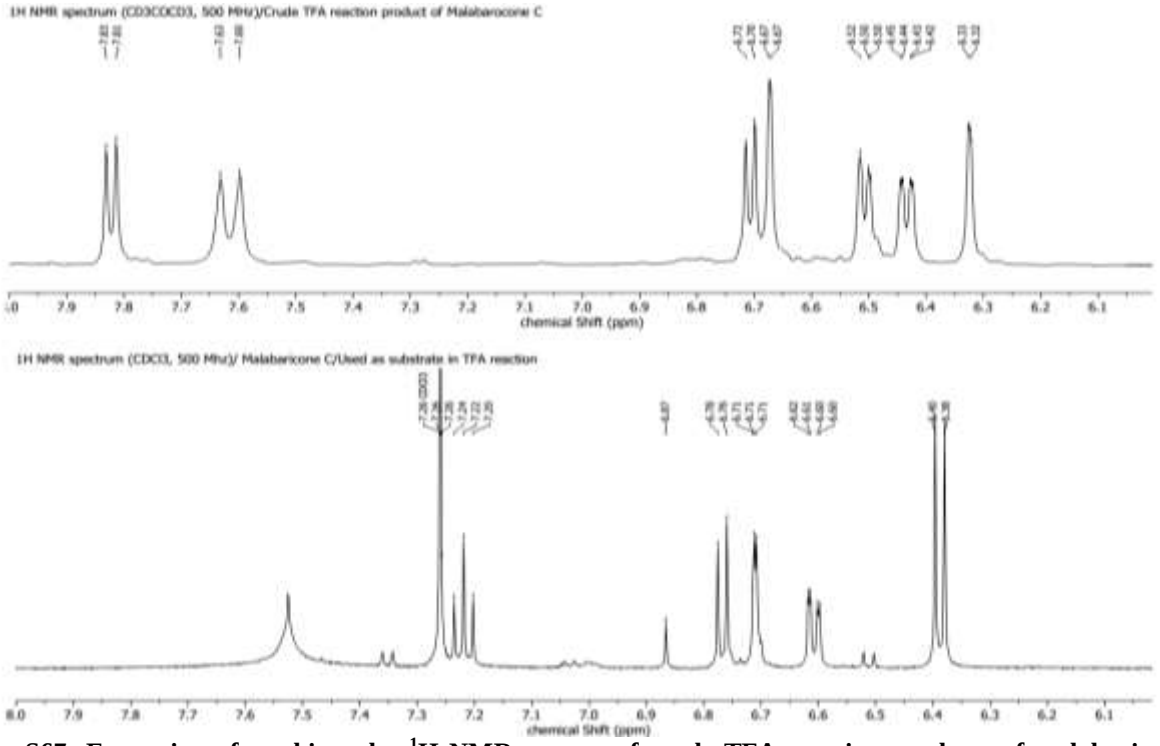

Figure S67: Expansion of stacking plot ^{1}H NMR spectra of crude TFA reaction products of malabaricone D (CD_3COCD_3, 500 MHz) and malabaricone D ($CDCl_3$, 500 MHz).

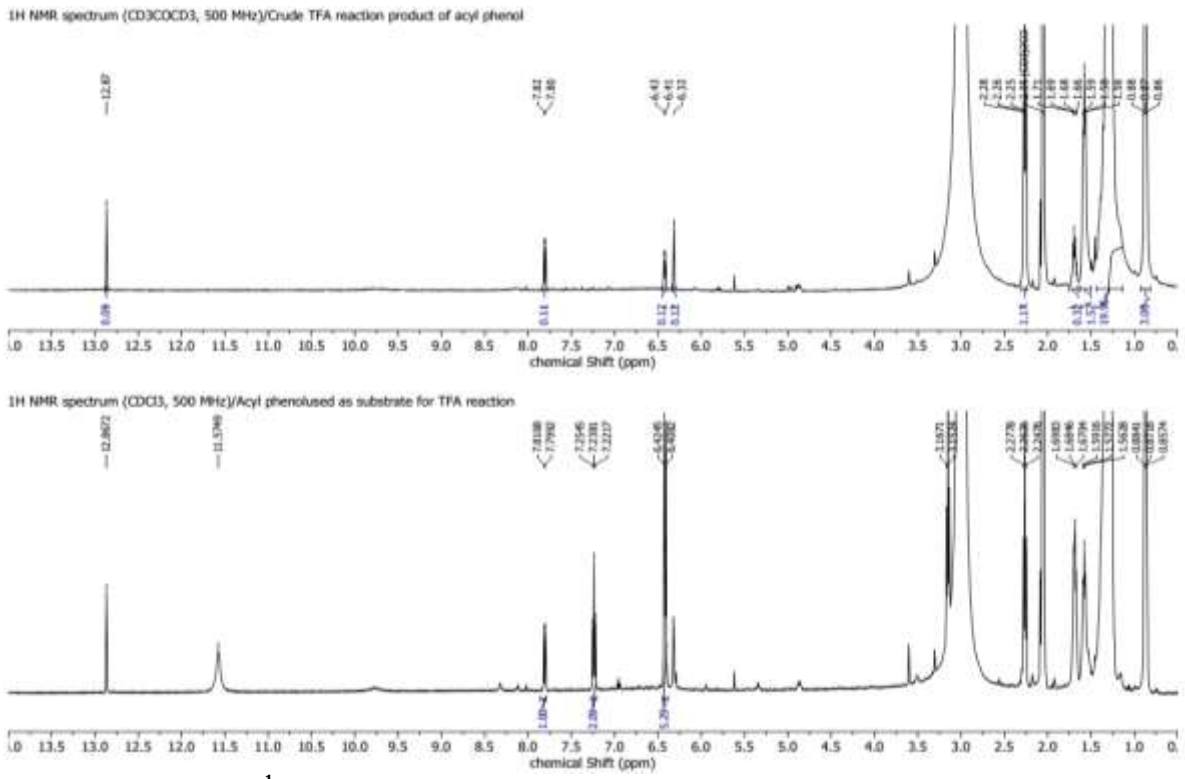

Figure 68: Stacking plot of ^{1}H NMR spectrum of acyl phenol (CD_3COCD_3, 500 MHz) and its crude TFA reaction products (CD_3COCD_3, 500 MHz).

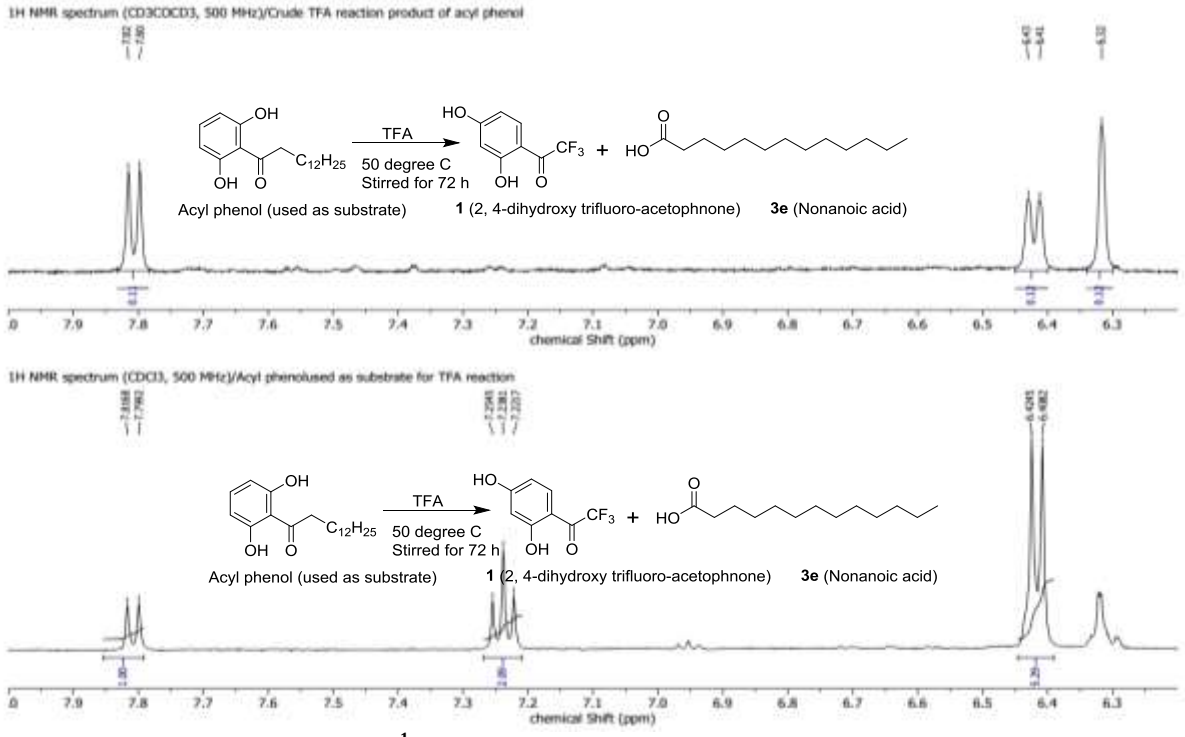

Figure 69: Expansion stacking plot of ^{1}H NMR spectrum of acyl phenol (CD_3COCD_3, 500 MHz) and its crude TFA reaction products (CD_3COCD_3, 500 MHz).

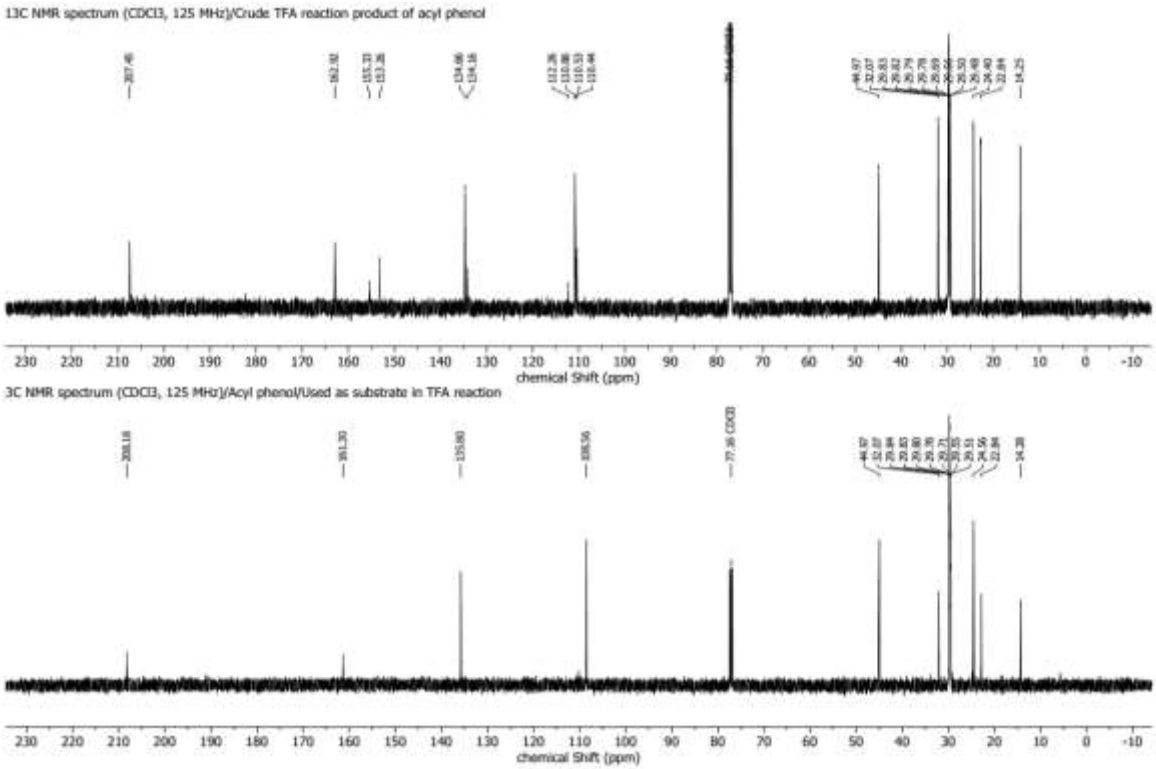

Figure 70: Stacking plot of ^{13}C NMR spectrum of acyl phenol (CD_3COCD_3, 125 MHz) and its crude TFA reaction products (CD_3COCD_3, 125 MHz).

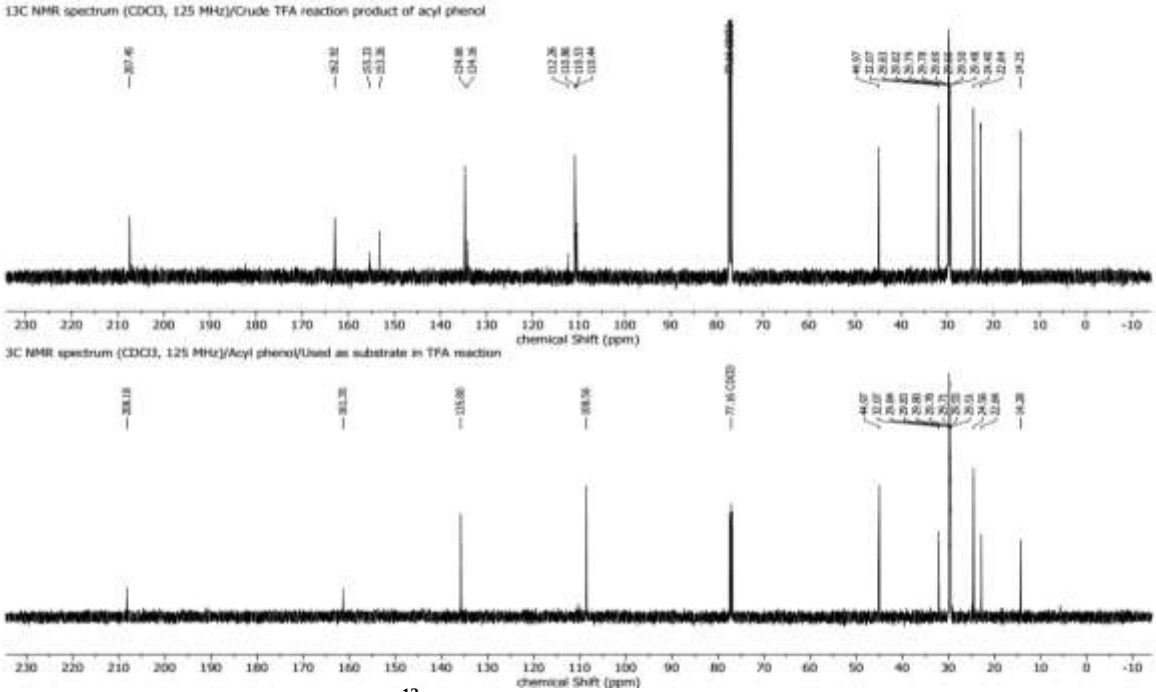

Figure 71: Expansion of stacking plot of ^{13}C NMR spectrum of acyl phenol (CD_3COCD_3, 125 MHz) and its crude TFA reaction products (CD_3COCD_3, 125 MHz).

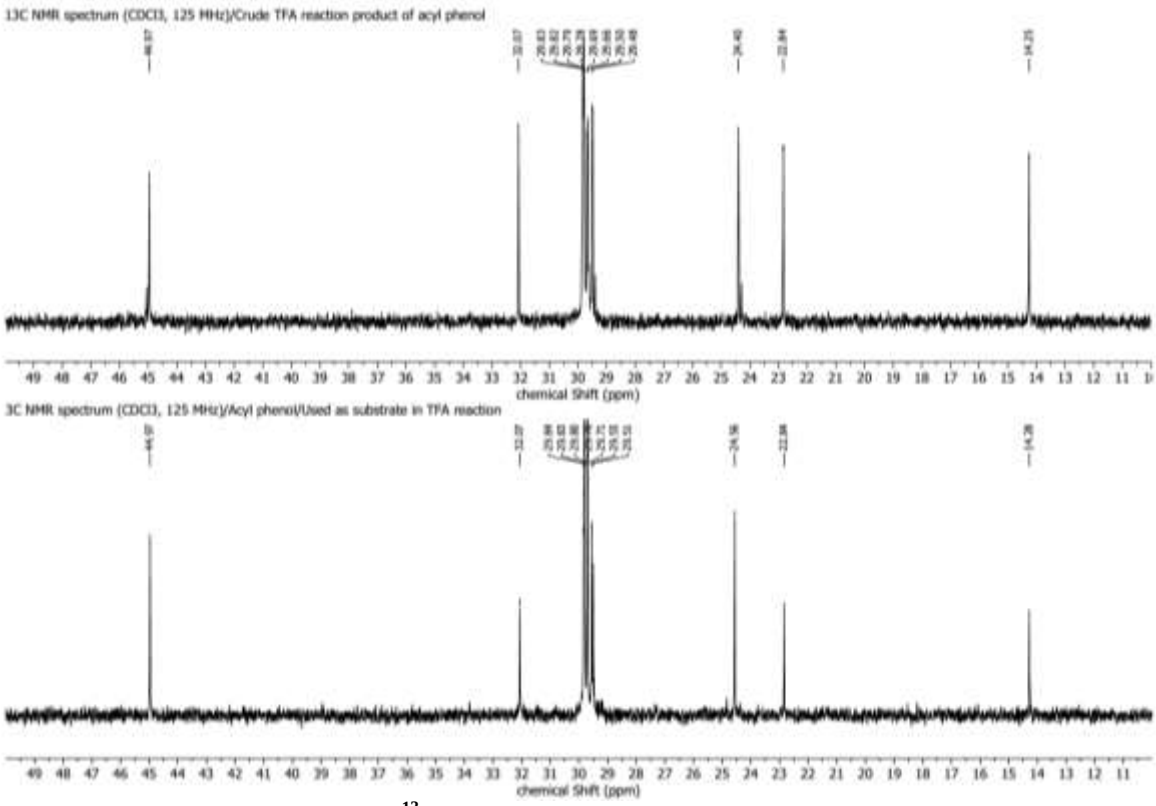

Figure 72: Expansion of stacking plot of ^{13}C NMR spectrum of acyl phenol (CD_3COCD_3, 125 MHz) and its crude TFA reaction products (CD_3COCD_3, 125 MHz).

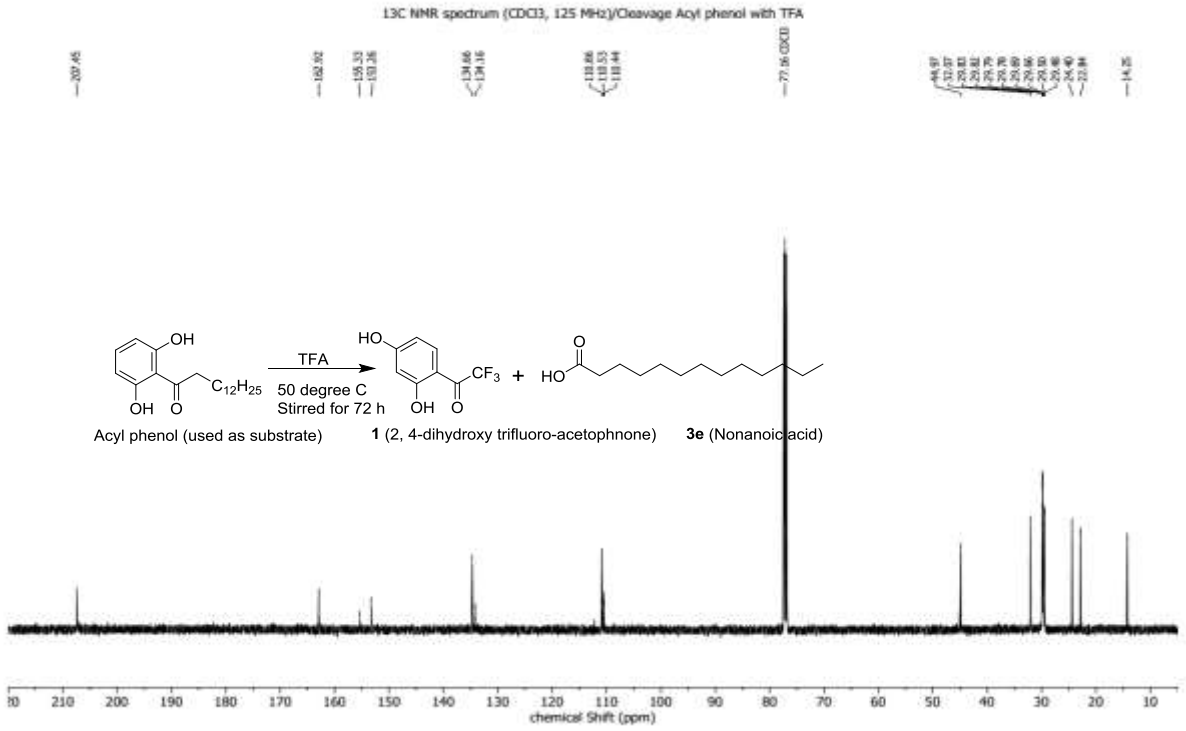

Figure S73: ^{13}C NMR spectrum ($CDCl_3$, 125 MHz) of crude TFA reaction products of acyl phenol.

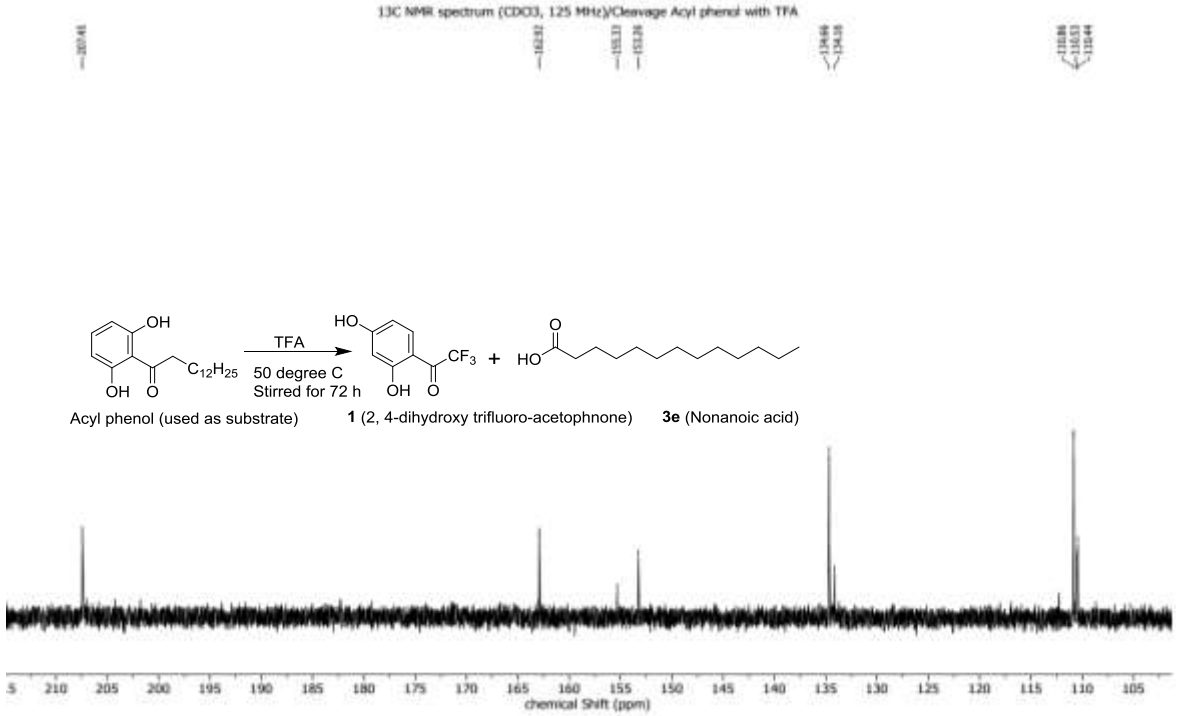

Figure 74: Expansion of ^{13}C NMR spectrum ($CDCl_3$, 125 MHz) of crude TFA reaction products of acyl phenol.

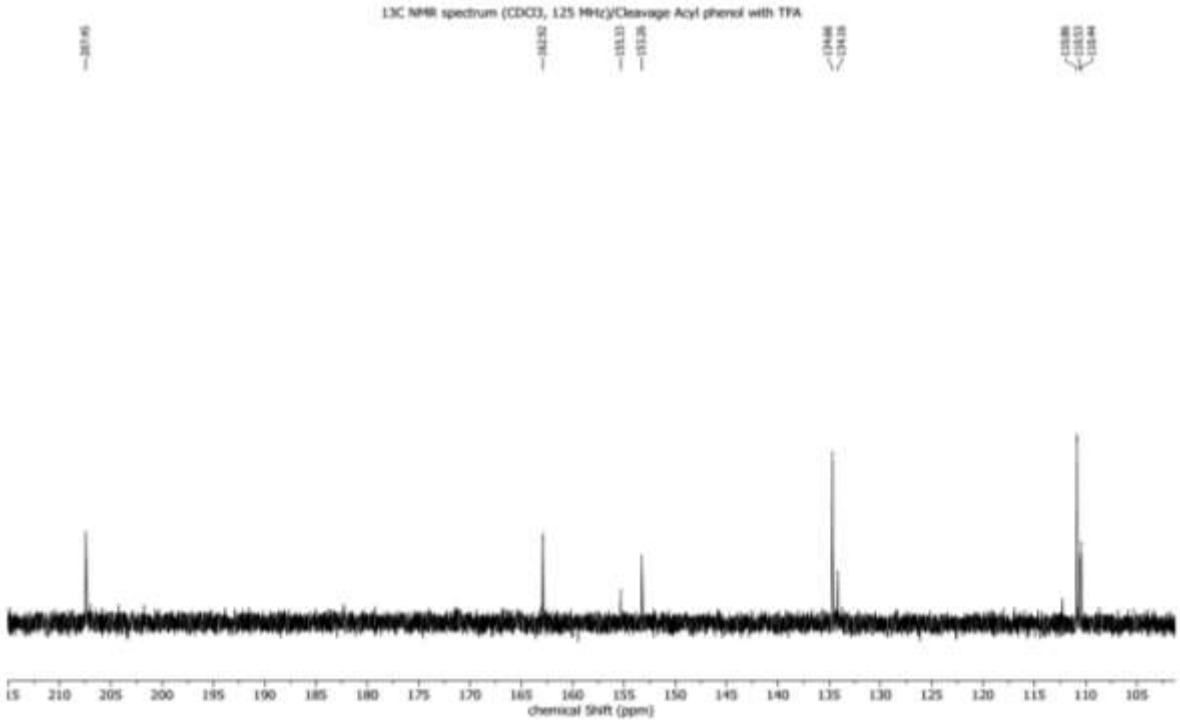

Figure 75: Expansion of ^{13}C NMR spectrum ($CDCl_3$, 125 MHz) of crude TFA reaction products of acyl phenol.

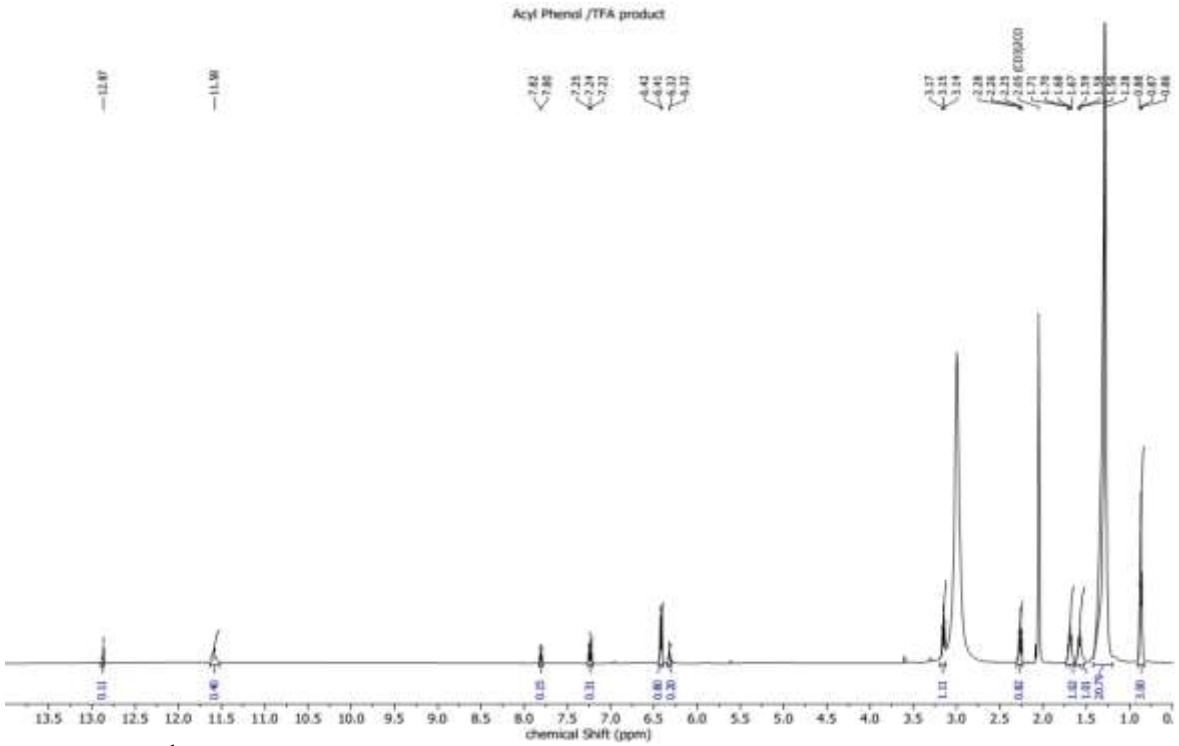

Figure 76: ^{1}H NMR spectrum ($CDCl_3$, 500 MHz) of crude TFA reaction products of acyl phenol.

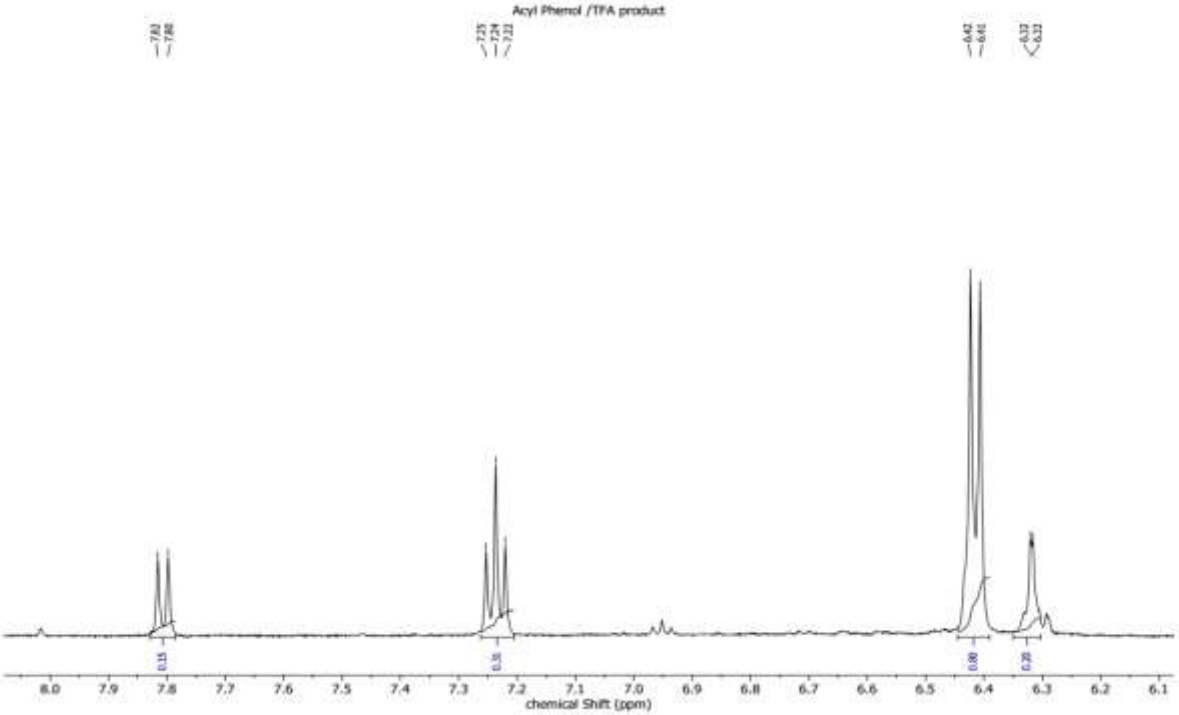

Figure 77: Expansion of ^{1}H NMR spectrum ($CDCl_3$, 500 MHz) of crude TFA reaction products of acyl phenol.

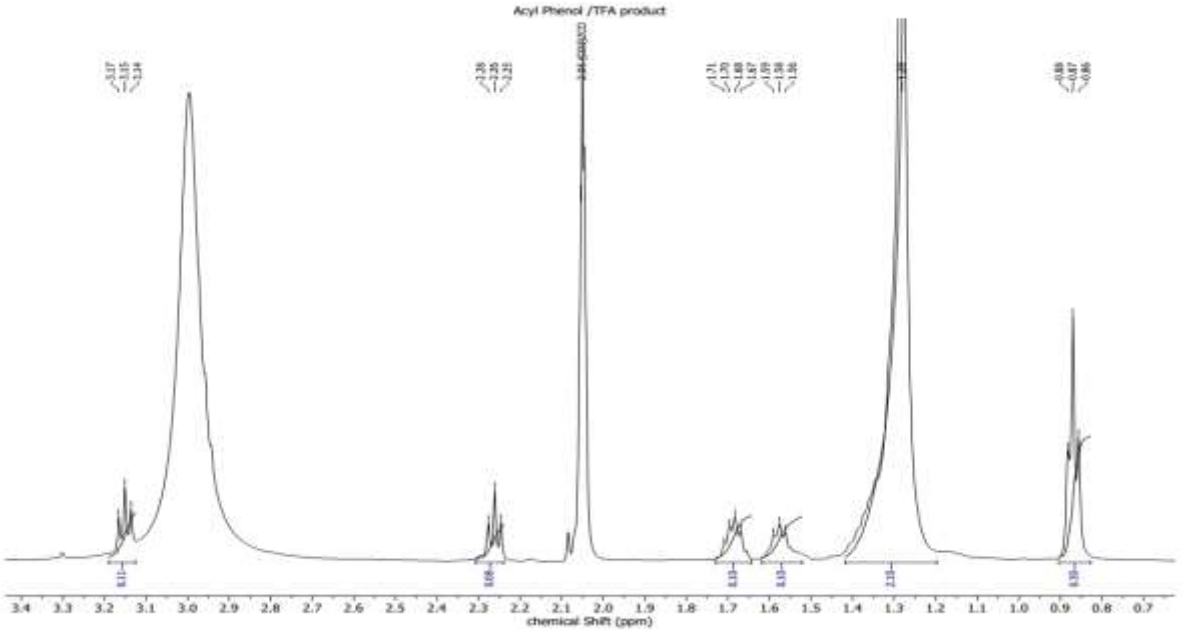

Figure 78: Expansion of ^{1}H NMR spectrum ($CDCl_3$, 500 MHz) of crude TFA reaction products of acyl phenol.

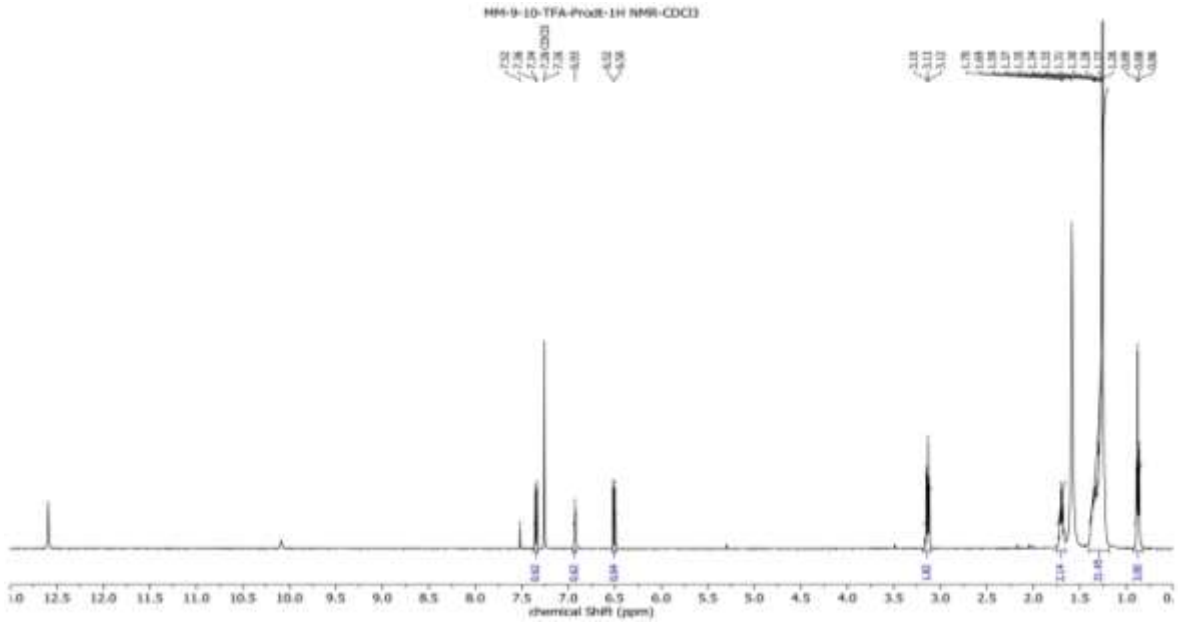

Figure S79: ^{1}H NMR spectrum ($CDCl_3$, 500 MHz) of crude TFA reaction product of acyl phenol.

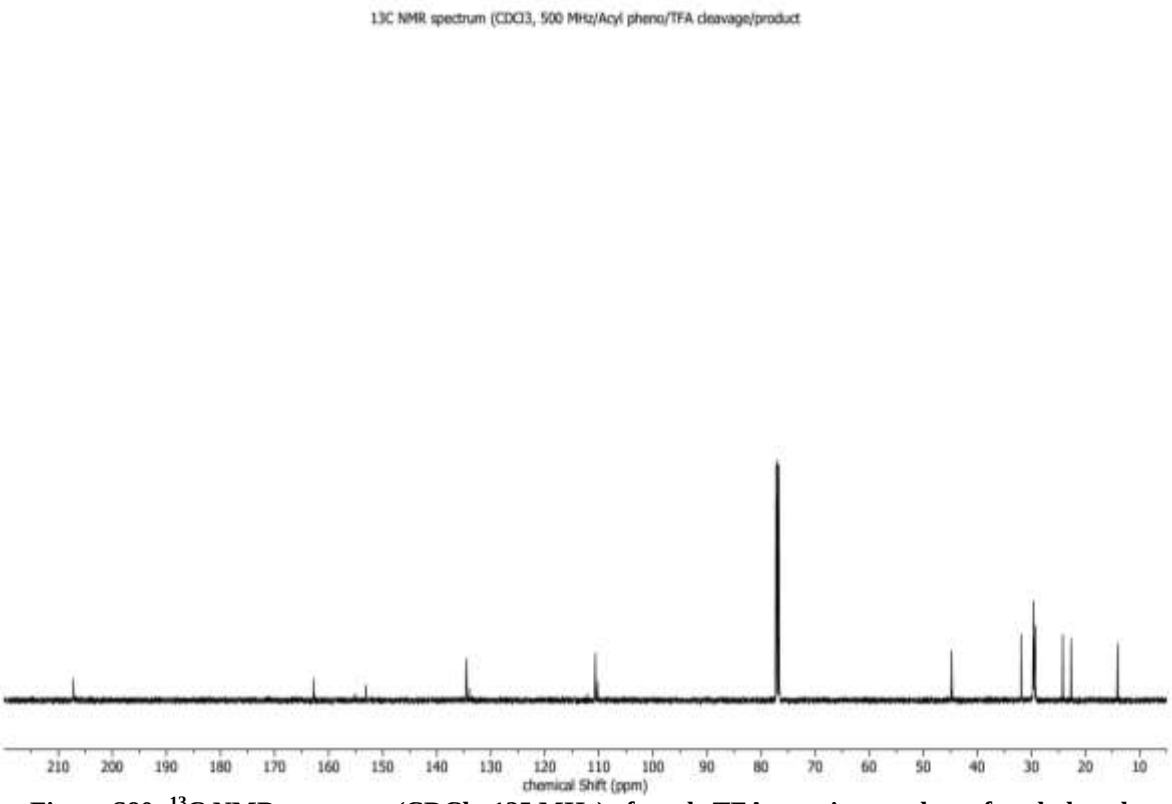

Figure S80: ^{13}C NMR spectrum ($CDCl_3$, 125 MHz) of crude TFA reaction product of acyl phenol.

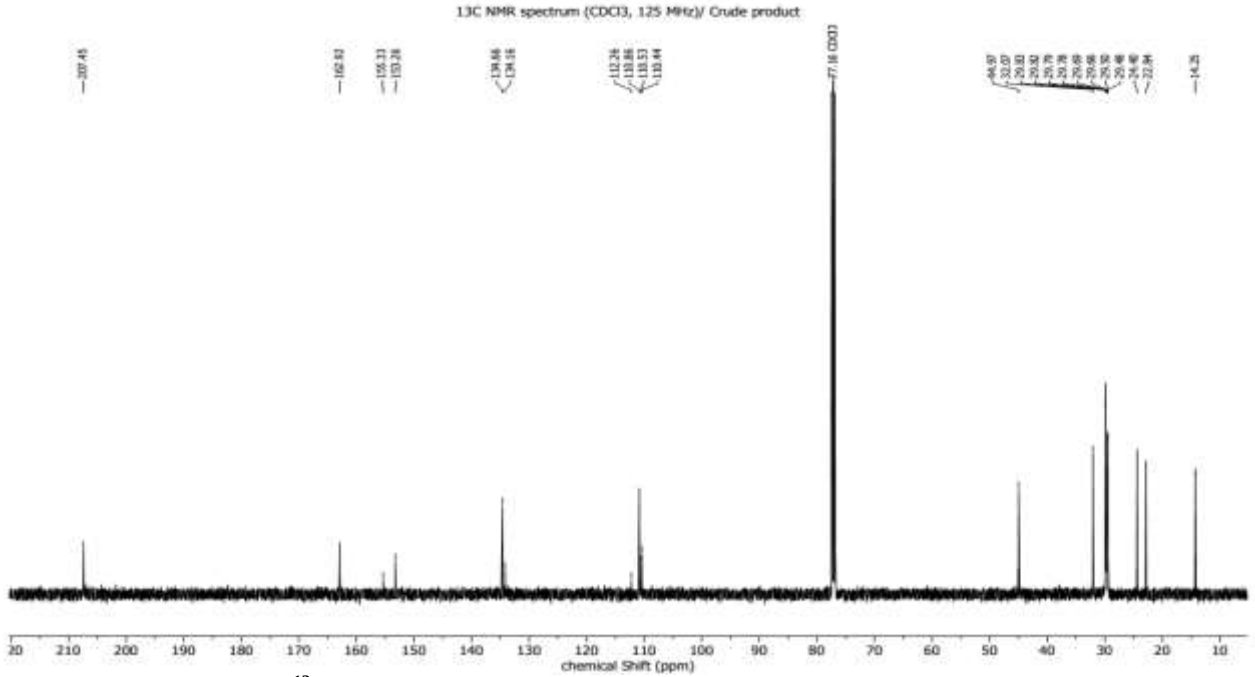

Figure S81: Expansion of ^{13}C NMR spectrum ($CDCl_3$, 125 MHz) of crude TFA reaction product of acyl phenol.

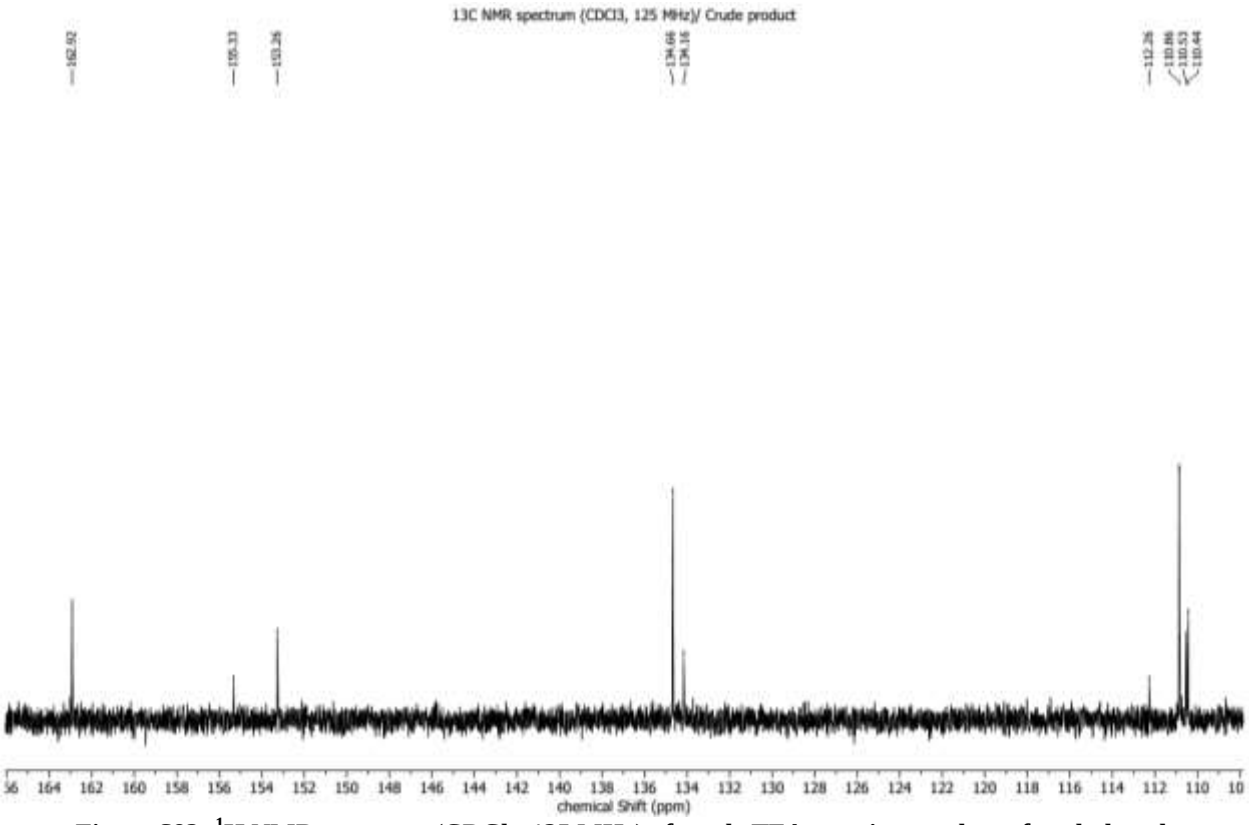

Figure S82: ^{1}H NMR spectrum ($CDCl_3$, 125 MHz) of crude TFA reaction product of acyl phenol.

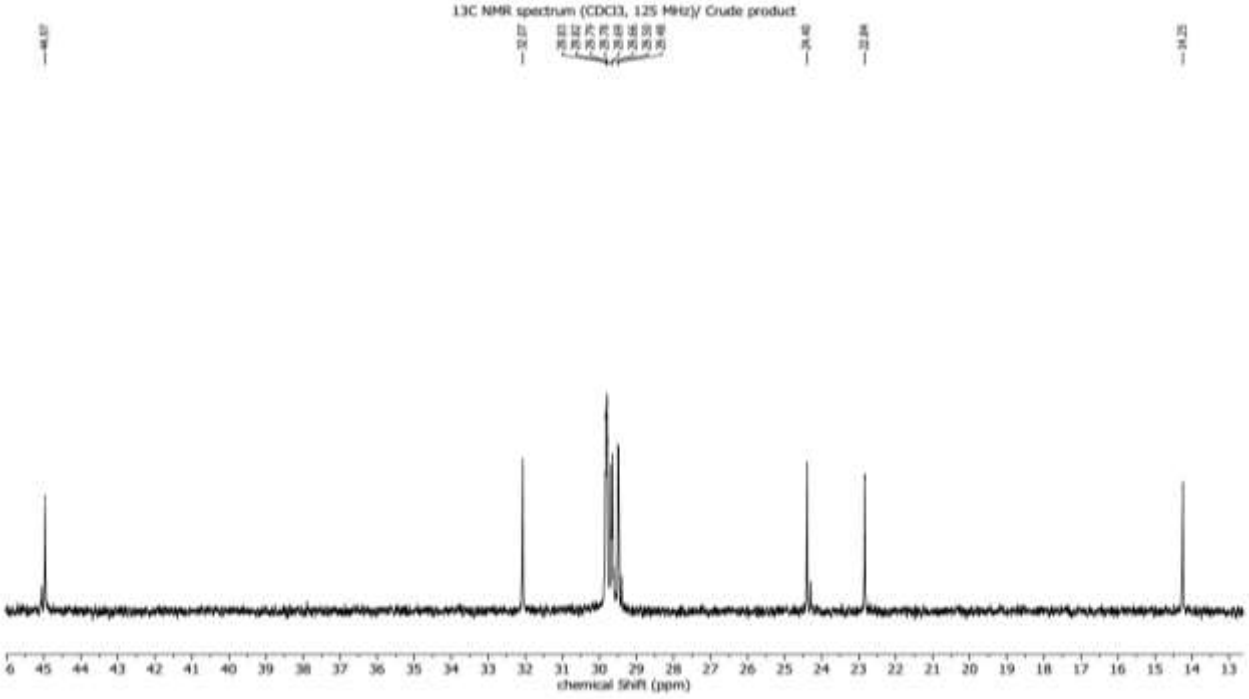

Figure S83: ^{1}H NMR spectrum ($CDCl_3$, 125 MHz) of crude TFA reaction product of acyl phenol.

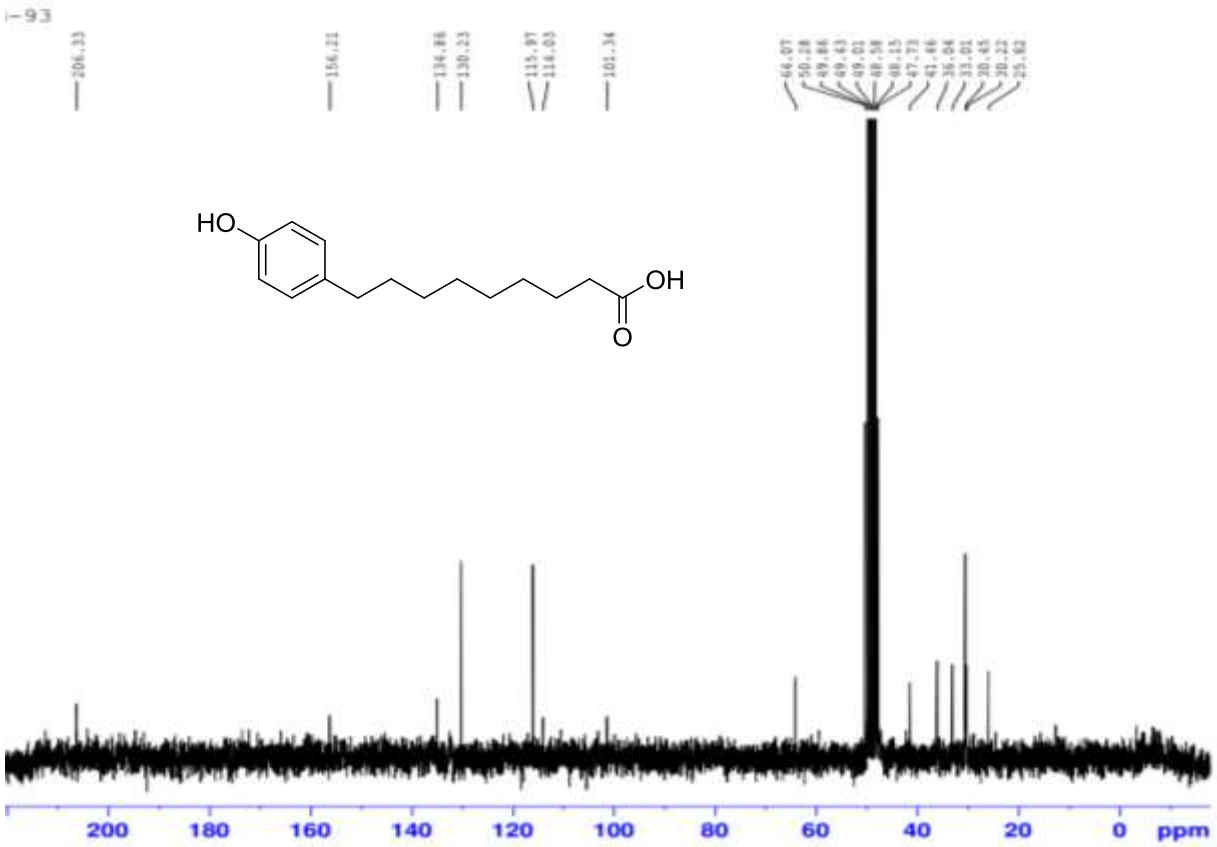

Figure S84: ^{13}C NMR spectrum (CD_3COCD_3, 125 MHz) of [9(4-hydroxy phenyl) nonanoic acid].

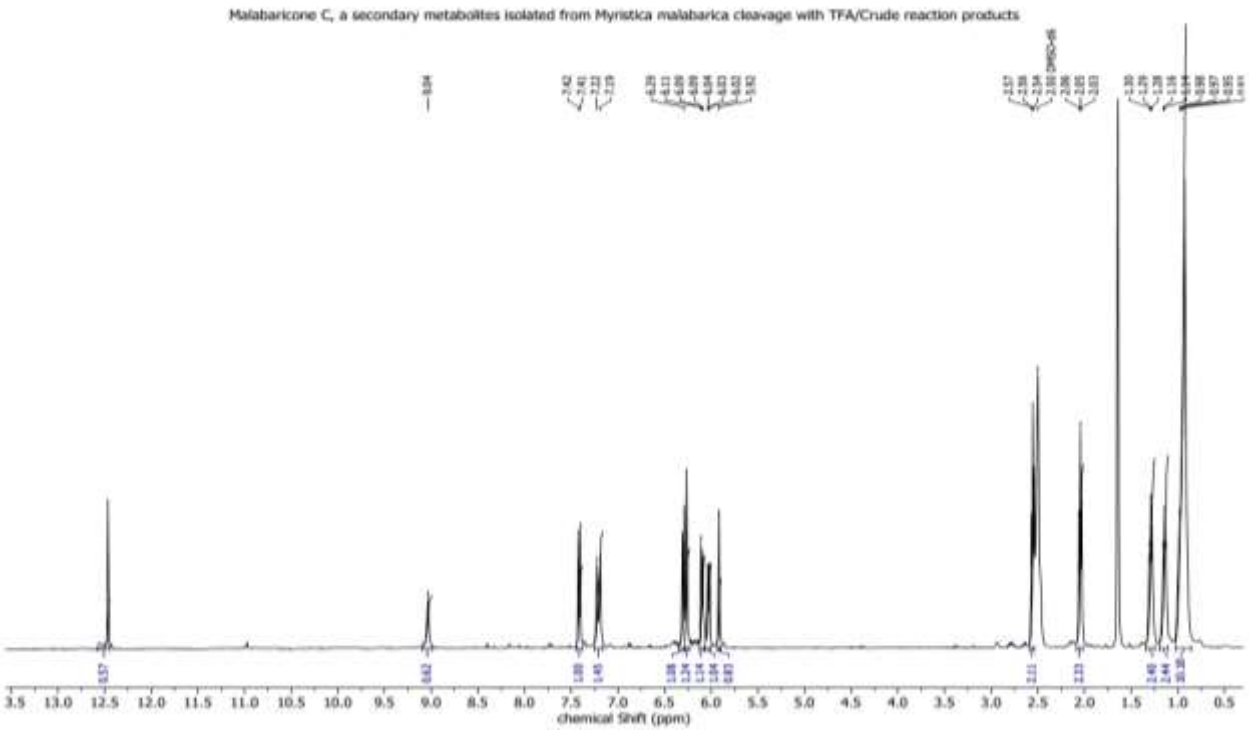

Figure S85: ^{1}H NMR spectrum ($CDCl_3$, 500 MHz) of crude TFA reaction products of malabaricone C.

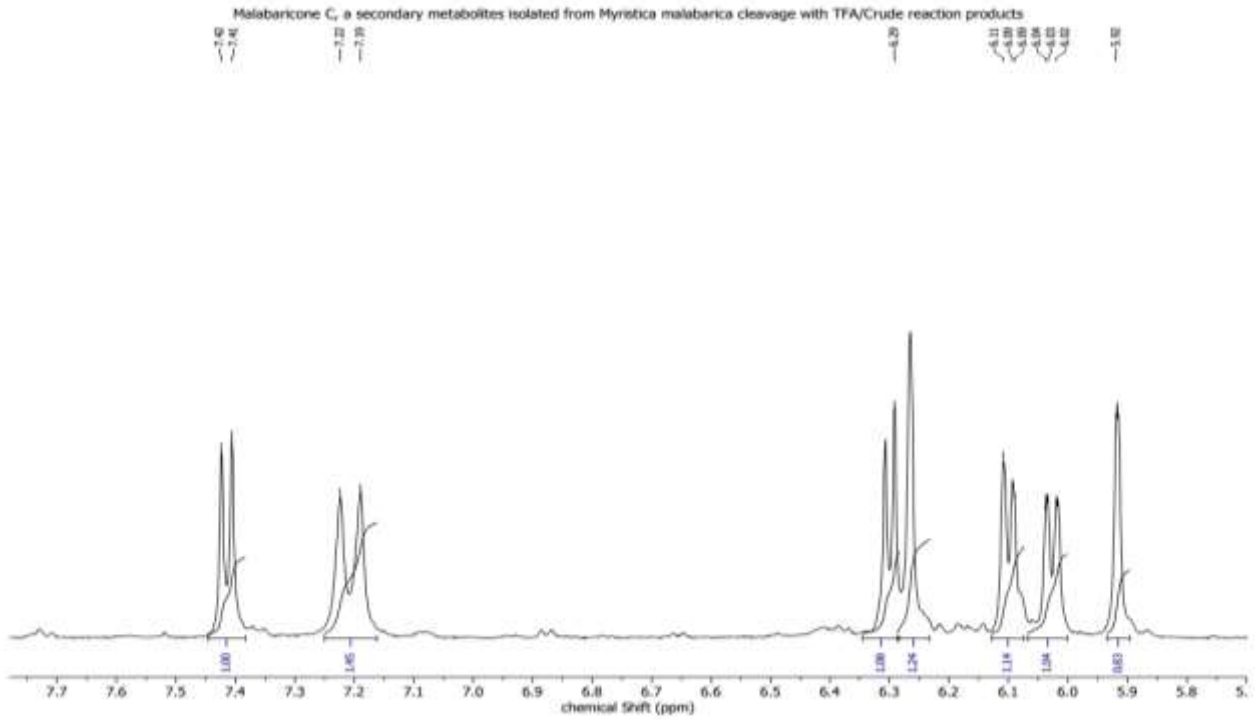

Figure S86: Expansion of ^{1}H NMR spectrum (CD_3COCD_3, 500 MHz) of crude TFA reaction products of malabaricone C.

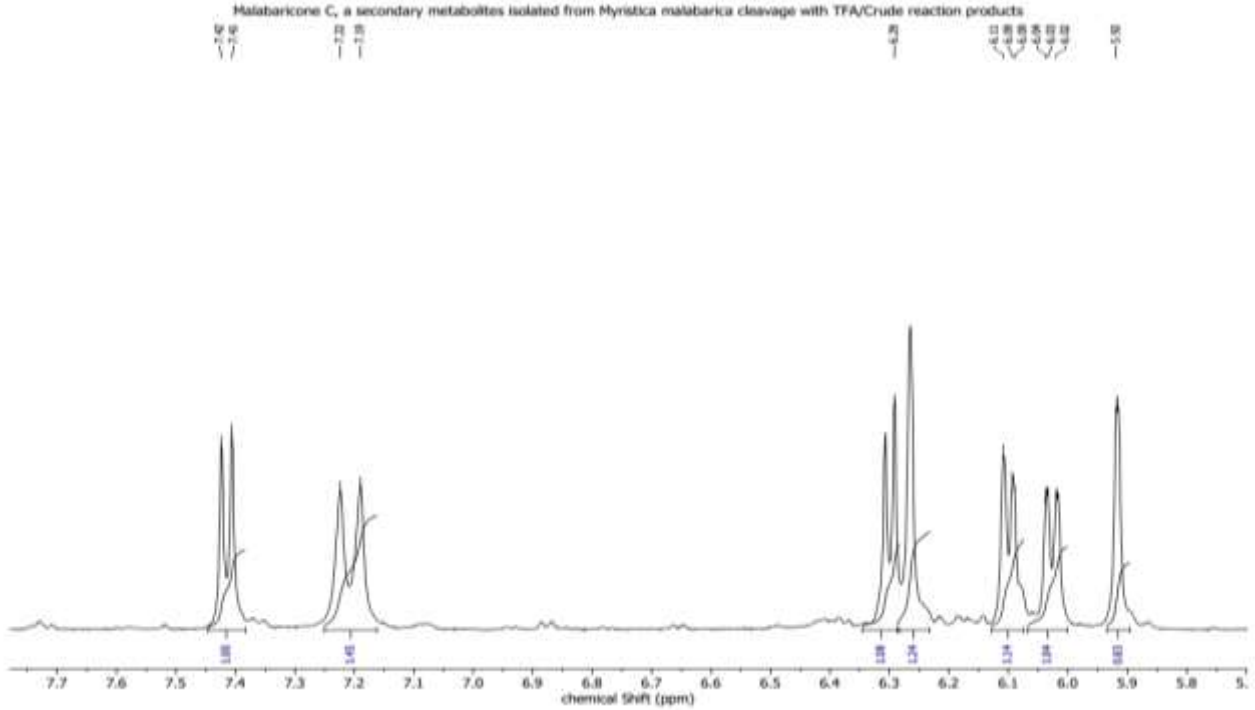

Figure S87: Expansion of ^{1}H NMR spectrum (CD_3COCD_3, 500 MHz) of crude TFA reaction products of malabaricone C.

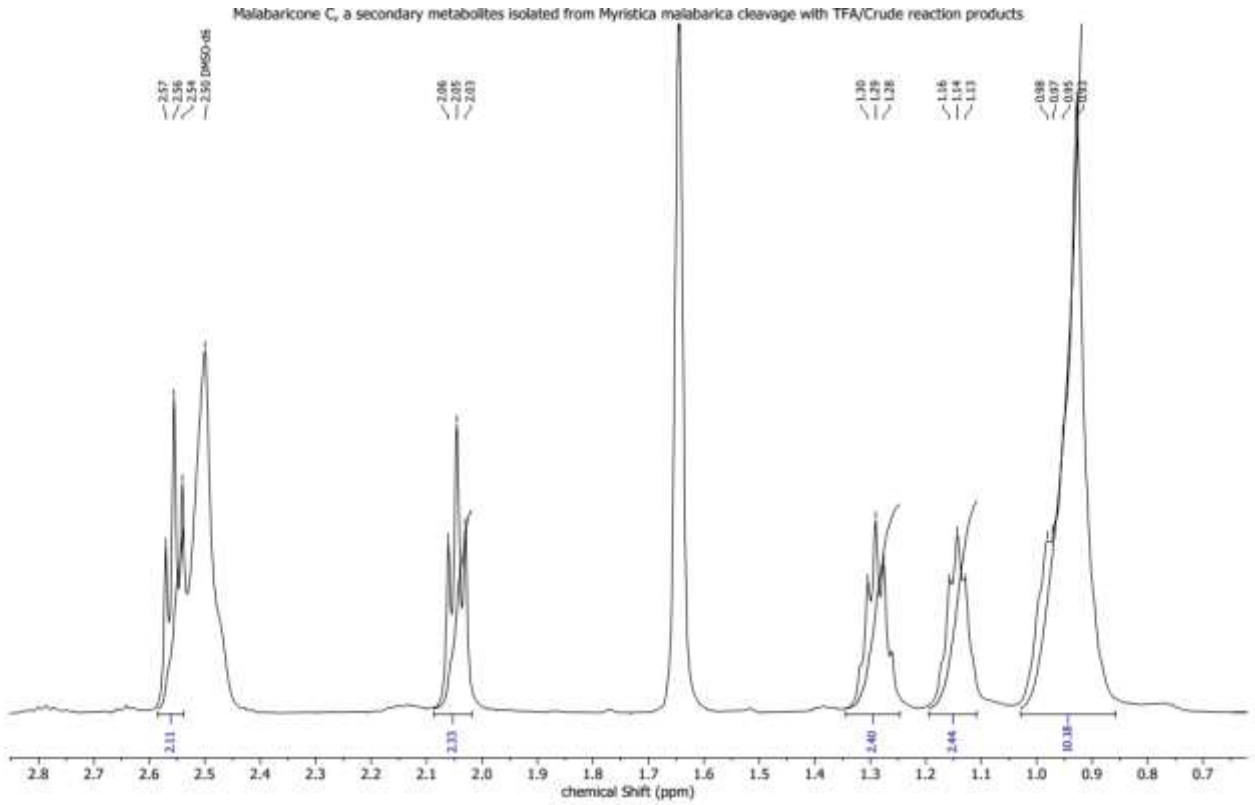

Figure S88: Expansion of ^{1}H NMR spectrum (CD_3COCD_3, 500 MHz) of crude TFA reaction products of malabaricone C.

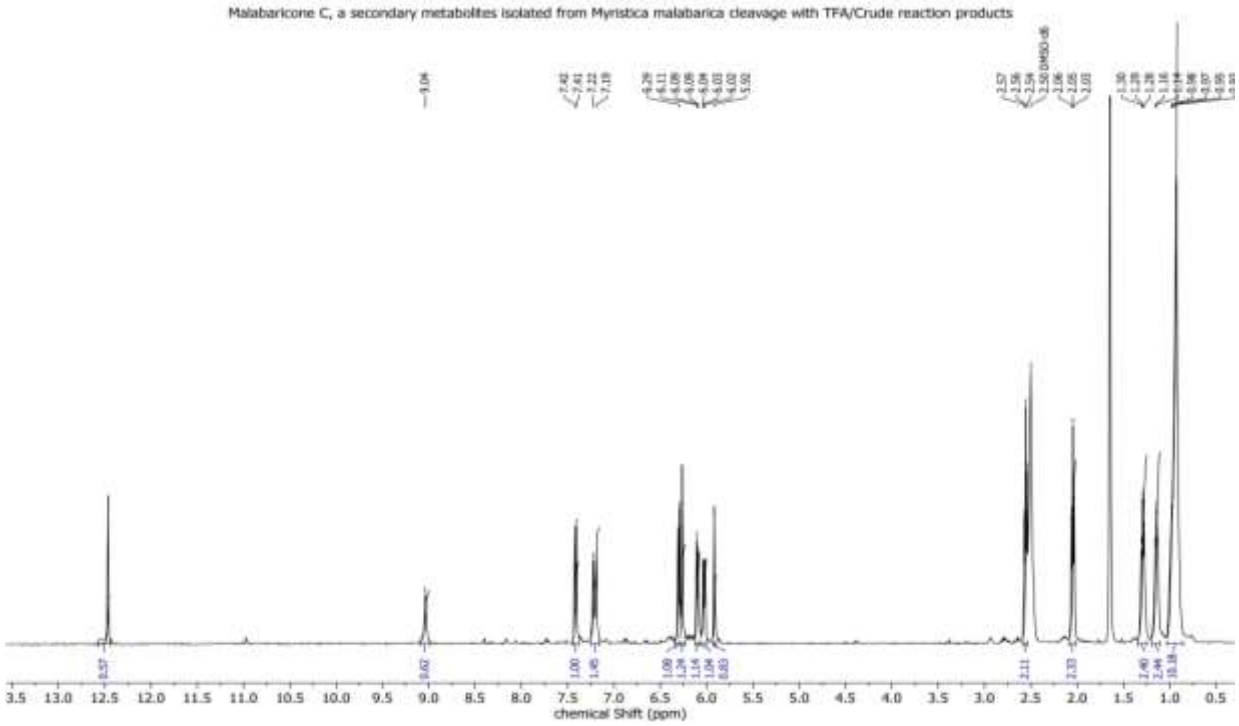

Figure S89: Stacking plot of ^{1}H NMR spectrum (CD_3COCD_3, 500 MHz) of malabaricone C and its crude TFA reaction products.

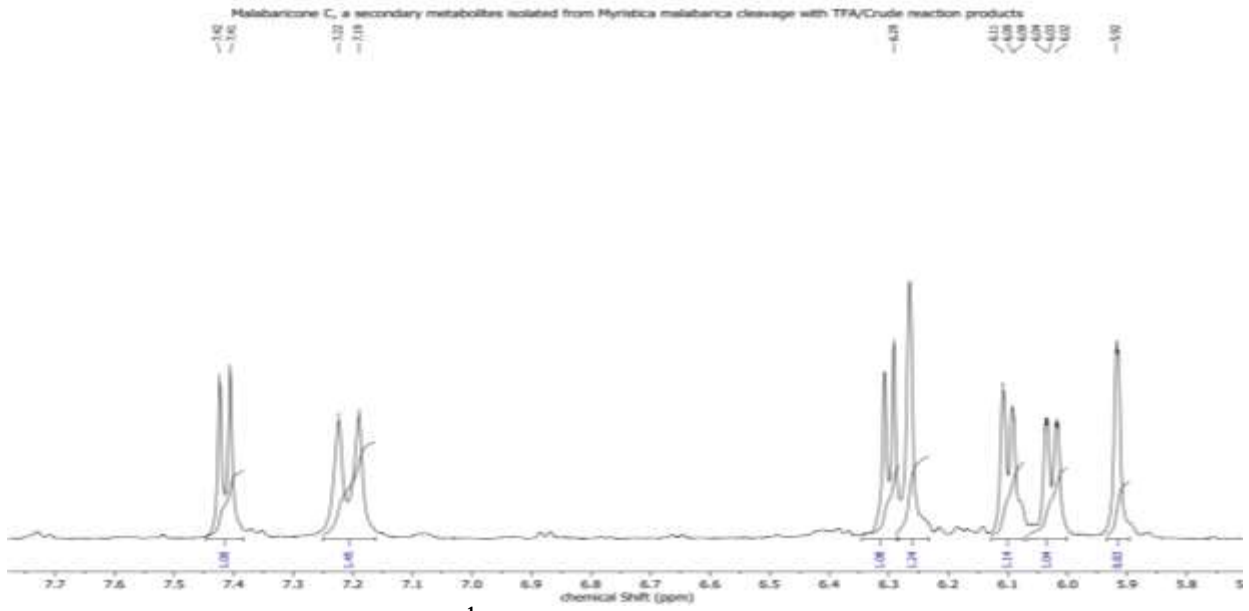

Figure S90: Expansion of stacking plot of ^{1}H NMR spectrum (CD_3COCD_3, 500 MHz) of malabaricone C and its crude TFA reaction products.

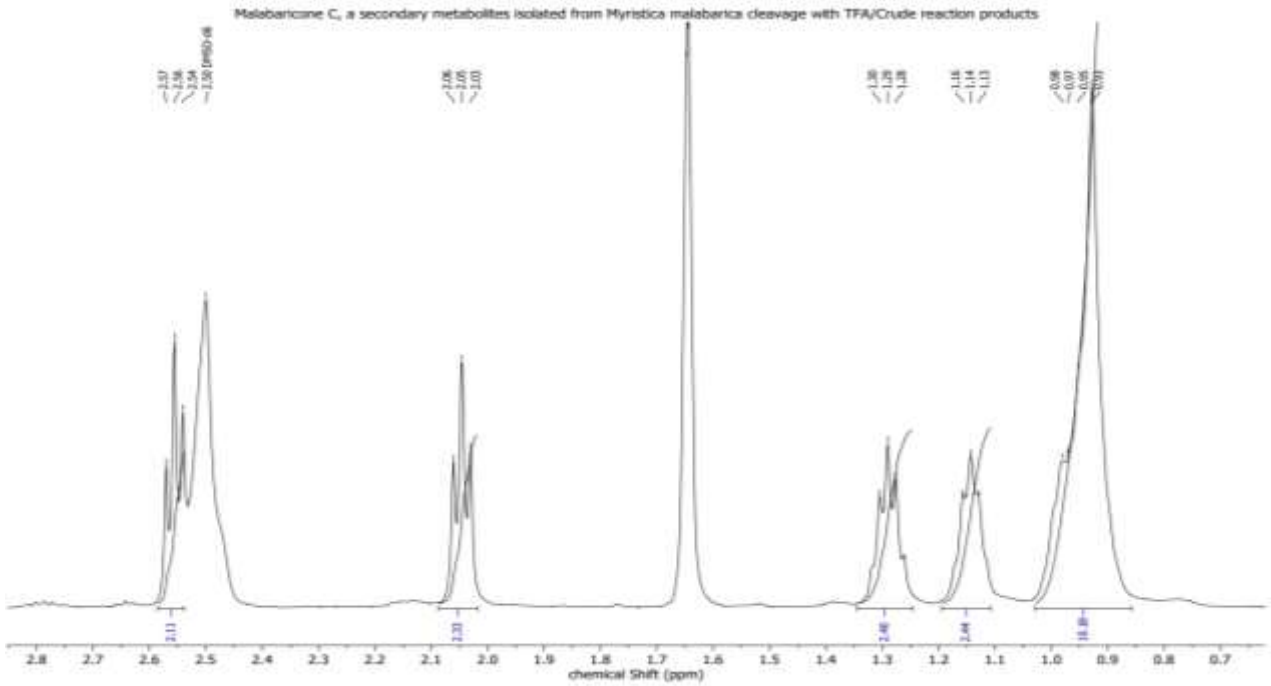

Figure S91: Expansion of stacking plot of ^{1}H NMR spectrum (CD_3COCD_3, 500 MHz) of malabaricone C and its crude TFA reaction products.

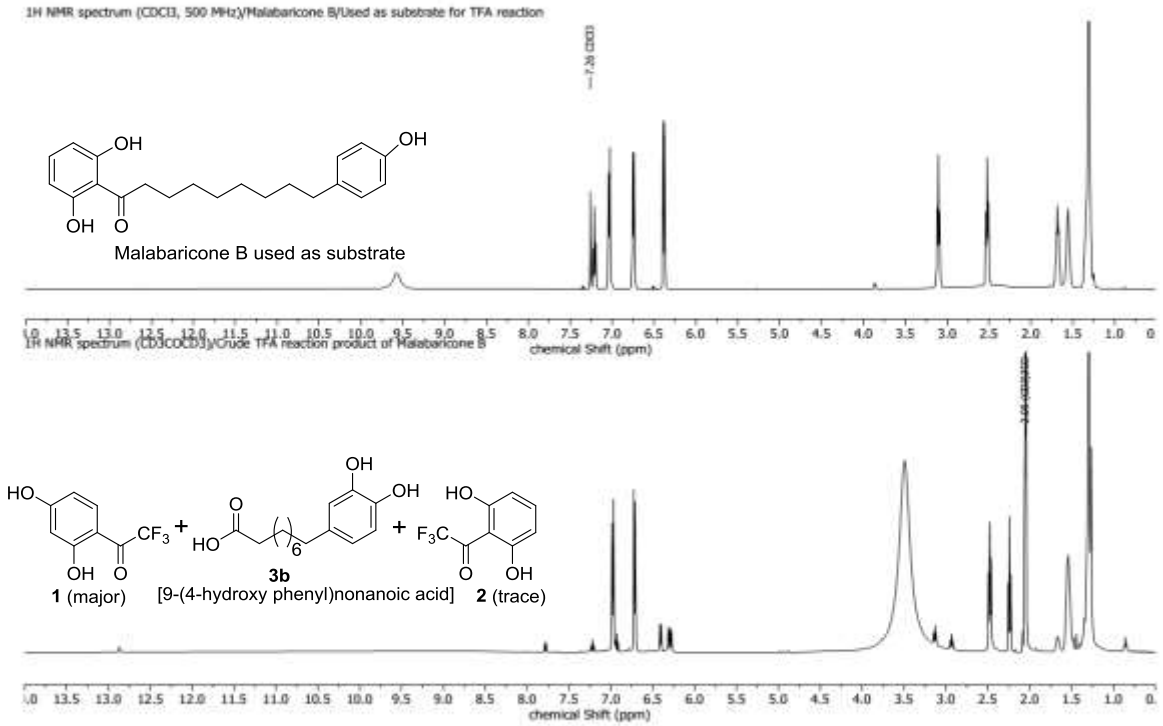

Figure S92: Stacking plot of ^{1}H NMR spectra ($CDCl_3$, 500 MHz) of malabaricone B and its TFA reaction products (CD_3COCD_3, 500 MHz).

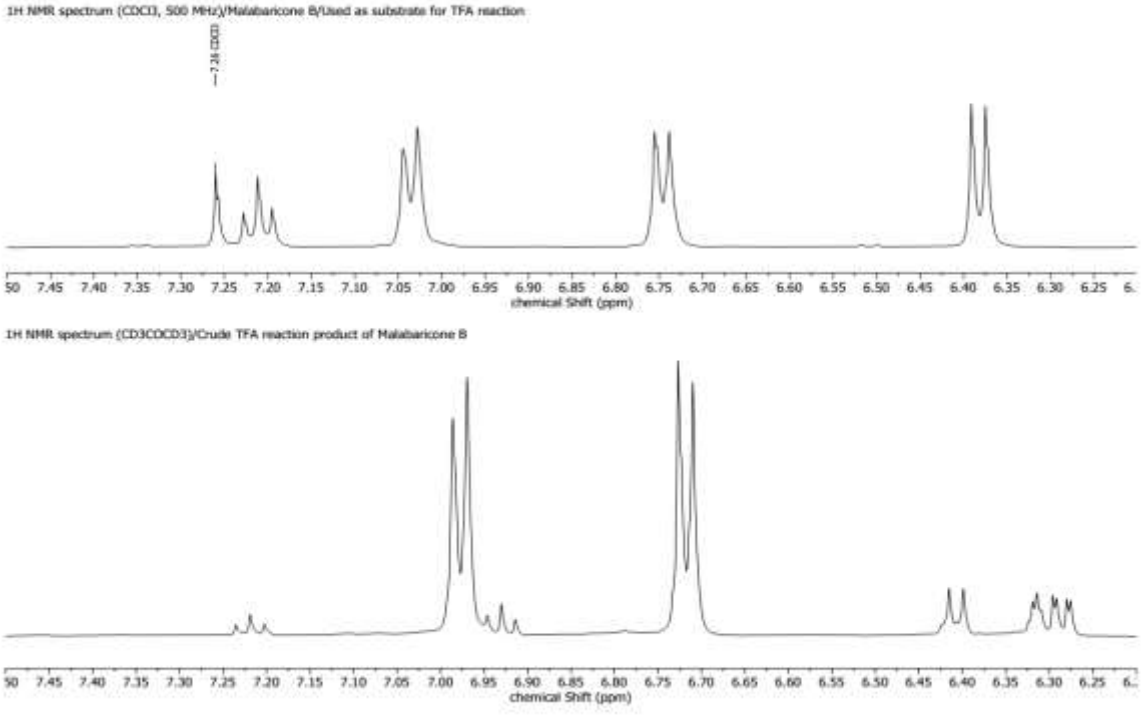

Figure S93: Expansion of stacking plot of ^{1}H NMR spectra ($CDCl_3$, 500 MHz) of malabaricone B and its TFA reaction products (CD_3COCD_3, 500 MHz).

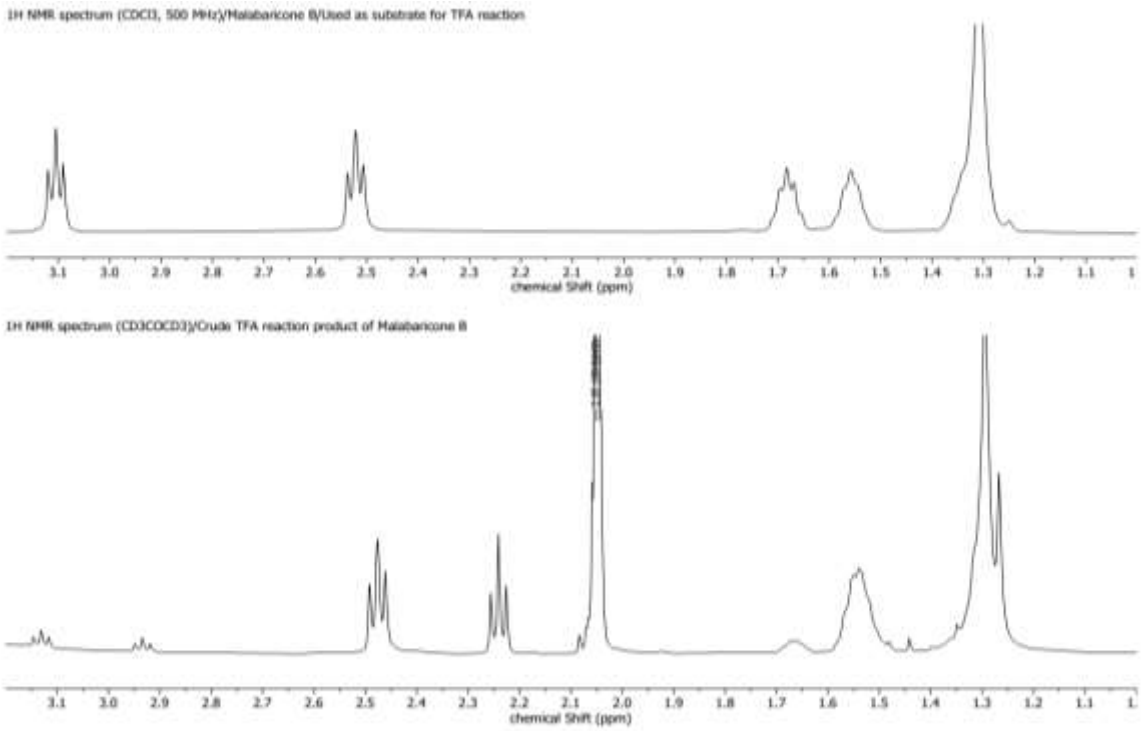

Figure S94: Expansion of stacking plot of ^{1}H NMR spectra ($CDCl_3$, 500 MHz) of malabaricone B and its TFA reaction products (CD_3COCD_3, 500 MHz).

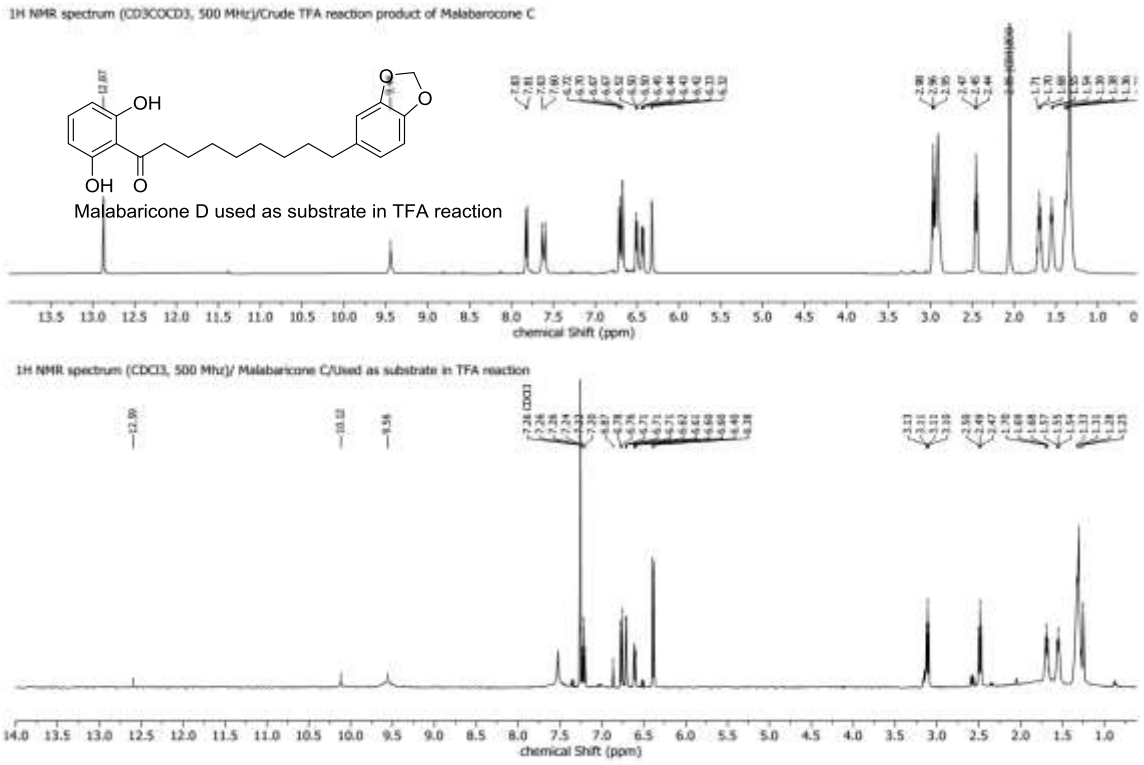

Figure S95: Stacking plot of ^{1}H NMR spectra ($CDCl_3$, 500 MHz) of malabaricone C and its TFA reaction products (CD_3COCD_3, 500 MHz).

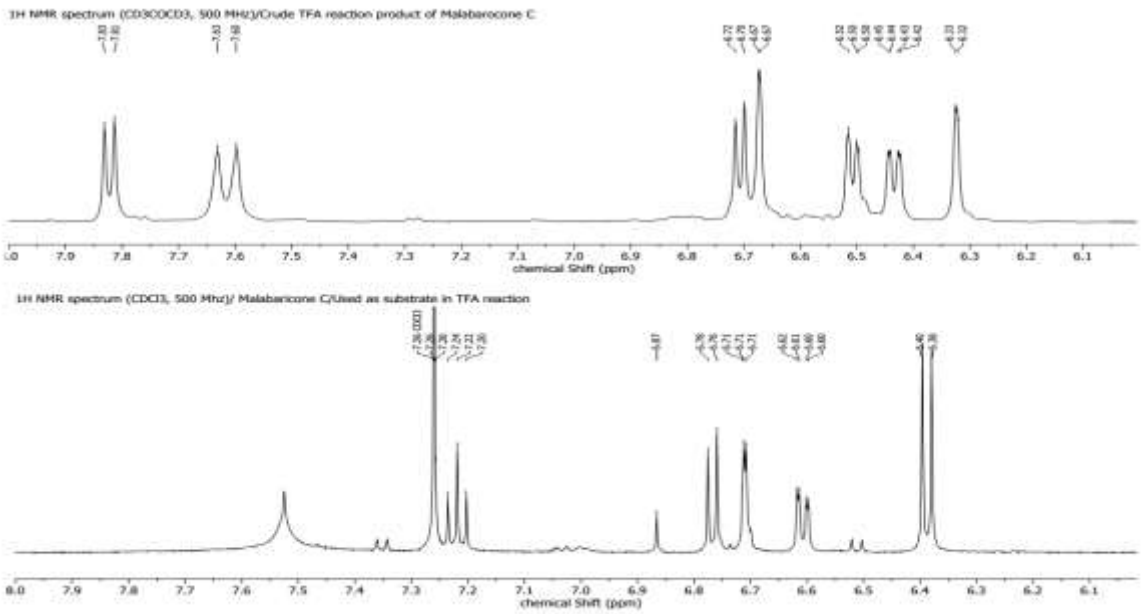

Figure S96: Expansion of stacking plot of ^{1}H NMR spectra ($CDCl_3$, 500 MHz) of malabaricone C and its TFA reaction products (CD_3COCD_3, 500 MHz).

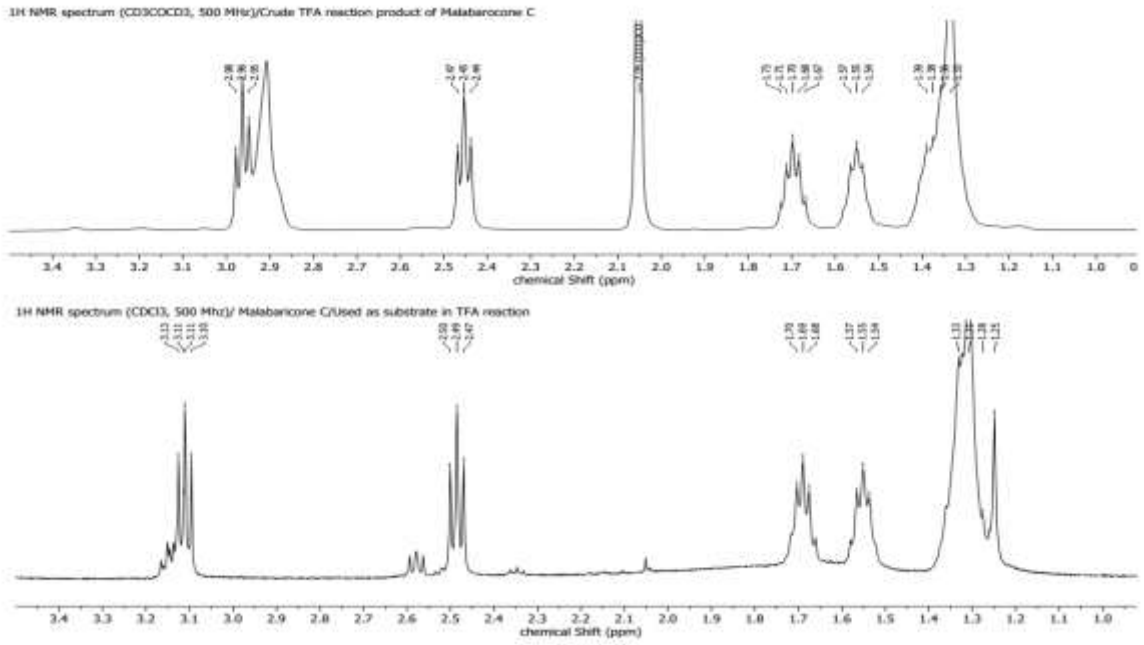

Figure S97: Expansion of stacking plot of ^{1}H NMR spectra ($CDCl_3$, 500 MHz) of malabaricone C and its TFA reaction products (CD_3COCD_3, 500 MHz).

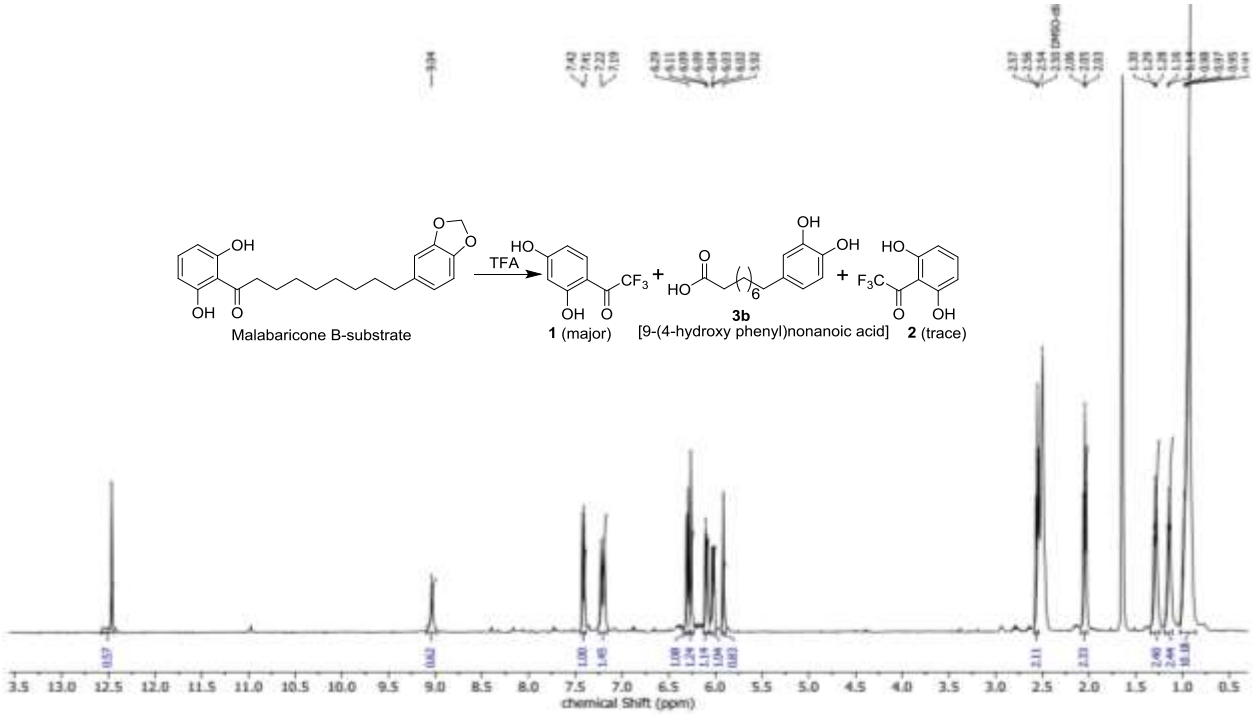

Figure S98: Stacking plot of ^{1}H NMR spectra ($CDCl_3$, 500 MHz) of malabaricone D and its TFA reaction products (CD_3COCD_3, 500 MHz).

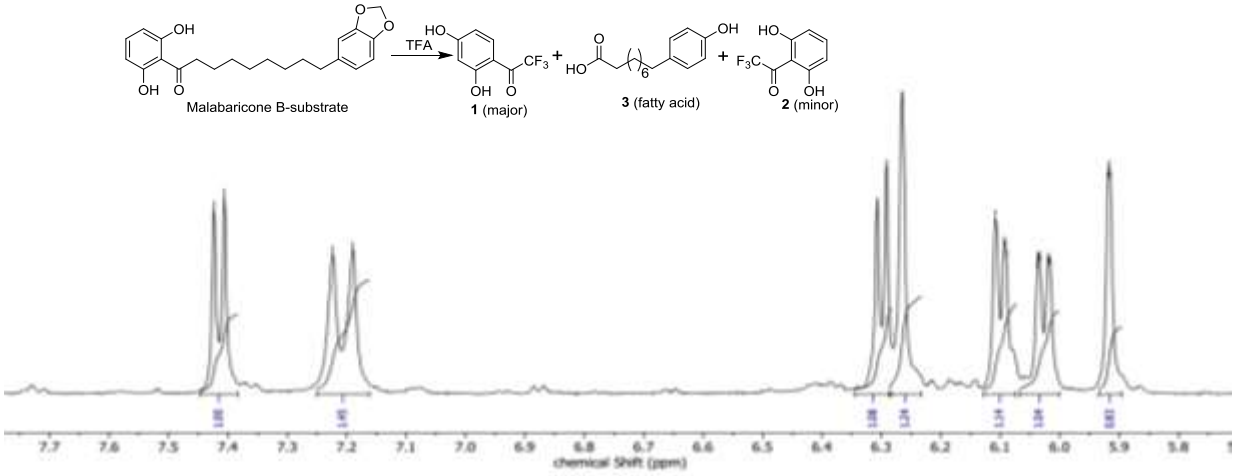

Figure S99: Expansion of stacking plot of 1H NMR spectra ($CDCl_3$, 500 MHz) of malabaricone D and its TFA reaction products (CD_3COCD_3, 500 MHz).

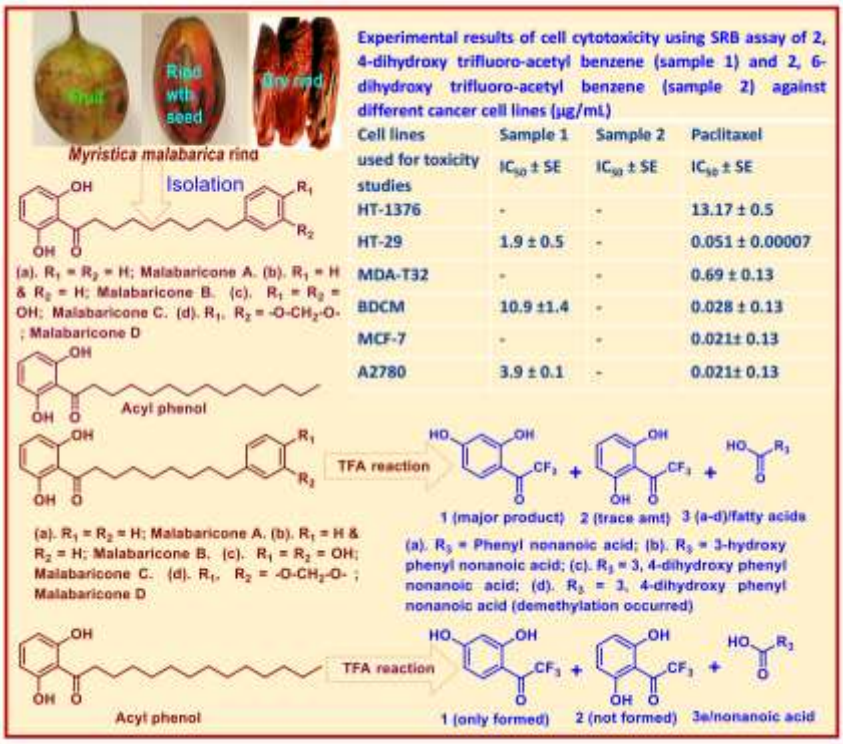

Experimental results of cell cytotoxicity using SRB assay of 2, 4-dihydroxy trifluoro-acetyl benzene (sample 1) and 2, 6-dihydroxy trifluoro-acetyl benzene (sample 2) against different cancer cell lines (µg/mL)

Cell lines used for toxicity studies	Sample 1 $IC_{50} \pm SE$	Sample 2 $IC_{50} \pm SE$	Paclitaxel $IC_{50} \pm SE$
HT-1376	-	-	13.17 ± 0.5
HT-29	1.9 ± 0.5	-	0.051 ± 0.00007
MDA-T32	-	-	0.69 ± 0.13
BDCM	10.9 ±1.4	-	0.028 ± 0.13
MCF-7	-	-	0.021± 0.13
A2780	3.9 ± 0.1	-	0.021± 0.13

Figure S100: Graphical abstract.